8-2018

Novel Tools to Study Modulation of Adenylyl Cyclase Isoforms

Monica Soto-Velasquez
Purdue University

NOVEL TOOLS TO STUDY MODULATION OF ADENYLYL CYCLASE ISOFORMS

by

Monica Soto-Velasquez

A Dissertation

Submitted to the Faculty of Purdue University

In Partial Fulfillment of the Requirements for the degree of

Doctor of Philosophy

Department of Medicinal Chemistry & Molecular Pharmacology

West Lafayette, Indiana

August 2018

THE PURDUE UNIVERSITY GRADUATE SCHOOL
STATEMENT OF COMMITTEE APPROVAL

Dr. Val J. Watts, Chair
Department of Medicinal Chemistry & Molecular Pharmacology

Dr. Gregory H. Hockerman
Department of Medicinal Chemistry & Molecular Pharmacology

Dr. Donald F. Ready
Department of Biological Sciences

Dr. Jean-Christophe Rochet
Department of Medicinal Chemistry & Molecular Pharmacology

Approved by:

Dr. Zhong-Yin Zhang
Head of the Graduate Program

A mis padres,
Monica y Alirio

ACKNOWLEDGMENTS

It has been a life-changing opportunity to complete this PhD journey at Purdue University, and it could not have happened without the unconditional support and encouragement of my colleagues, friends and family for the past six years. I am grateful for the guidance and advice of my Ph.D. mentor, Dr. Val J. Watts. As part of his lab, I have acquired a broad set of core skills that are the foundation for the next steps in my research career. His visionary drive to continuously incorporate innovative technologies kept me motivated and fostered my passion to the field of pharmacology and drug discovery. I would also like to thank Dr. Gregory Hockerman, Dr. Donald Ready, and Dr. Chris Rochet for their time and willingness to be part of my doctoral advisory committee, and for all their help and constructive feedback.

The achievements and the research reported herein could not have been possible without the help and effort from former and current members of the Watts lab. Since day one, Dr. Karin Ejendal welcomed me into the lab and kindly shared her knowledge and friendship. I want to thank her for the help learning the techniques and all those stimulating conversations about science, our research, life, and coffee. I also want to thank Dr. Tarsis Brust for being a great example on how it was possible to have a successful lab work and life balance as a graduate student, and Dr. Jason Conley for all the discussions and feedback during lab meetings and casual lab conversations. I would also like to thank the current members of the lab, Trevor Doyle and Dr. Michael Hayes who made the lab a fun and stimulating environment to share and troubleshoot experiments. I hope one day one of our million-dollar ideas gets to materialize. I also thank Dr. Zhong Ding and Yu Han-Hallett for their contributions to the Watts lab that one way or another were important for completing this work. I thank the numerous collaborators in the MCMP department (Flaherty, Parker, Dai, Dykhuizen, and Van Rijn labs), the University of Iowa (Roman lab), University of

Michigan (Smrcka lab) and the Institute of Organic Chemistry and Biochemistry of the Academy of Sciences of the Czech Republic (Janeba lab) for providing their expertise in biochemistry, genetics, behavioral science and synthetic chemistry to allow the work reported herein to move forward.

At the end of this journey and after many sleepless nights, I am extremely grateful for my MCMP friends, my husband Matt, Sophie, and my family for being my rock during those days the experiments did not work, and for kept reminding me then why I was here. We did it!

TABLE OF CONTENTS

LIST OF TABLES

LIST OF FIGURES

LIST OF ABBREVIATIONS

AC: Adenylyl cyclase

AKAP: A-kinase anchoring protein

ATP: Adenosine Tri-Phosphate

β2AR: β2-adrenergic receptor

Ca^{2+}: Calcium

CCE: Capacitative Ca^{2+} entry

CaM: Calmodulin

CaMKII: Ca^{2+}/calmodulin-dependent protein kinase II

cAMP: Cyclic AMP

CRISPR: Clustered regularly interspaced short palindromic repeats

CTE: Cyclase transducer element

DAG: Diacylglycerol

D2R: Dopamine D2 receptor

DSDB: Double-strand DNA break

EP_2R: Prostaglandin E2 receptor

Epac: Exchange proteins activated by cAMP

FDFM: Familial Dyskinesia with Facial Myokymia

FSK: Forskolin

GIRK: G protein-coupled inwardly rectifying K^+ channel

GlyR: Glycine receptor

GRK: G protein-coupled receptor kinase

GPCR: G protein-coupled receptor

IBMX: 3-isobutyl-1-methylxanthine

LTP: Long-term potentiation

mAC: Mammalian AC

MAPK: Mitogen-activated protein kinase

Mg^{2+}: Magnesium

MLCK: Myosin light chain kinase

NHEJ: Non-homologous end joining

NO: Nitric oxide

NIO: No Inhibition observed

PAINS: Pan-assay Interference compounds

PAM: Protospacer adjacent motif

PDE: Phosphodiesterase

PDGFR: Platelet-derived growth factor receptor

PI3K: Phosphatidylinositol 3-kinase

PKA: Protein Kinase A

PKC: Protein Kinase C

PLC: Phospholipase C

RTK: Receptor tyrosine kinase

sAC: Soluble AC

SAR: Structure-activity Relationship

sgRNA: single guide RNA

SPR: Surface Plasmon Resonance

ABSTRACT

Author: Soto Velasquez, Monica, P. PhD
Institution: Purdue University
Degree Received: August 2018
Title: Novel Tools to Study Modulation of Adenylyl Cyclase Isoforms
Committee Chair: Val J. Watts

Adenylyl cyclases (AC) are a major component of the cAMP signaling pathway. The differential regulatory properties and tissue expression patterns of the nine transmembrane AC isoforms provide unique mechanisms to regulate cAMP signaling in a precise and organized manner. However, the understanding of the individual roles of AC isoforms in the overall cellular response presents considerable challenges due to the expression of multiple AC isoforms in cells, and the lack of available tools to accurately detect isoform-specific AC expression or selectively modulate its catalytic activity. For these reasons, the research aims of this study were to develop a series of tools to characterize isoform-specific AC responses. In the first approach, a cell line with low cAMP levels in response to drug-stimulated conditions was developed by disrupting the expression of two of the most abundant ACs (i.e. AC3 and AC6) expressed in HEK293 cells using the CRISPR-Cas9 gene editing technology. Our HEK-ACΔ3/6 cell line displayed a substantially reduced cAMP response to forskolin (less than 95%) and to endogenous Gα_s-coupled receptors, β2AR and EP_2R (75% and 85% reduction respectively), compared to the cAMP responses of the parental HEK293 cells. Characterization of the cAMP responses of the nine membrane-bound AC isoforms to stimulatory and inhibitory paradigms in the HEK-ACΔ3/6 knockout cell line indicated that the regulatory properties of the AC isoforms previously reported in the literature were recapitulated. Furthermore, a comparison of the cAMP responses of a series of AC1 mutants demonstrated that the HEK-ACΔ3/6 cell line provided an enhanced signal window over the

parental HEK293 cells to characterize AC constructs with reduced catalytic activity. A second approach to better understand the individual role of AC isoforms in biological responses is by exploiting isoform-specific interactions with AC regulators to modulate AC activity. Thus, it was also determined in these studies that juxtamembrane domains derived from AC2 could modulate Gβγ-mediated AC activity. Based on the high degree of sequence homology between the juxtamembrane region of the C2a domain of Gβγ-stimulated cyclases, AC2, AC4, and AC7, together with surface plasmon resonance analysis with a C2a derived peptide (C2-20), it was demonstrated that Gβγ subunits bind with high affinity to this C2a juxtamembrane region. In addition, a minigene expressing the C2-20 peptide downstream of a membrane-anchoring domain, CD8, abolished Gβγ-mediated potentiation of PMA-stimulated AC2 activity. Mutagenesis studies indicated that several residues towards the middle of the sequence of the C2-20 peptide mediated the inhibitory activity on Gβγ-signaling, and the inhibitory effects of the minigene appeared to be selective for Gβγ-mediated stimulation of AC2. In the last approach to study isoform-specific AC responses, a series of structure activity relationship (SAR) studies were carried out towards the development of potent and selective AC1 and AC8 inhibitors. Initial SAR studies included analogs of the selective AC1 inhibitor, ST034307, that revealed a structure relationship between AC1 and AC8 selective inhibition. Furthermore, two new scaffolds were identified from a 10,000-compound screening campaign from the Life Chemicals compound collection, that showed dual inhibitory activity of calcium-stimulated AC1 and AC8 activity or selective inhibition of AC1 activity with sub-micromolar potency. Preliminary SAR analysis of various analogs of the dual AC1/AC8 inhibitory scaffold led to analogs with differential selectivity profiles for AC1 and AC8 and improved potency on both Ca^{2+}/calmodulin-stimulated AC isoforms. In conclusion, throughout this work, a cellular model, a peptide/minigene, and a series of inhibitor scaffolds were

developed as cellular and pharmacological tools to facilitate the study of the individual responses and respective roles of AC isoforms in cellular signaling.

CHAPTER 1. INTRODUCTION

1.1 Cyclic AMP(cAMP) Signaling Pathway

Cyclic adenosine monophosphate (cAMP) is one of the major secondary messengers of cellular signaling. At the molecular level, cAMP is responsible for multiple biological processes because it plays a critical role in the mechanism by which extracellular signals are translated into cellular responses. The cAMP signaling cascade initiates when an extracellular stimulus in the form of a photon, hormone, neurotransmitter, odorant, or lipid is recognized by the cell-surface receptors, G-protein coupled receptors (GPCR) (Ji et al., 1998). Ligand-activated GPCR associates to the heterotrimeric G-protein and promotes the dissociation of the Gαs-subunit from the heterotrimeric complex (Mahoney and Sunahara, 2016). The Gαs-subunit subsequently modulates the activity of the enzyme adenylyl cyclase (AC) which is responsible for the catalytic conversion of ATP into cAMP (Sunahara and Insel, 2016). Dynamic equilibrium between AC activation and cAMP degradation by cyclic nucleotide phosphodiesterase enzymes (PDEs) determines the duration of the cAMP signal in a given cell (Sassone-Corsi, 2012). An increase of intracellular cAMP levels then leads to the activation of three main cAMP effectors: protein kinase A (PKA), the exchange proteins activated by cAMP (EPAC), and/or cyclic-nucleotide-gated ion channels (reviewed in Cheng et al., 2008; Kaupp and Seifert, 2002; Skalhegg and Tasken, 2000). **Fig. 1.1** provides an overview of the cAMP signaling pathway. The cAMP effectors ultimately mediate a myriad of cellular responses by activating several other enzymes, changing membrane potential or regulating gene expression.

When cAMP was discovered in 1958 by Nobel laureate Earl W. Sutherland, it was thought impossible that numerous physiological changes in response to various hormones other than

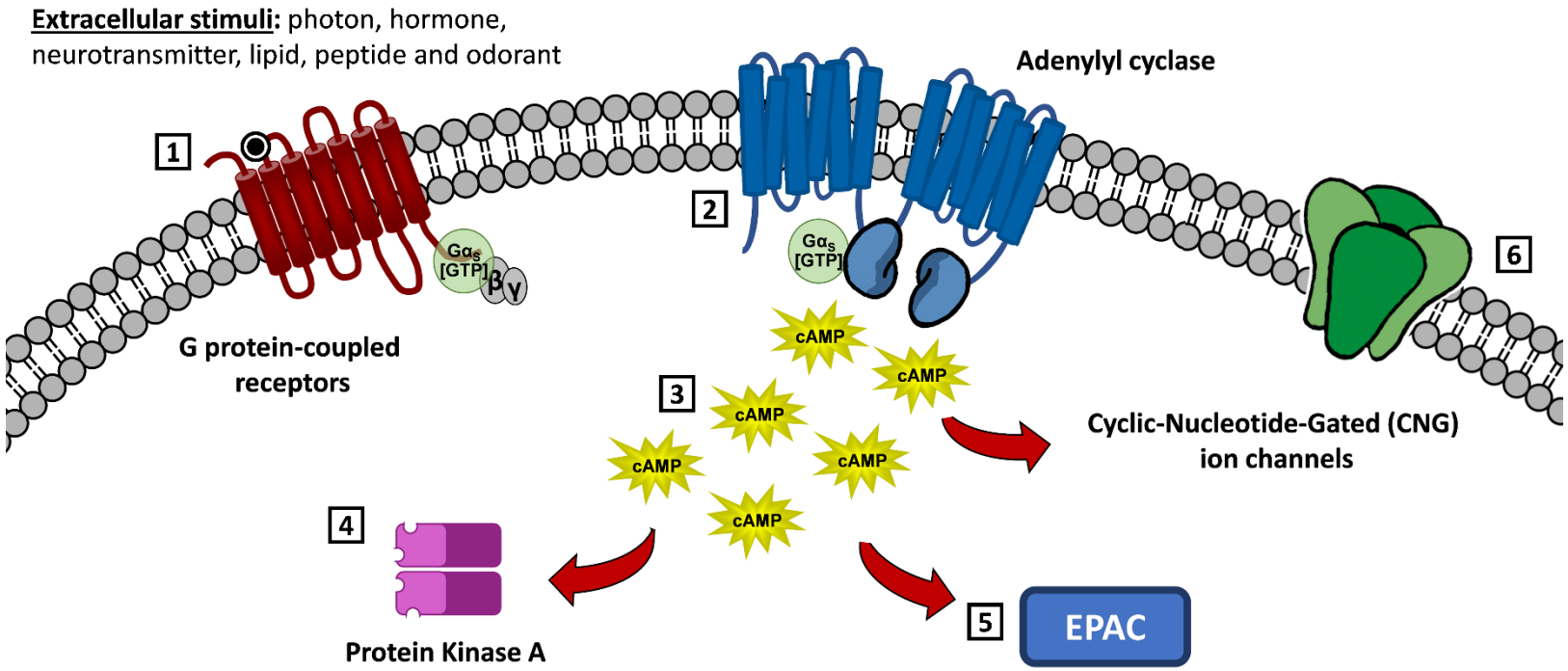

Figure 1.1 *Overview of the cAMP signaling pathway.*

An extracellular signal is recognized by G protein-coupled receptors **(1)**, triggering the dissociation of the heterotrimeric G-protein into a GTP-bound $G\alpha_s$ subunit and the $G\beta\gamma$ complex. Subsequently, the $G\alpha_s$ subunit activates the membrane-bound enzyme, adenylyl cyclase **(2)** which is responsible of synthesizing cAMP from ATP **(3)**. An increase of intracellular levels activates the cAMP effectors: protein kinase A (PKA) **(4)**, Epac **(5)** or cyclic-nucleotide-gated ion channels (CNGs) **(6)**, ultimately leading to a cellular response.

epinephrine were mediated intracellularly by a common secondary messenger (Sutherland and Rall, 1958). Sutherland and Rall initially proposed that hormones did not cross the plasma membrane, thus, receptors at the cell surface recognized the extracellular stimuli and translated into cAMP. Decades later, in the laboratory of Nobel laurate Alfred Gilman it was determined that the surface receptor and adenylyl cyclase were separate proteins, and that the receptor triggers AC activation via an intermediary, the GTP-dependent G-protein (Ross et al., 1978). Upon recognition of an extracellular stimuli by the GPCR, the G-protein couples to the receptor, and the receptor promotes the exchange of GDP for GTP to activate the G-protein (Sprang, 1997). GPCRs can be linked to three major classes of Gα-proteins that not only stimulate ($G\alpha_s$) or inhibit ($G\alpha_i$) AC activity, but also activate ($G\alpha_q$) phospholipase C (PLC) which can mediate the release of Ca^{2+} from intracellular stores (reviewed in McCudden et al., 2005). GPCRs are the largest family of surface receptors and because of their versatile mechanisms of activation, they have been a therapeutic target of great interest for numerous human diseases (Sriram and Insel, 2018).

However, the cAMP signaling cascade has demonstrated not to be a simple chain reaction downstream of GPCRs. Since the discovery of cAMP more than 60 years ago, our understanding of the cAMP signaling pathway has evolved from a linear signaling cascade to a dynamic network of signaling events. Emerging evidence supports that the regulatory properties and the spatiotemporal distribution of the cAMP network components (AC, PDE, cAMP effectors) create local cAMP domains that orchestrate organized and precise cellular processes (Arora et al., 2013). As mentioned earlier, the propagation of the cAMP signal within the cell results from the balance of cAMP synthesis and degradation by ACs and PDEs (Sassone-Corsi, 2012). Ten different AC isoforms have been cloned, and 21 isoforms of PDEs exist. AC isoforms are regulated by various mechanisms other than G-protein activation, and PDE isoforms also exhibit different regulatory

properties and binding affinities for cAMP (Dessauer et al., 2017; Maurice et al., 2014). Hence, multiple signal inputs besides GPCRs can trigger or prevent an increase of intracellular cAMP levels, and isoform-specific regulatory properties along with specific cell and tissue expression patterns of AC and PDE isoforms are additional mechanisms by which a given cell can mediate specific cAMP responses (Bender and Beavo, 2006; Hanoune and Defer, 2001).

High resolution microscopy and fluorescence sensors most recently have allowed precise monitoring of the different components of the cAMP signaling pathway (Calebiro and Maiellaro, 2014). It has become apparent that the cAMP signal does not spread uniformly across the cell, and distinct cAMP pools act in subcellular microdomains. Cyclic AMP diffuses freely in the cytosol; however, distinct GPCRs, ACs or PDEs sequestered at these subcellular compartments create a localized increase of cAMP levels that only causes selective activation of nearby effectors and does not allow the cAMP signal to rapidly diffuse (Arora et al., 2013). As more evidence for the existence of subcellular pools of cAMP is emerging, the roles of scaffolding/anchoring proteins such as caveolin and A-kinase anchoring proteins (AKAPs) in cAMP compartmentalization is also becoming more evident (Kapiloff et al., 2014; Ostrom and Insel, 2004). Specific interactions between ACs and/or cAMP effectors with anchoring/scaffolding proteins mediate the formation of signalosome complexes that coordinate the effects of cAMP (Dessauer, 2009). Therefore, localized cAMP signaling is another mechanism by which cAMP levels in the cell are fine-tuned to induce a precise cellular response.

In conclusion, the diversity of GPCR signaling is not the only basis that controls cAMP signaling and determines the signaling outcome. Intracellular inputs mediated by adenylyl cyclases and PDEs in combination with the spatiotemporal control of the cAMP signal, also enables fine-tuning of the cAMP-mediated cellular responses. Hence, further understating of the interplay

between the cAMP network components opens novel avenues that should be explored for the development of therapeutic agents that can modulate cAMP signaling.

1.2 Adenylyl Cyclases (AC), a key determinant of cAMP-mediated cellular responses

The term of adenyl cyclase was first introduced by Sutherland in 1962 when describing the enzyme responsible for cAMP production (Sutherland et al., 1962). It was not until 1989 that the first mammalian AC (mAC) was cloned by Krupinski in the Gilman laboratory, and since then additional 8 membrane-bound ACs and one soluble AC have been characterized in mammals (Bakalyar and Reed, 1990; Buck et al., 1999; Defer et al., 1994; Feinstein et al., 1991; Gao and Gilman, 1991; Ishikawa et al., 1992; Katsushika et al., 1992; Krupinski et al., 1989; Paterson et al., 1995; Watson et al., 1994). All membrane-bound mACs share an N-terminus and two transmembrane regions (M1 and M2) of six-spanning helices that are connected by two cytosolic/catalytic domains (C1 and C2) and comprise the enzyme's active site (Hurley, 1999) (**Fig.1.2**). The soluble AC (sAC) shares homologous cytosolic/catalytic domains to the mACs, except they are connected by a cytosolic linker instead of the transmembrane domains (Steegborn, 2014).

Adenylyl cyclases catalyze the formation of cAMP from ATP by removing the two terminal phosphates groups from the triphosphate "tail" and linking the remaining phosphate to the sugar ring of the ATP molecule (Tang and Hurley, 1998). The catalytic site on the cyclase is formed within a cleft at the interface of the C1 and C2 domain when the two domains heterodimerize (Tesmer et al., 1997). On the opposite site of the ATP binding site, a pseudo symmetric site is also formed at the interface where the diterpene forskolin or bicarbonate binds to tmAC 1-8 or sAC,

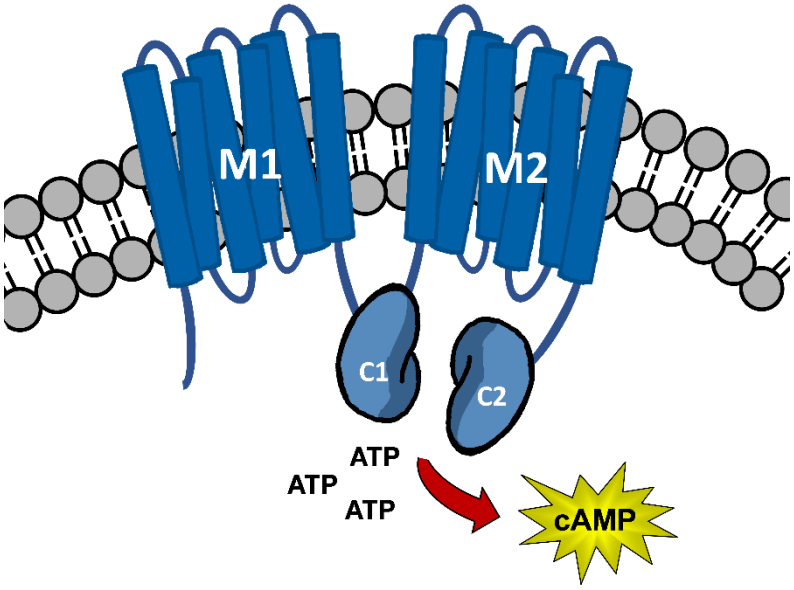

Figure 4.2 *Topology of transmembrane adenylyl cyclases*

The basic structure of membrane-bound adenylyl cyclases consist of a cytosolic N-terminus, followed by two domains (M1 and M2) of six membrane-spanning α-helices and two highly conserved catalytic domains (C1 and C2) that form the ATP-binding site at the C1-C2 interface.

respectively (Kleinboelting et al., 2014; Tesmer et al., 1997). GPCR/G-protein activation has been described as the major mechanism of AC regulation; however, ACs can also be regulated by protein kinases, Ca^{2+}/Calmodulin, divalent cations, ethanol, bicarbonate and nitric oxide depending on the AC isoform (Dessauer et al., 2017). AC isoform-specific cAMP responses that arise from the regulatory effects of the different AC modulators exemplifies another mechanism, independent of GPCR activation, by which intracellular levels of cAMP mediate many different signaling events (Hanoune and Defer, 2001). Despite the fact that ACs are ubiquitously expressed and cells/tissues express more than one AC isoform, several AC isoforms have been associated with specific physiological processes and emerge as interesting targets for cAMP modulation (Pierre et al., 2009; Sadana and Dessauer, 2009).

1.3 Adenylyl cyclase Regulation

1.3.1 G protein-coupled receptors

G protein-coupled receptors are seven transmembrane receptors that comprise the largest family of membrane proteins. Activated by a diverse class of ligands including photons, small molecules, peptides, odorants, or lipids, GPCRs translate extracellular signals into intracellular signals by coupling to G-proteins (Ji et al., 1998). The inactive G-protein complex is a heterotrimeric structure composed of a Gα, Gβ, and Gγ subunits (Wall et al., 1995). The heterotrimeric complex is localized at the plasma membrane in an inactive GDP-bound state, but upon GPCR activation, the receptor undergoes a conformational change that promotes the exchange of bound GDP to GTP on the Gα subunit causing the dissociation of Gα from the Gβγ complex (reviewed by Oldham and Hamm, 2008). Both Gα and Gβγ are then free to activate their

corresponding downstream targets such as protein kinases, ion channels, or membrane-bound enzymes (Cabrera-Vera et al., 2003).

Depending on the Gα protein subtype that couples to the GPCR, receptor activation primarily promotes the stimulation ($G\alpha_s$) or inhibition ($G\alpha_i$, $G\alpha_o$) of adenylyl cyclase activity or triggers the release of Ca^{2+} from intracellular stores by activating phospholipase C (PLC) via Gαq (Exton, 1996; Taussig and Zimmermann, 1998). Once the G-protein has been activated, G protein-coupled receptor kinases (GRKs) translocate to the activated receptor and phosphorylate its C-terminus (Benovic et al., 1986). The phosphorylated C-terminus interacts with arrestins which block further coupling of the receptor with the G-protein and mediates receptor internalization for subsequent signal termination (Lohse et al., 1990). For a detailed review of the roles of GRKs and arrestins in GPCR desensitization/trafficking, referred to Moore et al., 2007.

Over the past three decades, GPCRs have been a prominent target for treatment of a wide range of diseases (Sriram and Insel, 2018). Exceptional progress has been done trying to elucidate the pharmacology, structure and biology of more than 800 homologous GPCR genes identified in humans (Fredriksson et al., 2003; Katritch et al., 2012). It has become clear that GPCRs functions are not limited to G-proteins, and arrestins can mediate GPCR signaling as well (reviewed by Smith and Rajagopal, 2016). Furthermore, certain ligands can induce specific receptor conformations that activate a specific intracellular pathway (G-protein vs arrestin) and this phenomenon is referred as *functional selectivity* or *biased signaling* (Goupil et al., 2012). Since the breakthrough of the β2-adrenergic receptor crystal structure in 2011 that earned Brian Kolbika the Nobel prize in 2012 (shared with Robert Lefkowitz), the number of GPCR crystal structures solved also keeps increasing (Rasmussen et al., 2011). Ongoing efforts are trying to explore new

GPCR targets (orphan receptors), develop GPCR-based drugs with fewer side effects, and decipher GPCR signaling networks (Jacobson, 2015; Ngo et al., 2016).

G protein-coupled receptors linked to $G\alpha_s$ and $G\alpha_i$ proteins are the primary regulators of mAC activity, whereas sAC is insensitive to GPCR activation. $G\alpha_s$ stimulates all nine transmembrane AC isoforms by direct interaction with the C1-C2 catalytic domains of the AC, and $G\alpha_i$ inhibits cAMP production of several AC isoforms, but its mechanism of action is not fully understood yet (Taussig and Zimmermann, 1998; Tesmer et al., 1997). The $G\beta\gamma$ complex conditionally modulates AC activity after GPCR activation, however depending on the isoform it has stimulatory or inhibitory effects (Khan et al., 2013).

1.3.1.1 $G\alpha_s$-protein

Activation of adenylyl cyclases by $G\alpha_s$ subunits was the first described mechanism resulting from GPCR activation. Stimulation of the catalytic activity by $G\alpha_s$ protein has been confirmed for all transmembrane adenylyl cyclases *in vitro* (Sunahara et al., 1996). Studies with purified C1 and C2 catalytic domains were the first indication that $G\alpha_s$ triggers cAMP production by promoting C1-C2 dimerization (Sunahara et al., 1997). The crystal structure of the heterodimer of the C1 (AC5) and C2 (AC2) catalytic domains in complex with $G\alpha_s$ and forskolin, revealed that the $G\alpha_s$-protein primarily interacts with the C2 domain by inserting a switch helix motif into a groove formed by two helices of the AC (Tesmer et al., 1997). The residues important for the interaction with the AC are positioned on the surface of the $G\alpha_s$ protein that faces the plasma membrane and that undergoes a conformational change upon GTP binding (Berlot and Bourne, 1992). In cells, the stimulatory effect of $G\alpha_s$-coupled receptors is not uniform across AC isoforms, and it is strictly dependent on expression levels of the GPCR and the subcellular localization of the receptor and the AC (Ostrom and Insel, 2004).

1.3.1.2 $G\alpha_i$-protein

Inhibition of AC activity by $G\alpha_i$ has been demonstrated for AC1, AC5, and AC6 (Taussig et al., 1993a). The degree of inhibition by $G\alpha_i$ depends on the stimulation mechanism, and high concentrations of forskolin or $G\alpha_s$ can overcome the inhibitory effects of the G-protein (Taussig et al., 1994). A $G\alpha_i$-binding site has been characterized on the C1 domain of AC5 by mutagenesis studies. Analogous to the $G\alpha_s$-AC interaction, the $G\alpha_i$-protein interacts with two alpha helices of the C1 catalytic domain—directly opposite to the $G\alpha_s$-binding site (Dessauer et al., 1998). In contrast to $G\alpha_s$, it appears that the interaction of $G\alpha_i$ with the AC inhibits catalytic activity by decreasing the apparent affinity of C1 for C2 (Dessauer et al., 2002). It is worth noting that AC2 is insensitive to $G\alpha_i$ *in vitro* (Taussig et al., 1993a), but activation of $G\alpha_i$-coupled receptors in cells induces an enhancement of AC2 activity (Watts and Neve, 1997). However, the stimulatory effects are mediated by Gβγ subunits, not by the $G\alpha_i$-protein.

1.3.1.3 Gβγ subunits

The Gβγ complex can function independently from the Gα subunits and modulates a broad range of downstream effectors (Khan et al., 2013). Depending on the AC isoform, Gβγ conditionally stimulates or inhibits AC activity (Taussig et al., 1993b). AC2, AC4 and AC7 have been described as Gβγ-stimulated cyclases, whereas AC1, AC3 and AC8 are inhibited by the Gβγ complex (Diel et al., 2006; Sunahara et al., 1996). The regulation of AC5 and AC6 by Gβγ appears to be complex since there are contradictory reports in the literature of both stimulatory and inhibitory effects (Bayewitch et al., 1998; Gao et al., 2007). Isoform-specific binding sites have been identified for Gβγ that are distributed across the N-terminus and the two catalytic domains of the ACs (Boran et al., 2011; Brand et al., 2015; Chen et al., 1995; Diel et al., 2008), however it is

not fully understood yet how the interaction of Gβγ with the cyclase distinctly promotes or interferes with the catalytic activity.

1.3.2 Ca^{2+}/Calmodulin (CaM)

Calcium is another critical secondary messenger that transmits signals throughout the cell. Changes in cytosolic calcium concentrations result from ion channel activation or the opening of intracellular Ca^{2+} stores triggered by GPCR ($G\alpha_q$) and PLC activation. An increase of Ca^{2+} in the cytosol of the cell is primarily detected by the calcium-binding protein, calmodulin (CaM), a small and flexible protein that upon Ca^{2+} binding undergoes a conformational change that enables its interaction with approximately 300 other proteins (Clapham, 2007). Major targets of calmodulin include Ca^{2+}/calmodulin-dependent protein kinase II (CaMKII), calcineurin, the myosin light chain kinase (MLCK) and both bacterial (edema factor and CyaA) and mammalian (AC1 and AC8) adenylyl cyclases (Tidow and Nissen, 2013). Calcium and cAMP signaling pathways are not two isolated signaling events, and crosstalk between different components of each pathway contributes to the complex and distinct cellular responses that arise from changes in cAMP or calcium levels (Bruce et al., 2003). One mechanism by which Ca^{2+} regulates the cAMP pathway is by regulating AC activity. Ca^{2+}/calmodulin stimulates the catalytic activity of AC1 and AC8, and high concentrations of intracellular Ca^{2+} inhibit AC5 and AC6 (Guillou et al., 1999; Halls and Cooper, 2011). Similarly, Ca^{2+} can also indirectly modulate AC activity by inhibiting or activating other AC regulators such as PKC and CaMKII.

1.3.2.1 Calcium

Calcium sensitivity was one of the primary properties evaluated besides G-protein and forskolin activation when AC isoforms were initially cloned and characterized (Choi et al., 1992; Feinstein et al., 1991; Ishikawa et al., 1992; Katsushika et al., 1992). The stimulatory properties of Ca^{2+} on membrane-bound AC activity are mediated by the calcium binding protein, calmodulin, and the inhibitory properties are a direct consequence of Ca^{2+} (Halls and Cooper, 2011). When AC5 and AC6 were first cloned, it was established *in vitro* that Ca^{2+} inhibited their catalytic activities in a dose-dependent manner (Katsushika et al., 1992; Yoshimura and Cooper, 1992). Later, when the crystal structure of the C1(AC5)-C2(AC2) heterodimer bound to Ca^{2+} was solved, it revealed that the divalent cation competes for the binding site of the metal cofactor Mg^{2+} at the active site and stabilizes an inactive conformation of the C1 and C2 domains that ATP can't bind to (Mou et al., 2009). Ca^{2+} inhibition appears to be biphasic, having a high-affinity binding site for AC5 and AC6 and a low-affinity binding site for the rest of the isoforms (Guillou et al., 1999). Soluble AC is insensitive to G-protein and forskolin activation, but is directly activated by Ca^{2+} (Litvin et al., 2003). In the crystal structure of sAC bound to Ca^{2+}, the Ca^{2+} binding site was localized at the interface of the catalytic domains and confirmed that the divalent cation promotes catalytic activity by increasing the affinity of the active site for ATP (Kleinboelting et al., 2014).

1.3.2.2 Calmodulin

Changes in intracellular Ca^{2+} levels and subsequent activation of calmodulin, has stimulatory effects on AC1 and AC8 activity (Cali et al., 1994; Tang et al., 1991). The responsiveness of AC1 and AC8 to Ca^{2+}/calmodulin is a critical property of these two isoforms (Ferguson and Storm, 2004). In the case of AC1, Ca^{2+}/calmodulin-stimulated activity can be observed in combination

with $G\alpha_s$ and forskolin, or it can be inhibited by $G\alpha_i$ and $G\beta\gamma$ subunits (Tang et al., 1991). Although the exact mechanism of activation of Ca^{2+}/calmodulin has not been established, it is known that the stimulatory effects of calmodulin are mediated by a direct interaction with the catalytic domains of AC1 and AC8 (Masada et al., 2012). For AC1, the Ca^{2+}/calmodulin binding domain was found in the C1b domain when domain swapping of the C1b region of AC2 for the C1b domain of AC1 made AC2 responsive to Ca^{2+}/calmodulin (Levin and Reed, 1995). In contrast, AC8 has two binding domains for calmodulin, one in the N-terminus and one in the C2 domain that were determined by GST pull-down and mutagenesis studies (Gu and Cooper, 1999). Adenylyl cyclase type 3 (AC3) is also described as a Ca^{2+}/calmodulin-sensitive cyclase based on a limited set of studies. The activation of AC3 by Ca^{2+}/calmodulin appears to be conditional because in order to observe a stimulatory effect on AC3 activity, other mechanisms of activation such as $G\alpha_s$ and forskolin must be present (Choi et al., 1992; Mamluk et al., 1999).

1.3.3 Protein Kinases

Protein kinases are cytosolic enzymes that regulate about 30% of the human proteome by transferring a phosphate group from ATP onto a free hydroxyl group of its substrates (Cheng et al., 2011). This reversible post-translational modification induces conformational changes that alter the structure and function of the phosphorylated-protein. More than 500 protein kinases have been identified in humans, and they all have precise mechanisms to recognize their specific targets/substrates (Ubersax and Ferrell, 2007). Protein Kinase A (PKA) is the prominent effector of cAMP. When there is an increase of intracellular cAMP levels, the regulatory subunits of PKA bind cAMP causing a conformational change that provokes the release of the catalytic subunits (Cheng et al., 2011).

In addition, protein kinases also regulate the activity of several AC isoforms and phosphorylation sites have been identified on AC2, AC3, AC5, AC6 and AC8 (Iwami et al., 1995; Jacobowitz and Iyengar, 1994; Kawabe et al., 1994). PKA has an inhibitory effect on AC5 and AC6 activity by a negative feedback loop mechanism, PKC displayed stimulatory and inhibitory effects on AC2 and AC6, respectively (Jacobowitz et al., 1993; Lai et al., 1997), and Ca^{2+}/calmodulin-dependent protein kinase II (CaMKII) inhibits AC3 activity, but activates AC9 (Cumbay and Watts, 2005; Wei et al., 1996) .

1.3.3.1 Protein Kinase A

Evidence with purified enzymes demonstrated that PKA phosphorylates AC5 and it reduces AC activity by decreasing the catalytic rate of cAMP synthesis (Iwami et al., 1995). Phosphorylation inhibits $G\alpha_s$-mediated activation of AC6 but has no major effects on $G\alpha_s$-stimulated activity of AC1 and AC2 (Chen et al., 1997). PKA phosphorylates AC6 at Ser^{674}, within a region involved in $G\alpha_s$ activation; however, the phosphorylated residue is only conserved between AC5 and AC6 (Chen et al., 1997). Most recently, a phosphorylation site on the N-terminus of AC8 (Ser^{112}) was identified that decreases the cAMP response of the cyclase to Ca^{2+} (Willoughby et al., 2012). Analogous to AC5 and AC6 phosphorylation by PKA, the interaction with the A-kinase-anchoring protein, AKAP79/150, serves as platform for PKA to phosphorylate AC8 by colocalizing it in close proximity to the cyclase (Bauman et al., 2006; Beazely and Watts, 2006; Willoughby et al., 2012).

1.3.3.2 Protein Kinase C

PKC enzymes are activated by Ca^{2+} or diacylglycerol (DAG), and they are not cAMP-dependent (Huang, 1989). Enhancement of AC2 and AC7 activity by PKC has been demonstrated

in membrane preparations and intact cells (Jacobowitz et al., 1993; Nelson et al., 2003; Watson et al., 1994). Particularly, AC2 activity can be stimulated by PKC activators (PMA, TPA) alone or in combination with Gβγ subunits, forskolin, or Gαs (Jacobowitz and Iyengar, 1994; Watts and Neve, 1997; Yoshimura and Cooper, 1993). Three phosphorylation sites have been proposed on AC2, two sites on the C1 domain at Ser^{490} and Ser^{543}, and one site on the C2 domain at Thr^{1057} (Bol et al., 1997; Shen et al., 2012). Much less evidence exists for the regulation of other AC isoforms by PKC. For instance, only one study has provided evidence for the inhibitory effects of PKC on AC6 activity that appear to be through a calcium-independent mechanism (Lai et al., 1997). However, after chronic activation of the dopamine D2 receptor and activation of the PKC-Raf1 pathway, sensitization of AC6 activity is also potentiated (Beazely and Watts, 2005). In addition, several other reports have had conflicting results about PKC regulation of AC1, AC3, AC5 and AC9 activity (reviewed by Halls and Cooper, 2011).

1.3.3.3 Ca^{2+}/calmodulin-dependent protein kinase II (CaMKII)

CaMKII is one of the main effectors of the calcium binding protein, calmodulin. Ca^{2+}-bound CaM activates CaMKII by displacing an autoinhibitory domain that prevents substrate binding (serine/threonine residues) to the catalytic domain (Hanson and Schulman, 1992). Limited evidence is available on CaMKII regulation of AC3 activity, and only one report has shown the inhibitory effects of CaMKII on $G\alpha_s$- and forskolin-stimulated AC3 activity (Wei et al., 1996). Wei et al., 1996 showed that neither PKA nor PKC phosphorylated AC3, but rather CaMKII in a calcium-dependent manner phosphorylated Ser^{1076} of the C2 domain of AC3. Particularly, phosphorylation of Ser^{1076} was proved to be mediated by CaMKII in endogenous AC3 of mouse olfactory cilia and primary olfactory neurons, suggesting a role of the Ca^{2+}/calmodulin-dependent kinase in the regulation of cAMP responses associated with olfactory signaling (Wei et al., 1998).

CaMKII also appears to potentiate AC9 activity (Cumbay and Watts, 2005). By using the CaM inhibitor W7 and the CaMKII inhibitor KN62, it was determined that the enhancement of $G\alpha_s$-mediated stimulation of AC9 activity after $G\alpha_q$-coupled receptor activation, was induced by CaMKII activation (Cumbay and Watts, 2005).

1.3.4 Additional Isoform-specific Regulators

AC isoforms are also regulated by chemical compounds such as bicarbonate, ethanol and nitric oxide (Dessauer et al., 2017).

Bicarbonate: Although there is a high degree of homology between the catalytic domains of transmembrane ACs and the soluble AC, sAC accommodates a bicarbonate ion at the pseudo symmetric site rather occupied in the membrane-bound ACs by the diterpene forskolin (Kleinboelting et al., 2014; Steegborn, 2014). Binding of bicarbonate ions increases the V_{max} of the enzyme but has no effect on the affinity for ATP (Litvin et al., 2003). The ability of bicarbonate to directly regulate sAC depicts a mechanism by which changes in pH modulate cellular signaling.

Nitric oxide (NO): The inhibitory effects of nitric oxide on AC activity are selective for the closely related cyclases, AC5 and AC6. The inhibitory actions of NO are directly on the catalytic domains of the AC and are not a result of an indirect effect through other NO effectors such as G-proteins or phosphodiesterases (Hill et al., 2000). Evidence with NO and AC6 suggests that NO inhibits the catalytic activity of the AC by decreasing the V_{max} of the enzyme, and that it preferably binds to the inactive/basal conformation of the AC because occupancy of the active site by ATP diminished the ability of NO to inhibit AC6 activity (McVey et al., 1999).

Ethanol: The regulatory properties of ethanol on AC activity so far have only been demonstrated on AC7 (Nelson et al., 2003). Studies with purified catalytic domains or with cells overexpressing AC7 showed that ethanol alone potentiated AC activity, but it decreased the cAMP responses

induced by forskolin or/and $G\alpha_s$ (Qualls-Creekmore et al., 2017). The multiplicity of regulatory mechanisms that modulate adenylyl cyclase activity are other effective ways that the cell fine-tunes its responses to an extracellular signal. The regulatory properties of the AC isoforms previously described are summarized in **Table 1.1**.

To achieve a precise cellular response, the cAMP pathway requires additional levels of complexity, despite the diversity of the human GPCR family and the variety of ligands/signals that induce GPCR activation. Regulation of AC activity by a variety of intracellular agents also allows the integration of signal inputs from inside and outside of the cell (crosstalk) (Yan et al., 2016). In addition, identifying isoform specific responses to regulators is also critical to elucidate the contribution of each AC isoform to a cellular response given that adenylyl cyclase expression is ubiquitous across tissues, and cells tend to express more than one AC isoform. Furthermore, based on these isoform-specific regulatory properties, membrane-bound adenylyl cyclase isoforms are subdivided into 4 groups. Group 1 consists of the Ca^{2+}/calmodulin responsive ACs, AC1, AC3, and AC8, whereas the Gβγ-stimulated cyclases, AC2, AC4, and AC7 belong to Group 2. Group 3 include the Ca^{2+}-inhibited ACs, AC5 and AC6, and the forskolin-insensitive AC9 is the only member of Group 4 (Dessauer et al., 2017). Hence, the multiplicity of regulatory mechanisms that modulate adenylyl cyclase activity is another effective way the cell fine-tunes its responses to an extracellular signal.

1.4 Organization of Adenylyl Cyclases at the Cellular and Tissue levels

Apart from the diverse regulatory properties of the AC isoforms, their distinct subcellular localization and tissue expression pattern adds another aspect to the cAMP signaling network that enables the cell to tailor precise responses to an extracellular stimulus.

Table 1.1 *Regulatory properties of adenylyl cyclase isoforms*

Differential effects of regulators on the catalytic activity of AC isoforms. (+) stimulation, (–) inhibition, ($^{+}/_{-}$) complex regulation, (+ +) conditional stimulation/potentiation.

	ADENYLYL CYCLASE ISOFORM									
	AC1	AC2	AC3	AC4	AC5	AC6	AC7	AC8	AC9	sAC
Forskolin	+	+	+	+	+	+	+	+		
Gαs	+	+	+	+	+	+	+	+	+	
Gαi	–				–	–				
Gβγ	–	+ +	–	+ +	$^{+}/_{-}$	$^{+}/_{-}$	+ +	–		
Ca^{2+}					–	–				+
Ca^{2+}/Calmodulin	+		+					+		
PKA					–	–		–		
PKC	$^{+}/_{-}$	+	$^{+}/_{-}$		$^{+}/_{-}$	$^{+}/_{-}$	+		$^{+}/_{-}$	
CaMKII			–						+ +	
Bicarbonate										+
Nitric Oxide					–	–				
Ethanol							+ +			

Although, the relative expression level of AC isoforms has been assessed in different cell models and human tissues by quantifying mRNA and protein levels, the selectivity of commercially available antibodies is not ideal to distinguish between AC isoforms, and mRNA levels don't always correlate with protein expression (Dessauer et al., 2017).

Furthermore, most cells express more than one AC isoform, implying a potential functional redundancy in response to a shared stimulant/activator; however, different cAMP responses still arise as a result of the subcellular organization into membrane microdomains of specific AC isoforms (Ostrom and Insel, 2004). At these subcellular compartments, GPCRs, cAMP effectors, phosphodiesterases and AKAPs are also confined, causing a local cAMP response with unique cellular and physiological outcomes (reviewed in Halls and Cooper, 2017).

1.4.1 AC Subcellular Compartmentalization

At the cellular level, AC isoforms are found in lipid rafts and non-raft membrane domains (Ostrom and Insel, 2004). The interactions of the AC isoforms with caveolin and/or AKAPs, or post-translational modifications on the cytosolic domains of the ACs, determine their specific cellular localization (Dessauer, 2009). For instance, caveolin serves as a scaffolding protein for AC6 and β2AR in lipid raft domains of cardiac myocytes, and colocalization of AC6 and β2AR in caveolin-rich domains appears to be the major determinant of AC6-selective coupling to β2AR in these type of cells (Ostrom et al., 2002; Ostrom et al., 2000). Conversely, the EP_2R localizes at non-raft domains, and it exhibits a more efficient coupling to AC isoforms localized at non-raft domains such as AC2 and AC4, than mediating the activation of other ACs localized in lipid-rafts such as AC3 and AC6 (Bogard et al., 2012; Ostrom et al., 2001; Ostrom et al., 2002).

Similarly, Ca^{2+}/Calmodulin regulation of AC1 and AC8 can be restricted to a microdomain because the source of intracellular Ca^{2+} that triggers AC activation may also be specific (Willoughby et al., 2010). Indeed, stimulation of AC activity by capacitative Ca^{2+} entry (CCE) has been shown to be selective for AC8 which localizes at lipid rafts, so when the microdomain is disrupted by degrading sphingomyelins, CCE fails to stimulate AC8 activity (Pagano et al., 2009; Smith et al., 2002).

AKAPs primary role is to scaffold PKA, and they not only restrict the movement of ACs, but also anchored other signaling components of the cAMP pathway creating a platform for dynamic interactions that facilitate selective coupling with distinct upstream and downstream effectors (Johnstone et al., 2017; Logue and Scott, 2010). More than 50 different isoforms of AKAPs have been identified and those that interact with ACs, have different specificities for different AC isoforms. Some AC-AKAP interactions have been characterized for AKAP79/150 with AC5/6, Yotiao with AC1, AC2, AC3 and AC9, and mAKAP with AC2 and AC5 (Dessauer, 2009). Most recently, the advancement of imaging techniques and the development of sensors with high spatiotemporal resolution have allowed a better characterization of these multiprotein complexes and localized cAMP signaling networks in living cells (Paramonov et al., 2015). The importance of cellular compartmentalization of the cAMP pathway is then an emerging concept; thus, additional evidence is still needed in order to associate a specific cellular response with a multicomponent complex of a unique GPCR-AC-AKAP-PDE combination. However, it is becoming more evident that via these signaling complexes, a single cell can achieve spatiotemporal control of its cellular responses.

1.4.2 Tissue Pattern Expression of ACs

Quantification of AC isoform expression in tissues has been a challenging task for various reasons. Commercially available antibodies are not specific enough to distinguish between AC isoforms, and the protein expression level of endogenous ACs is near the limit of detection by western blot and immunohistochemistry (Antoni et al., 2006). Hence, most of the studies that have reported the relative gene expression of AC isoforms in mammalian tissues are based on RNA quantification methods such as RT-qPCR, Northern analysis, in-situ hybridization and micro arrays (Atwood et al., 2011; Defer et al., 2000; Ludwig and Seuwen, 2002; Sanabra and Mengod, 2011). **Table 1.2** summarizes the relative expression of the AC isoforms in human tissues. Although the relative mRNA levels may indicate gene expression, this data must be interpreted cautiously because mRNA levels do not always reflect the protein expression levels due to the fact other factors such as translation efficiency and protein turn-over are also significant determinants of protein abundance (Maier et al., 2009).

1.5 Physiological Roles of Adenylyl Cyclase Isoforms

Despite the fact that cells and tissues express more than one adenylyl cyclase isoform, it is the combination of the unique regulatory properties of the different AC isoforms with their subcellular organization and tissue-specific expression patterns that distinct physiological and pathophysiological conditions have been associated with particular AC isoforms (Dessauer et al., 2017). Knockout and overexpression studies have been the main approaches utilized to determine the physiological functions regulated by isoform-specific AC activities (Sadana and Dessauer, 2009).

Table 1.2 *Relative tissue distribution of AC isoforms*

Expression profile for the nine membrane-bound AC isoforms in human tissues based on the results of semi-quantitative RT-qPCR analysis carried out by Ludwig and Seuwen, 2002.

	ADENYLYL CYCLASE ISOFORM								
	AC1	**AC2**	**AC3**	**AC4**	**AC5**	**AC6**	**AC7**	**AC8**	**AC9**
Brain	X	X	X		X	X	X	X	X
Colon		X	X		X	X	X		
Heart	X	X		X	X	X	X		X
Kidney						X			X
Liver							X		X
Lung			X	X			X		X
Ovary	X	X	X	X	X	X	X		X
Peripheral blood leukocytes	X						X		X
Pancreas	X								X
Placenta			X	X			X		X
Prostate		X			X	X			
Skeletal Muscle	X	X							X
Small Intestine				X	X	X			
Spleen	X		X	X			X		
Testis	X	X	X	X	X	X		X	X
Thymus			X				X		

Likewise, the identification of genetic polymorphisms in the adenylyl cyclase (ADCY) genes and their association with a particular phenotype have also provided complementary evidence of the isoform-specific contributions to a particular disease (Chen et al., 2012; Grarup et al., 2018; Pitman et al., 2014). Consequently, AC isoforms have emerged as potential therapeutic targets for various pathophysiological conditions, and isoform-selective modulation of AC activity becomes an additional approach—besides modulating GPCRs—by which the cAMP signaling pathway can be regulated (Pierre et al., 2009).

1.5.1 Group I: Adenylyl cyclases 1, 3 and 8

Ca^{2+}/calmodulin-stimulated cyclases, AC1 and AC8, are highly expressed in the brain (Sanabra and Mengod, 2011; Xia et al., 1991). Single and double knockout studies of AC1 and AC8 have demonstrated that both cyclases play a critical role in learning and memory (reviewed by Ferguson and Storm, 2004). AC1- and/or AC8-deficient mice exhibited impaired long-term potentiation (LTP) in various regions of the brain including the hippocampus, cerebellum, hypothalamus and thalamus (Schaefer et al., 2000; Storm et al., 1998; Villacres et al., 1998; Wang et al., 2003; Wong et al., 1999). However, the role of these Ca^{2+}/calmodulin-stimulated cyclases in memory and learning appears to be redundant given that in the single-knockout mice of AC1 or AC8, memory and learning were attenuated to a lesser extent than in the double-knockout mice (Wong et al., 1999). Moreover, LTP can be reestablished by forskolin in AC1- and/or AC8-deficient mice, suggesting that stimulation of AC activity compensates for AC1/AC8-induced cAMP signaling (Villacres et al., 1998; Wong et al., 1999). Likewise, mice overexpressing AC1 in the forebrain also showed improved contextual memory—in accordance with its role in memory formation—however over expression of AC1 has also impaired spatial memory in elderly mice (Garelick et al., 2009; Wang et al., 2004). In addition, mice overexpressing AC1 were also

hyperactive and displayed reduced sociability (Chen et al., 2015). Studies with double-knockout mice of AC1 and AC8 have also associated both of these AC isoforms with opioid withdrawal and hyperlocomotion produced by morphine (DiRocco et al., 2009; Li et al., 2006; Zachariou et al., 2008). Single-knockout mice of AC1 and AC8 have also revealed specific functions for each AC isoform (Sadana and Dessauer, 2009). For instance, AC1-deficient mice displayed reduced responses to chronic and inflammatory pain (Vadakkan et al., 2006), advocating for selective AC1 inhibitors as non-opioid based strategies for chronic pain management (Skyba et al., 2004; Watts, 2018). Likewise, AC1-knockout mice showed reduced excitotoxicity to overactivation of the NMDA and AMPA receptors (Wang et al., 2007; Watts, 2007). In contrast, AC8-knockout mice failed to exhibit stress-induced anxiety-like behaviors, so this AC isoform has emerged as a potential target to treat mood disorders (Bernabucci and Zhuo, 2016).

In the case of AC3, its high expression in the olfactory epithelium and olfactory sensory neurons was the first indication of its role in olfaction (Bakalyar and Reed, 1990; Bishop et al., 2007). AC3-deficient mice were unable to detect odorants and pheromones, and social, learning, and sexual behaviors dependent on olfactory signals were also significantly altered (Cao et al., 2016; Wang et al., 2006; Wang and Storm, 2011; Wong et al., 2000). In addition, AC3-knockout mice became obese, exhibited diminished short-term memory for novel objects and were unable to show extinction of contextual fear (Wang et al., 2009; Wang et al., 2011b). Most recently, the identification of polymorphisms within the ADCY3 (AC3) gene that cause weight gain or weight loss have provided converging evidence that implicates loss of AC3 activity with the development of obesity and type 2 diabetes (Grarup et al., 2018; Pitman et al., 2014; Saeed et al., 2018). For example, loss-of-function mutations in the ADCY3 gene have been associated with severe cases of obesity in humans (Grarup et al., 2018; Saeed et al., 2018). Likewise, the characterization of a

mouse strain that remains unaffected during high-fat diet consumption because of a single gain-of-function mutation in the ADCY3 gene, also supports the role of AC3 activity in the mechanisms of body weight regulation (Pitman et al., 2014), and suggests that AC3 activators could be used in antiobesity therapies.

1.5.2 Group II: Adenylyl cyclases 2, 4 and 7

For the Gβγ-mediated cyclases, AC2 and AC4, there is no data available for knockout mice or overexpression studies that link these two cyclases to a specific physiological condition (Sadana and Dessauer, 2009). However, their high expression in airway smooth muscle cells may suggest their involvement in pulmonary function (Bogard et al., 2012; Bogard et al., 2011). Only a single study in a cellular model of Lesch-Nyhan syndrome, rat B103 neuroblastoma, has provided evidence that implicates the disease with diminished AC2 activity (Kinast et al., 2012). In contrast, the direct regulation of AC7 catalytic domains by ethanol (Yoshimura et al., 2006; Yoshimura and Tabakoff, 1995), and behavioral studies with female mice that exhibited reduced AC7-expression and consumed large volumes of ethanol, suggest that AC7 is linked to alcohol consumption (Desrivieres et al., 2011). In addition, AC7 plays a critical role in the immune system given its high expression levels in leukocytes, and its importance to increase cAMP levels in response to pathogens and microbes in B and T cells (Duan et al., 2010).

1.5.3 Group III: Adenylyl cyclases 5 and 6

AC5 and AC6 are the most abundant AC isoforms expressed in the heart that play a critical role in cardiac function (reviewed by Baldwin and Dessauer, 2018) . Despite these two cyclases are closely related, AC5 and AC6 knockout mice showed different phenotypic changes in the heart, implying specific roles of each isoform (Sadana and Dessauer, 2009; Vatner et al., 2013).

AC5-knockout mice exhibited diminished responses to β-AR stimulation in the left ventricle (Tang et al., 2006) , and decreased inhibition of cAMP production in response to $G\alpha_i$-coupled muscarinic receptors and Ca^{2+} (Okumura et al., 2003). Instead, cardiomyocytes from AC6-deficient mice displayed reduced responsiveness to β-AR activation (Tang et al., 2008), but overexpression of AC6 increased contractility of the cardiac muscle after persistent β_2AR activation (Roth et al., 1999; Tang et al., 2011; Tang et al., 2013; Wu et al., 2017). The beneficial effects of AC6 overexpression appear not to be cAMP-dependent given that inactive catalytic domains exerted the same effects as active C1 and C2 domains (Gao et al., 2011). Consequently, overexpression of AC6 catalytic domains has been evaluated as a cardioprotective gene therapy strategy to improve cardiac function (Gao et al., 2016; Hammond et al., 2016).

AC5-deficient mice also displayed increased life-span compared to wild-type subjects and prevented the development of age-related cardiac myopathy (Chester and Watts, 2007; Vatner et al., 2015; Vatner et al., 2009; Yan et al., 2007). Loss of AC5 had also additional metabolic benefits such as decreased body weight under regular and high-fat diets (Ho et al., 2015), and abolished the locomotive, addictive and analgesic effects of opioid receptor agonists (Kim et al., 2006). Also, AC5 activity appears to be important for acute pain sensation in response to thermal and mechanical stimuli (Kim et al., 2007). However, deletion of AC5 also resulted in increased alcohol intake (Kim et al., 2011) and caused movement impairment syndromes such as bradykinesias (Iwamoto et al., 2003). Furthermore, in agreement with the role of AC5 in motor functions, ADCY5 polymorphisms within the catalytic domains of the cyclase have also been linked to the autosomal-dominant movement disorder, familial dyskinesia with facial myokymia (FDFM) (Chen et al., 2012). Besides the cardioprotective roles of AC6, this isoform is highly expressed in the kidneys and based on studies with AC6-deficient mice, it plays a major role in water

homeostasis (reabsorption) and renin secretion (Aldehni et al., 2011; Chien et al., 2010), and it also mediates the development of renal cysts (Rees et al., 2014).

1.5.4 Group IV: Adenylyl cyclase 9

Initial attempts to generate an AC9-knockout mouse strain suggested that an AC9-deficient phenotype was embryonic lethal, so the reports that have associated AC9 with the immune system and myelogenous leukemia have been based on microRNA-mediated downregulation of AC9 expression (Huang et al., 2009; Risoe et al., 2011; Zhuang et al., 2014). However, an AC9-deficient mice was recently developed by disrupting AC9 expression using a gene-trap mutagenesis strategy (Li et al., 2017). The changes in phenotype associated with the loss of AC9 indicated that this forskolin-insensitive isoform is involved in cardiac function (Li et al., 2017). Indeed, the protein-protein interactions between AC9 and the AKAP protein, Yotiao, or the heat shock protein 20 (Hsp20) appear to mediate the cardioprotective role of AC9 (Baldwin and Dessauer, 2018; Li et al., 2012).

Table 1.3 summarizes the major pathophysiological conditions associated with the individual AC isoforms. A comprehensive understanding of the physiological roles of certain isoforms is still elusive due to various challenges when studying adenylyl cyclases. As summarized in **Table 1.2**, cells and tissues express more than one AC isoform, and some isoforms only respond to general activators of adenylyl cyclase activity, making it difficult to tease out the contribution of each specific AC. Likewise, the lack of good antibodies to accurately detect AC isoform protein expression or the scarcity of selective AC modulators (Brand et al., 2013), also pharmacologically limits the ability to study ACs at the molecular level.

Table 1.3 *Classification and major pathophysiological conditions associated with AC isoforms.*

	AC Isoforms	Regulatory properties	Pathophysiological condition
GROUP 1	AC1 AC3* AC8	Ca^{+2}/Calmodulin regulated	**AC1:** Chronic pain and opioid withdrawal **AC3:** Obesity **AC8:** Stress-induced anxiety
GROUP 2	AC2 AC4 AC7	Conditionally stimulated by Gβγ subunits	**AC2:** Lesch-Nyhan syndrome **AC7:** Alcohol consumption
GROUP 3	AC5 AC6	Inhibited by sub-micromolar [Ca^{+2}]	**AC5:** Pain, addiction and movement disorders **AC6:** Congestive heart failure (CHF) and renal dysfunction
GROUP 4	AC9	Insensitive to the diterpene FSK	**AC9:** Immune responses and cardiac function

Nonetheless, the existing reports with knockout mice and overexpressing animal models have encouraged screening campaigns to develop selective AC modulators as new therapeutics for various diseases (Brust et al., 2017; Conley et al., 2013; Pierre et al., 2009; Wang et al., 2011a).

1.6 Scope of the work

The objective of the work reported here was to develop a series of tools to characterize isoform-specific AC responses. In order to do so, three aims were achieved:

AIM #1: CRISPR/Cas9-based cell line (HEK-ACΔ3/6) CHAPTER 2

Develop a HEK293 cell line with low cAMP levels through the use of CRISPR/Cas9 technology

Functional characterization of the cAMP responses of the nine membrane-bound ACs to forskolin, G protein-coupled receptors, Ca^{2+} and protein kinase C in the HEK-ACΔ3/6 cells. Comparison of the cAMP responses of AC1wt and AC1 mutant construct in the parental HEK293 cells and the knockout cell line.

AIM #2: CD8-C2-20 minigene CHAPTER 3

Determine whether juxtamembrane domains of adenylyl cyclase type 2 (AC2) could modulate Gβγ activity

The binding affinity for Gβγ was determined for a peptide derived from the C2a domain of AC2 using SPR. A minigene was subsequently utilized to evaluate the biological activity of the C2a domain on Gβγ-mediated pathways.

Carry out structure activity relationship studies for inhibitors of type 1 and type 8 adenylyl cyclases

A series of structure activity relationship (SAR) studies were carried out for a set of analogs of the selective AC1 inhibitor, ST034307, and completion of a high-throughput screen of 10,000 compounds yielded two promising scaffolds that exhibit AC1 selective and dual AC1/AC8 activity.

CHAPTER 2. A NOVEL CRISPR/CAS9-BASED CELLULAR MODEL TO EXPLORE ADENYLYL CYCLASE AND CYCLIC AMP SIGNALING

Functional characterization of adenylyl cyclase isoforms has proven to be challenging in mammalian cells due to the endogenous expression of multiple AC isoforms, and the high background cAMP levels induced by non-selective AC activators. To simplify the characterization of individual mAC isoforms, we generated a HEK293 cell line with low cAMP levels by knocking out two highly expressed ACs, AC3 and AC6, using the clustered regularly interspaced short palindromic repeats (CRISPR)-associated system (Cas) technology. Stable HEK293 cell lines were generated lacking either AC6 (HEK-ACΔ6) or both AC3 and AC6 (HEK-ACΔ3/6). Knock out was confirmed genetically and by comparing cAMP responses of the knockout cells to the parental cell line. HEK-ACΔ6 and HEK-ACΔ3/6 cells revealed an 85% and 95% reduction in the forskolin-stimulated cAMP response. Forskolin- and $G\alpha_s$-coupled receptor-induced activation was examined for the nine recombinant mAC isoforms in the HEK-ACΔ3/6 cells. Forskolin-mediated cAMP accumulation for AC1-6 and AC8 revealed 10- to 250-fold increases over the basal cAMP levels.. All nine mAC isoforms, except for AC8, also exhibited significantly higher cAMP levels than the control cells following β_2-adrenergic receptor (β_2AR) and prostaglandin EP_2 receptor (EP_2R) activation. Isoform specific AC regulation by Gαi-coupled receptors, protein kinases and Ca^{2+}/calmodulin was also recapitulated in the knockout cells. In addition, the HEK-ACΔ3/6 cells allowed the characterization of the cAMP responses of novel AC1 constructs containing mutations within the forskolin binding site. We have developed a HEK293 cell line deficient of endogenous AC3 and AC6 with low cAMP background levels for future studies of cAMP signaling, AC isoform regulation, and high throughput screening assays for AC modulators.Introduction

Adenylyl cyclases are key transduction mediators of G-protein coupled receptor signaling by catalyzing the conversion of ATP into the secondary messenger, cyclic AMP. Nine mammalian mACs (AC1-AC9) have been cloned and one soluble mammalian AC has also been characterized. Although mAC isoforms exhibit high structural homology, they are differentially regulated by G-proteins subunits, Ca^{2+}/Calmodulin and protein kinases; and depending on these regulatory properties, mACs are classified into four groups (reviewed in Dessauer et al., 2017). Group 1, comprising AC1, AC3 and AC8 is characterized for being activated by Ca^{2+}/Calmodulin. Group 2, which includes AC2, AC4 and AC7, is described to be conditionally stimulated by Gβγ subunits. AC5 and AC6 belong to Group 3 and both are inhibited by Ca^{2+}. Lastly, AC9, the only mAC that is insensitive to the diterpene forskolin, is the sole member of Group 4. This differential regulation of mAC isoforms, coupled with their tissue-specific expression patterns, correlates with knockout and overexpression studies that have implicated particular mACs with various physiological processes (Sadana and Dessauer, 2009). Consequently, adenylyl cyclase signaling dysfunction has emerged as a potential therapeutic target, and considerable efforts have been made to identify potent and selective AC modulators (Dessauer et al., 2017; Pierre et al., 2009; Seifert et al., 2012).

Overexpression of mAC isoforms in various cellular models such as HEK293, COS-7, and CHO cells has allowed *in vitro* and *in vivo* characterization of AC activity (Brust et al., 2017; Mann et al., 2009). However, mammalian cells usually express multiple AC isoforms, resulting in high background cAMP responses arising from these endogenous ACs. Therefore, cautious interpretation is required when evaluating $G\alpha_s$-coupled receptor- and forskolin-mediated stimulation of individual mAC isoforms in these heterologous systems. Other approaches to examine mAC activity have also utilized the Sf9 cell line from *Spodoptera frugiperda* which has been widely used to study membrane-bound proteins. This insect cell line expresses recombinant

proteins in high yields, exhibits low cAMP levels, and the recombinant proteins expressed undergo similar folding and post-translational modifications to those observed in mammalian cellular systems (Schneider and Seifert, 2010). *In vitro* studies to assess AC activity for all nine membrane isoforms and to characterize mAC inhibitors' activity and selectivity, have been successfully performed in Sf9 cells (Brand et al., 2013; Pinto et al., 2008). However, Sf9 cells also express an endogenous AC that is stimulated by forskolin and can be inhibited by P-site AC inhibitors (Gille et al., 2004; Pinto et al., 2008). In addition, possible disadvantages of using these insect cells is the difficulty of monitoring in real-time the spatiotemporal dynamics of the cAMP pathway, and the potential lack of expression of key upstream regulators or downstream effectors of AC isoforms.

In an effort to facilitate the selective characterization of AC isoforms' activity and regulation, it was the objective of this study to generate an isolated mammalian cell model with low cAMP production at drug-stimulated conditions. To do so, the CRISPR-Cas 9 technology was employed to knockout, in HEK293 cells, two abundant endogenous ACs (AC3 and AC6) **(Fig. 2.1)**. Our HEK-ACΔ3/6 cell line showed little to no response to forskolin and $G\alpha_s$-coupled receptor agonists and demonstrated to be a suitable cellular model to evaluate the individual responses of the nine mammalian mAC isoforms to forskolin, G-protein coupled receptors, and other regulators such as calcium and protein kinases. The HEK-ACΔ3/6 cells were also used to stably express representative AC isoforms for membrane-based in vitro assays. Lastly, this new cellular model proved to be a valuable tool to functionally characterize the activity profiles of a series of AC1 forskolin-binding site mutants that were difficult to interpret in the parental HEK293 cells due to the high cAMP background.

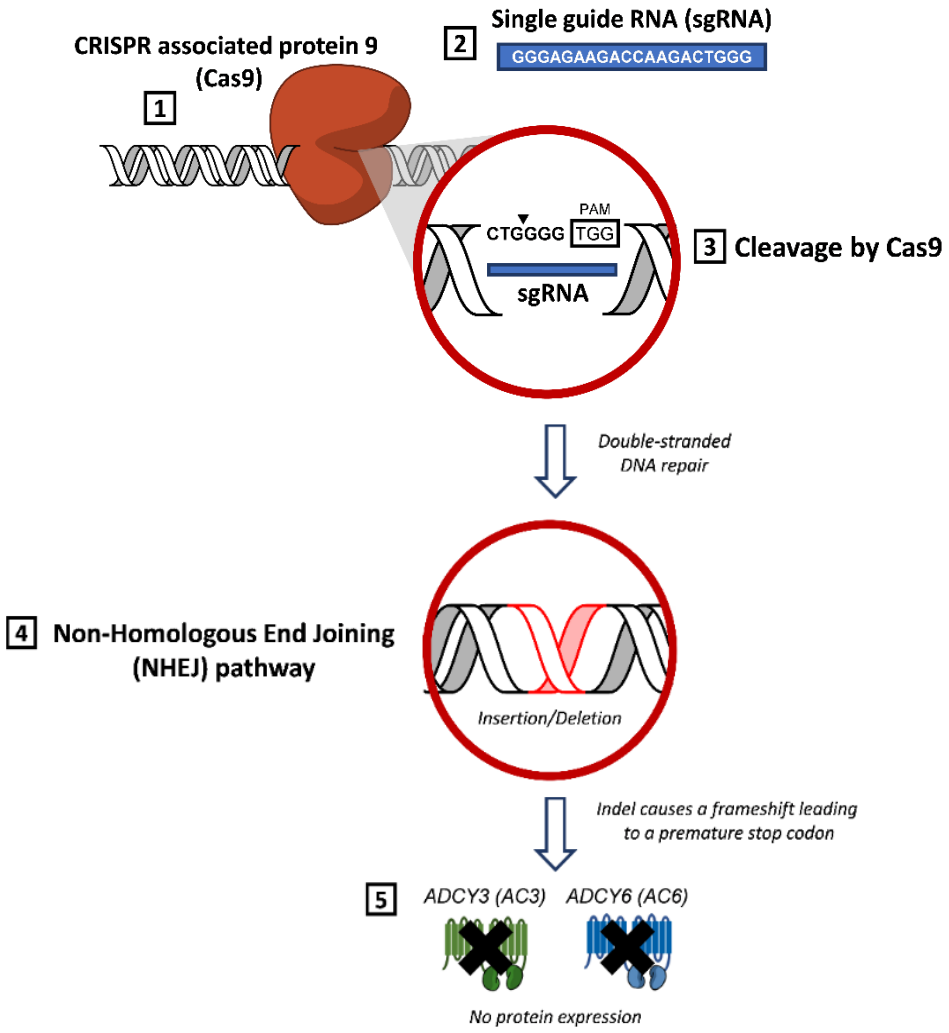

Figure 2.1 *Schematic diagram of the CRISPR/Cas9 genome editing technology.*

The CRISPR-Cas9 technology was engineered from the bacterial immune system to cut the DNA at a desired location (Ran et al., 2013). The CRISPR-Cas9 endonuclease **(1)** recognizes the targeted location within the genome based on the 20-nucleotide sequence of the single guide RNA (sgRNA) **(2)**. CRISPR-Cas9 cleaves the DNA (triangle) between a Protospacer Adjacent Motif (PAM) sequence and the complimentary sequence to the sgRNA **(3)**. The double-strand DNA break (DSDB) event triggers a repair mechanism at the cleavage site that directly ligates the blunt ends of the DNA, but due to the lack of a DNA template, generally leads to the insertion/deletion of base pairs **(4)**. The introduction of these indels at the repair site cause a frameshift mutation that prompts a premature stop codon and subsequently causes loss of protein expression **(5)**.

2.2 Methods

2.2.1 Materials

The sgRNA oligos and primers for plasmid construction were synthesized by Integrated DNA Technologies (IDT) (Coralville, IA). Dulbecco's modified Eagle's medium (DMEM), penicillin-streptomycin-amphotericin B solution (Antibiotic-Antimycotic), cell dissociation buffer, phosphate-buffered saline (PBS), and OptiMEM were purchased from Life Technologies (Carlsbad, CA). The HEK293 cell line was obtained from ATCC (Manassas, VA). Bovine Calf serum (BCS), Fetal Clone I (FCI), and HEPES were obtained from Hyclone (GE Healthcare, Pittsburgh, PA). Lipofectamine 2000 was purchased from Invitrogen (Carlsbad, CA), and XtremeGENE HP was obtained from Roche (Basel, Switzerland). A23187, adenosine 5′ -triphosphate (ATP) disodium salt hydrate, bovine serum albumin (BSA), 3-isobutyl-1-methylxanthine (IBMX), (−)-Isoproterenol (+)-bitartrate salt, magnesium chloride ($MgCl_2$) anhydrous, puromycin, and Tween 20 were purchased from Sigma-Aldrich (St. Louis, MO). The Pierce BCA protein assay kit was obtained from Thermo Fisher Scientific (Waltham, MA), and forskolin, phorbol 12-myristate 13-acetate (PMA), and prostaglandin E2 (PGE-2) from Tocris (Bio-Techne, Minneapolis, MN). The 384-well white opaque plates (Catalog# 6007680) were from PerkinElmer (Waltham, MA), and the cAMP detection reagents, HTRF cAMP Dynamic 2, were obtained from Cisbio (Bedford, MA). The QuickExtract DNA extraction solution was purchased from Epicentre Biotechnologies (Illumina, Madison, WI), and the BbsI restriction enzyme and Phusion High-Fidelity DNA polymerase were from New England Biolabs (Ipswich, MA).

2.2.2 Plasmids

The CRISPR/Cas9 vector, pSpCas9(BB)-2A-Puro (PX459) was a gift from Feng Zhang (Addgene plasmid # 62988). The plasmids encoding for human AC1, AC3, AC4 and AC7 genes were synthesized, codon optimized for mammalian expression, and cloned into a pcDNA3.1+ expression vector by Genscript Biotech (Piscataway, NJ). The pcDNA3.1+/hAC5, pcDNA3.1+/hAC9, and pQE60/Gα_s-His vectors were a gift from Carmen Dessauer. The pReceiver/hAC8 vector was purchased from GeneCopoeia (Rockville, MD), and the pcDNA3.1+/hAC2 plasmid was obtained from Genscript. The corresponding DNA mutations of the mutant AC1 constructs (pcDNA3.1+/AC1-W419A, pcDNA3.1+/AC1-V423G, pcDNA3.1+/AC1-N878A, and pcDNA3.1+/AC1-S924P) were incorporated into the pcDNA3.1+/hAC1 plasmid by Genscript. All the adenylyl cyclase genes encoded for untagged proteins.

2.2.3 Design and construction of CRISPR-Cas9 plasmids

Two abundant ACs in HEK293 cells are AC3 and AC6 encoded by the ADCY3 and ADCY6 genes respectively. To generate the HEK-ACΔ6 and HEK-ACΔ3/6 knockout cell lines we utilized the CRISPR/Cas9 system developed by the Zhang lab in which the pSpCas9(BB)-2A-Puro (PX459) vector coexpresses the single guide RNA(sgRNA), the human-codon optimized Cas9 nuclease, and a puromycin resistance gene (Ran et al., 2013). The specific sgRNAs for each gene were selected from the CRISPR/Cas9 screening library designed by *Wang. et al.*, and these targeting sequences for the ADCY3 and ADCY6 genes were:
5’ GGGAGAAGACCAAGACTGGG 3’ and 5’ TGGGTGGCTCTGCATCCCGG 3’, respectively (Wang et al., 2014). To insert the customized sgRNAs into the PX459 vector, two oligos per sgRNA (*ADCY3:* 5’-CACC-G*GGGAGAAGACCAAGACTGGGG*-3’ and

5’-AAAC-C*CCCAGTCTTGGTCTTCTCCC*-3’, *ADCY6*: 5’-CACC-G*TGGGTGGCTCTGCATCCCGG*-3’ and 5’-AAAC-*CCGGGATGCAGAGCCACCCA*C-3’) were synthesized by IDT, annealed according to the protocol by *Ran et al.*, and cloned into the BbsI site of the PX459 backbone vector. Correct insertion to the sgRNAs was confirmed by Sanger sequencing.

2.2.4 Stable knockout cell lines generation and validation

HEK293 cells were transfected with either the sgRNA for AC6 (HEK-ACΔ6) or both AC3 and AC6 sgRNAs (HEK-ACΔ3/6) using Lipofectamine 2000. After 24-hour transfection, the media was replaced with puromycin (2mg/mL) containing media to select for sgRNA- and Cas9-expressing cells. Transfected cells were then seeded sparsely into 10cm-dishes after they had been exposed to puromycin for 72-hours, and cell colonies were allowed to form for 2-3 weeks in regular HEK293 media consisting of DMEM supplemented with 5% bovine calf serum (BCS), 5% fetal clone I (FCI) and 1% Penicillin-Streptomycin-Amphotericin B Solution. HEK-ACΔ6 and HEK-ACΔ3/6 cell clones were screened for loss of function of AC3 and AC6 genetically, and by comparing cAMP responses between the knockout cells and the parental HEK293 cell line. For genotypic characterization of the clones, genomic DNA was extracted from the HEK-ACΔ6 and HEK-ACΔ3/6 clones with QuickExtract DNA extraction solution according to the manufacturer’s instructions. A portion of the ADCY3 and ADCY6 genes around the sgRNA site was amplified by polymerase chain reaction (PCR) from the genomic DNA with the following AC3 and AC6 set of primers (*ADCY3:* 5’-GTTAAAGCCCGTCTAGTATTG-3’ and 5’-CATCAGTCGACCACACGTCG-3’, *ADCY6*: 5’-ATGTCATGGTTTAGTGGCCTCC-3’ and 5’-CGTGTAGGCGATGTAGACAA-3’). The PCR conditions were as follows: after initial denaturation at 98 °C for 30 seconds, 30 cycles were performed of denaturation at 98 °C for

10 seconds, annealing at 52 °C for 30 seconds and extension at 72 °C for 30 seconds followed by a final extension at 72°C for 10 minutes. The PCR products were analyzed by agarose gel electrophoresis and by Sanger sequencing. The resulting gene mutation for the isolated HEK-ACΔ6 cell line was a single base pair insertion in both alleles of the ADCY6 gene that caused a frame shift and subsequent disruption of ADCY6 protein expression (**Fig.S1b**). For the isolated HEK-ACΔ3/6 cell line, ADCY3 expression was disrupted by a single base pair deletion for one allele and two-base pair insertion for the other allele, whereas loss of function of ADCY6 was a result of a single base pair deletion in both alleles of the gene (**Fig. S1c**). Phenotypic changes in the HEK-ACΔ6 and HEK-ACΔ3/6 cell lines were assessed by comparing the forskolin- and $G\alpha_s$-coupled receptor-stimulated cAMP responses in the knockout cells and the parental HEK293 cell line.

2.2.5 cAMP assays in cells

Parental HEK293, HEK-Δ6, and HEK-ACΔ3/6 cells were washed with PBS, dissociated from the culture plate with cell dissociation buffer, and centrifuged twice at 150 x g for 5 minutes. The cell pellet was resuspended in Opti-MEM, and cells were counted and seeded in a white opaque 384-well plate at a cell density of 15,000 cells per well for the functional characterization of the knockout cells, and 10,000 cells per well for the experiments with the transient transfected HEK-ACΔ3/6 cells. Cells were incubated for 2 hours at 37°C with 5% CO_2 before drug-treatment to ensure cells had adhered to the plate.

2.2.5.1 Stimulation assays

HEK293, HEK-ACΔ6, HEK-ACΔ3/6 or transiently transfected HEK-ACΔ3/6 cells were treated with forskolin for 1-hour, the EP_2R agonist, PGE-2 for 15 minutes or the β_2AR agonist, isoproterenol, for 5 minutes. For Ca^{2+}- and protein kinase C-mediated AC activation, and the

synergistic experiments, cells were stimulated for 1-hour with 40 μM (4x) A23187 or 4 μM (4x) PMA in the absence or presence of 40 μM (4x) PGE-2 or 200 μM (4x) forskolin respectively. AC activity was triggered in HEK293 and HEK-ACΔ3/6 cells transiently expressing wild-type AC1 (AC1-WT) or mutant AC1 (AC1-W419A, AC1-V423G, AC1-N878A and AC1-S924P) cells with increasing concentrations of forskolin in the presence or absence of 12μM (4x) A23187 for a period of 1-hour. All the drug-treatments were performed in the presence of the phosphodiesterase inhibitor, IBMX. Intracellular cAMP levels were detected after each corresponding incubation period using the Cisbio HTRF cAMP detection kit as described below.

2.2.5.2 Acute Inhibition assay ($G\alpha_i$-coupled receptors)

Transfected HEK-ACΔ3/6 cells transiently expressing D2R and mACs were treated with vehicle or 12μM (4x) quinpirole followed by the addition of the corresponding stimulant for each transfection condition in the presence of IBMX. Cyclic AMP was stimulated in Venus-, AC3-, and AC5-transfected cells with forskolin, and AC1- and AC8-expressing cells were stimulated with A23187. AC2-expressing cells were stimulated with PMA and cells expressing AC4 were treated PGE-2. After 1-hour incubation with quinpirole and the corresponding stimulant, for all AC conditions except AC4-expressing cells that were drug-treated for only 15 minutes, cAMP levels were detected using the Cisbio HTRF cAMP detection reagents as described below.

2.2.5.3 Sensitization assay

Same transiently transfected cells used for the acute inhibition assays were incubated for 2-hours with 9μM (3x) quinpirole at 37°C with 5% CO2 prior stimulation of AC activity. Venus-, AC3- and AC5-expressing cells were treated with forskolin to trigger AC activity, AC1- and AC8-expressing cells were stimulated with A23187, and AC4 activity was induced with PGE-2.

All drug-treatments were performed in the presence of IBMX and the D2R antagonist, spiperone. After a period of incubation of 1-hour with the AC stimulants, except for AC4-expressing cells that were incubated with PGE-2 for 15 minutes; cAMP levels were detected as described below.

2.2.5.4 cAMP Detection

Cisbio HTRF cAMP detection reagents, d2-labeled cAMP and anti-cAMP cryptate, were added to all wells after the corresponding incubation times for the treatment conditions, and time-resolved fluorescence was measured at dual emission wavelengths (620nm and 665nm) after 1-hour incubation at room temperature. Cyclic AMP accumulation per well was calculated using GraphPad Prism by interpolating the 620/665 signal ratios from a cAMP standard curve ran in parallel with every experiment.

2.2.6 ACs transient transfections

HEK293 or HEK-ACΔ3/6 cells were plated overnight prior transfection in a 12-well plate. The cells were then transiently transfected with Lipofectamine 2000 in a 1:2 (DNA:Lipofectamine) ratio or with XtremeGENE HP in a 1:1.5 or a 1:3 (DNA:XtremeGENE HP) ratio according to the manufacturer's protocol. Lipofectamine 2000 was used to transfect Venus, AC1-AC6, AC8, and mutant AC1 constructs for the forskolin, A23187, and protein kinase C experiments. For the acute and sensitization experiments, Lipofectamine 2000 was also used to cotransfect the Dopamine D2 receptor (D2R) and the corresponding mAC isoform into the HEK-ACΔ3/6 cells in a 1:2 DNA ratio (receptor:mAC). XtremeGENE HP was used in a 1:1.5 ratio to transfect all mAC isoforms for the calcium- and $G\alpha_s$-mediated AC activation assays, and it was used in a 1:3 ratio to transfect AC7 and AC9 in the forskolin experiments. After transfection, cells were cultured for 40 hours before cAMP responses were measured as described above.

2.2.7 AC1, AC2, AC5 and AC8 stable cell pool generation

HEK-ACΔ3/6 cells were seeded overnight in a 6-well plate to ensure that at the time of transfection, the cells had recovered and had reached 70% confluency. XtremeGENE was used in a 1:3 ratio (DNA:XtremeGENE) to transfect the pcDNA3.1+/hAC1, pcDNA3.1+/hAC2, pcDNA3.1+/hAC5 and pReceiver/hAC8 constructs. Media was replaced after 48-hour transfection to G418 (600ug/mL) or Puromycin (4µg/mL) containing media for the cells transfected with the pcDNA3.1 or the pReceiver expression vectors, respectively. The HEK-ACΔ3/6-AC1-, HEK-ACΔ3/6-AC2, and HEK-ACΔ3/6-AC5 pool cell lines were maintained and proliferated for cell-based and cellular membrane assays in media containing G418 (300ug/mL), and the HEK-ACΔ3/6-AC8 pool cell line was maintained in media containing puromycin (2µg/mL).

2.2.8 Isolation of cellular membranes

HEK-ACΔ3/6, HEK-ACΔ3/6-AC1, HEK-ACΔ3/6-AC2, HEK-ACΔ3/6-AC5, and HEK-ACΔ3/6-AC8 cells were proliferated in 15-cm cell culture dishes to a 90% confluency. Media was decanted and replaced with 10mL of ice cold lysis buffer containing: 1mM HEPES, 2 mM EDTA and 1mM EGTA at pH 7.4. The cell culture dish was incubated for 10 minutes with the lysis buffer on ice, and cells were scraped off using a disposable cell lifter. The cell suspension was transferred to a high-speed centrifuge tube and centrifuged at 30,000 x g for 20 minutes at 4°C. Supernatant was discarded, and the cell pellet was resuspended in binding buffer containing 4 mM $MgCl_2$ and 50 mM Tris at pH 7.4. After the cell suspension was homogenized using a Kinematica homogenizer, it was divided into 1mL-aliquots. Aliquots were centrifuged at 10,000 x g for 10 minutes at 4°C, supernatant was discarded, and membrane pellets were frozen and stored at -80°C until the day of the assay.

2.2.9 $G\alpha_s$ Purification and Activation

Recombinant $G\alpha_s$-His protein was expressed and purified using immobilized metal affinity and ion exchange chromatography as described previously (Lee et al., 1994) and stored at -80°C until it was activated for membrane assays. The purified $G\alpha_s$ protein was activated by incubation on ice in 50 mM HEPES, 2mM DTT, 250 μM GTPγS, and 1mM $MgCl_2$ for 20 minutes, followed by a 30 minute incubation at 30°C (Chen-Goodspeed et al., 2005).

2.2.10 cAMP assays in membranes

Cells membranes were thawed on ice and resuspended in washing buffer containing 2 mM Tris, 1mM EGTA and 1mg/mL of BSA. Membrane suspension was centrifuged at 10,000 x g for 10 minutes at 4°C, supernatant was aspirated, and the washing step was repeated two more times. Following the final wash, the membrane pellet was resuspended in membrane buffer containing 33mM HEPES, 0.1% Tween 20, and 1 mM EGTA. Protein concentration of the membrane suspension was measured using the Pierce BCA Protein assay kit, and the protein concentration was adjusted to 250 μg/mL. Membrane suspensions were plated in a white opaque 384-well plate at 10 μL/well followed by the addition of increasing concentrations of Gαs or forskolin—prepared in membrane buffer without EGTA— and stimulation buffer containing: 33mM HEPES, 0.1% Tween 20, 2.5mM $MgCl_2$, 250 μM ATP and 500 μM IBMX at pH 7.4. Cellular membranes were incubated with the stimulants for 45 minutes at room temperature and cAMP accumulation was measured using the Cisbio HTRF cAMP detection kit as described above.

2.3 Results

2.3.1 CRISPR/Cas9-based HEK-ACΔ6 and HEK-ACΔ3/6 cell lines display remarkably low cAMP levels

HEK293 are a human expression system that is widely used to study recombinant proteins because of their easy maintenance, rapid reproduction, and high transfection efficiency. HEK293 cells express multiple AC isoforms that when stimulated by forskolin and/or endogenous Gαs-coupled receptors promote high levels of cAMP. It has been reported based on qPCR studies, along with our own qPCR results (data not shown), that HEK293 cells express AC1, AC2, AC3, AC5, AC6, AC7 and AC9 mRNA (Atwood et al., 2011; Ludwig and Seuwen, 2002; Yu et al., 2014). Therefore, to decrease cAMP levels in HEK293 cells, we cloned sgRNA sequences that targeted the two abundant endogenous ACs (AC3 and AC6) into a CRISPR/Cas9 expression system. HEK-ACΔ6 and HEK-ACΔ3/6 cell lines were generated lacking either AC6, or both AC3 and AC6, respectively. We characterized the genotype of the knockout cells **(Figure S1)** and determined loss-of-function of the ADCY3(AC3) and ADCY6(AC6) genes by comparing the drug-induced cAMP responses of the knockout cells with the parental cell line. The activity of the endogenous ACs was stimulated by two common mechanisms: direct AC activation with forskolin **(Fig. 2.2a)**, or $G\alpha_s$ subunit-mediated activation elicited by the β_2AR agonist, isoproterenol **(Fig. 2.2b)** or the EP_2R agonist, PGE-2 **(Fig. 2.2c)**. Knocking out the ADCY6 gene in the HEK-ACΔ6 cell line reduced the cAMP response to forskolin by nearly 85%, and by an additional 10% when AC3 expression was also disrupted, resulting in an overall reduction of cAMP accumulation by 95% in the HEK-ACΔ3/6 cells compared to the parental cell line **(Fig. 2.2a)**. Likewise, HEK-ACΔ6 cells exhibited 50% of the maximal response to isoproterenol **(Fig. 2.2b)**, whereas the HEK-ACΔ3/6 cells displayed >75% lower cAMP accumulation than the HEK293 parental cell line.

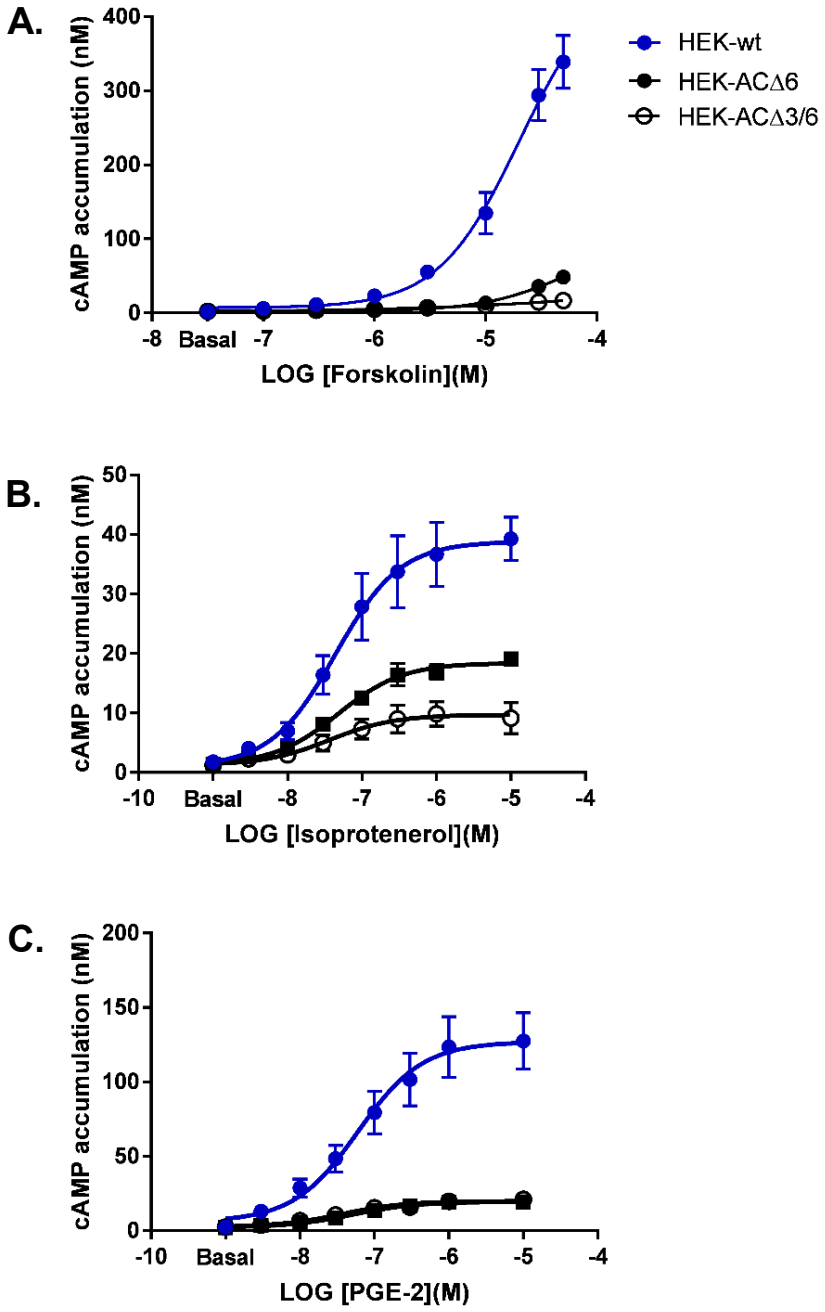

Figure 2.2 *Functional characterization of HEK-ACΔ6 and HEK-ACΔ3/6 cell lines.*

Parental HEK293 cells and the CRISPR-Cas9 based HEK-ACΔ6 and HEK-ACΔ3/6 cells were incubated at room temperature with increasing concentrations of the direct AC activator, forskolin (A), or the $G\alpha_s$-coupled receptors agonists, isoproterenol (B) or PGE-2 (C), and cAMP accumulation was measured. *The HEK-ACΔ6 and HEK-ACΔ3/6 responses to PGE-2 are overlapping in panel (C). Data represents the mean and SEM of at least three independent experiments conducted in duplicate.

In the case of the EP_2R-mediated activation, HEK-ACΔ6 cells showed >85% reduction of the maximal response to PGE-2, but no significant differences in PGE-2-stimulated cAMP levels were noted between the HEK-ACΔ6 and HEK-ACΔ3/6 cells (**Fig. 2.2c**).

2.3.2 Forskolin-mediated responses of the mAC isoforms in the knockout cells

Forskolin directly binds to a hydrophobic pocket at the interface between the AC catalytic domains, and it elicits stimulatory effects on ACs 1 to 8 by promoting a conformational change that facilitates cAMP synthesis (Tesmer et al., 1997). Hence, we employed our CRISPR-Cas9 based cell line to selectively assess forskolin-mediated responses in the nine mAC isoforms. Cyclic AMP levels were evaluated for increasing concentrations of forskolin in the HEK-ACΔ3/6 cell line expressing venus (control) or the or the individual mAC isoforms (**Fig. 2.3**). Forskolin induced cAMP production at a wide range of efficacies in the knockout cells expressing ACs, except for those transfected with AC7 and AC9. These forskolin-mediated responses ranged from 10- to a 250-fold increase over the basal cAMP levels for cells expressing AC1-AC6 and AC8, compared to a 4-fold increase over basal of the Venus-transfected cells. In particular, cells overexpressing AC5 and AC8 displayed the most robust cAMP response to forskolin relative to the other isoforms, and AC9-expressing cells were unresponsive to forskolin as has been previously described (Yan et al., 1998). Lack of selectivity of commercially available mAC antibodies or epitope tags on the constructs used here prevented the assessment of protein expression for a more rigorous comparison of forskolin-mediated cAMP responses across the other AC isoforms. Nonetheless, forskolin is a useful tool to selectively examine the activity of AC isoforms 1-6, and 8 in our HEK-ACΔ3/6 cells, given the increase in the signal window upon forskolin stimulation of AC in these knockout cells.

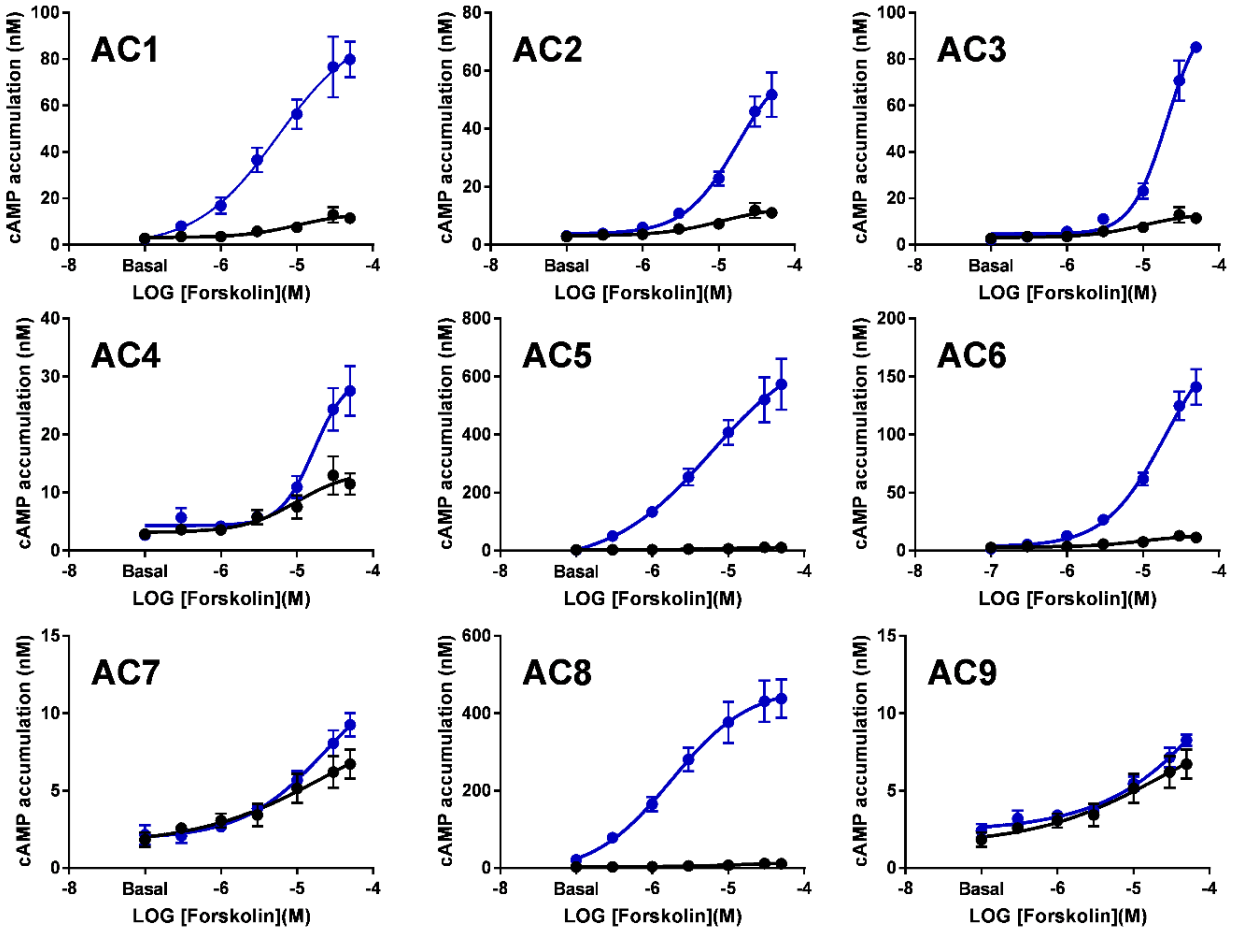

Figure 2.3 *Forskolin-stimulated cAMP responses for the nine mACs in the HEK-ACΔ3/6 cell line.*

HEK-ACΔ3/6 cells were transiently transfected with Venus (black) or the individual mAC isoforms (blue) as indicated. After 40 hours, cAMP accumulation was stimulated with increasing concentrations of forskolin at room temperature. Data represents the mean and SEM of at least three independent experiments conducted in duplicate.

2.3.3 $G\alpha_s$-protein coupled receptor signaling through mACs

Activation of GPCRs linked to $G\alpha_s$ is another major mechanism to activate ACs. Therefore, we evaluated the specific AC isoform responses following activation of the endogenously expressed β_2AR and EP_2R (Andressen et al., 2006; Atwood et al., 2011). HEK-ACΔ3/6 cells transiently transfected with the different mACs were treated with a saturating concentration of isoproterenol **(Fig. 2.4a)** or PGE-2 **(Fig. 2.4b)**. Activation of both $G\alpha_s$ -coupled receptors triggered a significant increase of cAMP levels in all AC isoforms, except for AC8, when compared to the control-transfected cells. AC8-expressing cells displayed high basal and forskolin-mediated activity, but cAMP levels did not increase significantly to $G\alpha_s$ stimulation above the basal response. Surprisingly, cells expressing AC4 showed the highest cAMP response to receptor activation—considering that this isoform was poorly activated by forskolin **(Fig. 2.3)**. Knockout cells transfected with AC7 and AC9 also showed a 2-fold increase over Venus-transfected cells when stimulated by $G\alpha_s$ -coupled receptors. This suggest that both isoforms are being expressed, and the lack of response of these isoforms to forskolin activation may reflect their unique regulatory properties (Hacker et al., 1998; Yan et al., 2001).

2.3.4 Selective regulation of mAC isoforms in the CRISPR/Cas9-based cell line

In addition to activation by forskolin and $G\alpha_s$ -proteins, AC isoforms are selectively activated by Ca^{2+} or protein kinases. Thus, we further explored AC1/AC8 and AC2/AC7 selective activation in the HEK-ACΔ3/6 cells by Ca^{2+} or protein kinase C (PKC), respectively **(Fig. 2.5)**. First, we examined the response of Ca^{2+}/calmodulin-stimulated cyclases, AC1 and AC8, in the HEK-ACΔ3/6 cell line **(Fig. 2.5a)**. An increase in intracellular Ca^{2+} with the calcium ionophore, A23187, elevated cAMP levels over basal in AC1-expressing cells by 5-fold and in AC8-expressing cells by 8-fold,

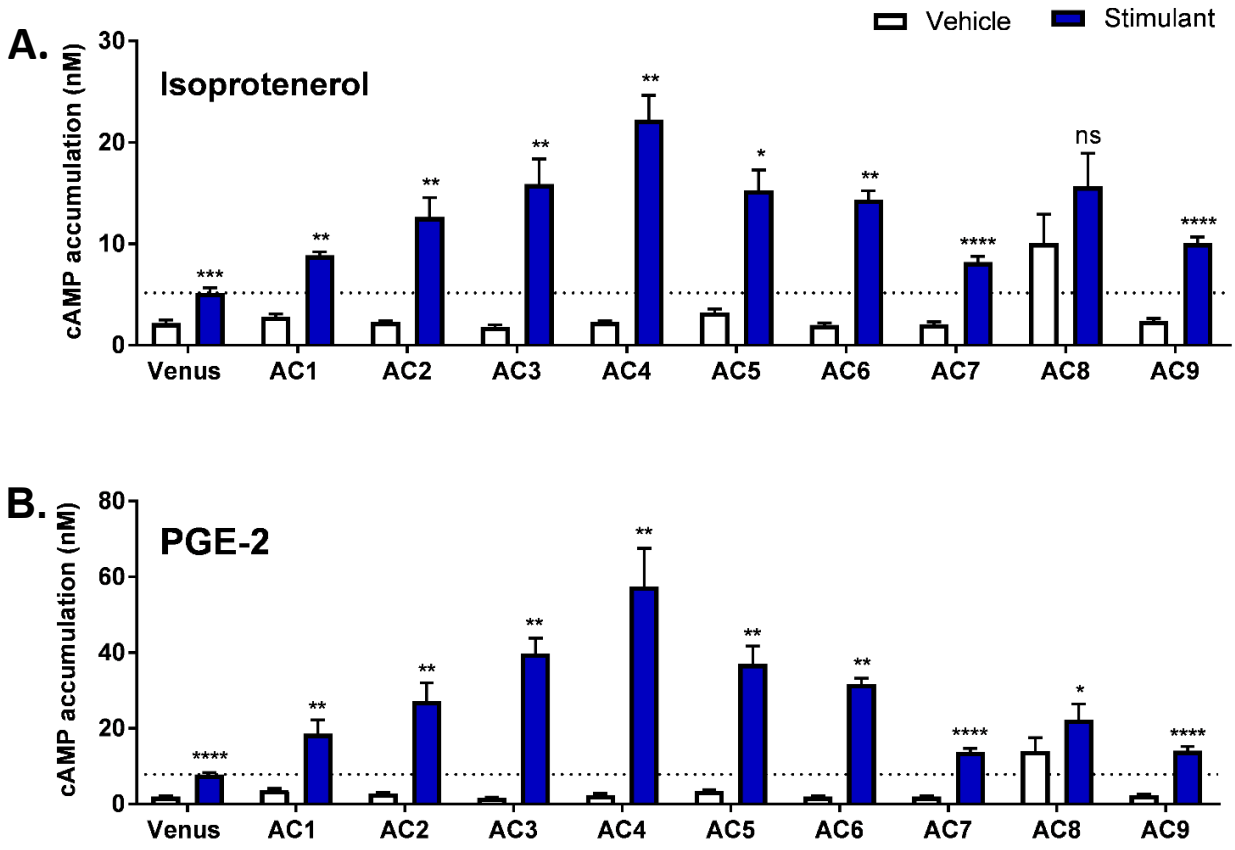

Figure 2.4 *$G\alpha_s$-coupled receptor-mediated activation of the nine mACs in the HEK-ACΔ3/6 cells.*

HEK-ACΔ3/6 cells were transiently transfected with venus or the individual mAC isoforms as indicated. After 40 hours, cAMP accumulation was stimulated with 10 μM isoproterenol **(A)** or 10 μM PGE-2 **(B)**. Data represents the mean and SEM of at least three independent experiments conducted in duplicate. Statistical analysis was performed using paired t-test. *P < 0.05, **P < 0.01, ***P < 0.001, ****P < 0.0001 compared to the cAMP levels of the vehicle-treated cells.

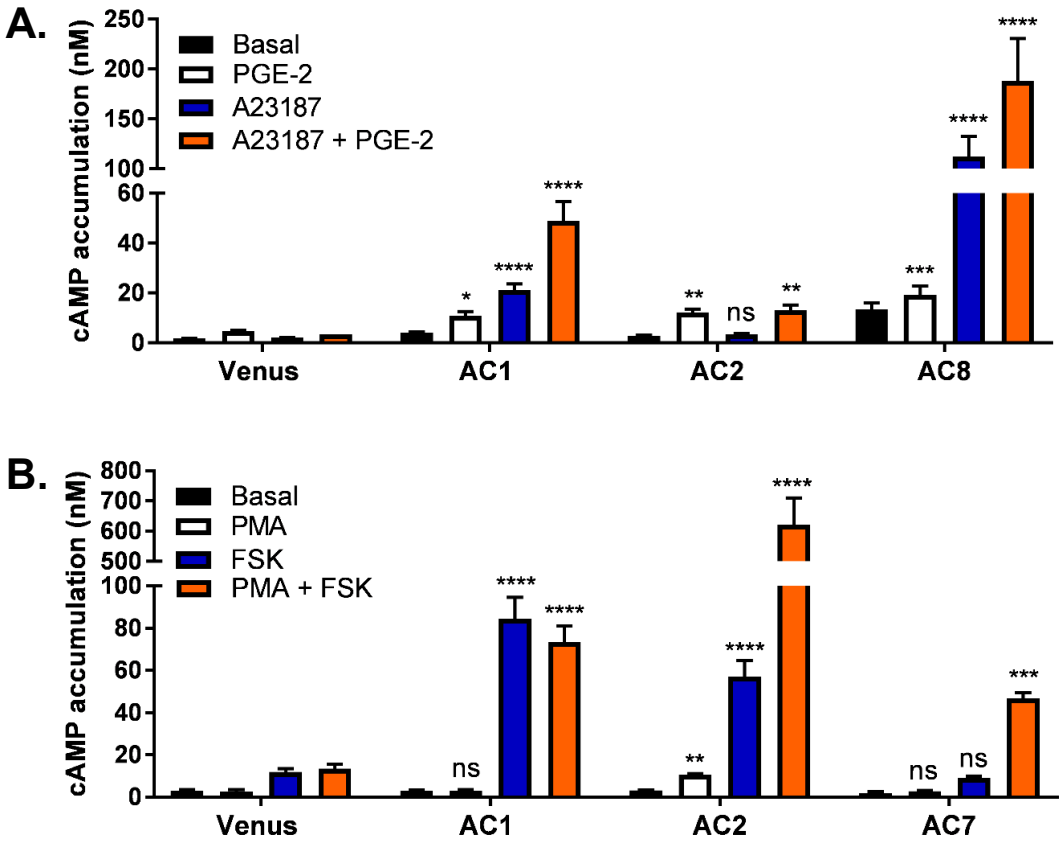

Figure 2.5 *Ca^{2+}/Calmodulin and PKC regulation of AC isoforms in the HEK-ACΔ3/6 cell line.*

(A). HEK-ACΔ3/6 cells were transiently transfected with the venus control plasmid, AC1, AC2, or AC8. Cells were incubated with the 10 μM A23187, 10 μM PGE-2, or a combination of both as indicated, and cAMP accumulation was measured. **(B).** Venus, AC1, AC2 or AC7-transfected HEK-ACΔ3/6 cells were incubated with 1 μM PMA, 50 μM forskolin, or a combination of both as indicated, and cAMP accumulation was measured. Data represents the mean and SEM of at least three independent experiments conducted in duplicate. Statistical analysis was performed using one-way ANOVA followed by a Dunnett's comparison. *P < 0.05, **P < 0.01, ***P < 0.001, ****P < 0.0001 compared AC-transfected cAMP responses to the responses of the Venus-transfected cells for each stimulation condition.

whereas Venus (mock) or AC2 (negative control) transfected cells failed to respond to Ca^{2+} influx. Additionally, we assessed whether Ca^{2+}-induced AC1 and AC8 activation was differentially modulated by simultaneous activation with $G\alpha_s$. Stimulation with A23187 and PGE-2 ($G\alpha_s$) elicited an apparent synergistic effect on HEK-ACΔ3/6 cells expressing AC1, since the cAMP response was greater for the combination of Ca^{2+} and $G\alpha_s$ stimulation than to the additive response to both drugs. AC8-expressing knockout cells showed a minimal response to $G\alpha_s$ that modestly potentiated Ca^{2+}–induced cAMP accumulation.

Protein kinases are another set of important regulators of ACs. Particularly, activation of PKC with the phorbol ester, PMA, directly stimulates AC2 and AC7 activity (Harry et al., 1997; Jacobowitz and Iyengar, 1994). To determine whether AC2 and AC7 expression will give rise to PKC-stimulated cAMP accumulation in the HEK-ACΔ3/6 cells, transiently transfected cells were incubated with PMA **(Fig. 2.5b)**. In the presence of the phorbol ester, AC2-expressing cells showed a 3-fold increase over basal levels. In contrast, cells expressing AC7 (or AC1) showed no significant response to PMA. However, when AC2 and AC7 activity was stimulated with PMA in the presence of forskolin, both isoforms appeared to exhibit a robust synergistic response. In the case of AC7, the PMA and forskolin combination was able to induce a cAMP signal that was significantly higher than control cells, despite a minimal or absent response to forskolin or PMA alone.

2.3.5 Regulation of mACs activity by $G\alpha_i$-coupled receptors

GPCRs, besides stimulating mAC activity via $G\alpha_s$-proteins, can also inhibit cAMP synthesis via activation of the inhibitory G-proteins, $G\alpha_{i/o}$. However, $G\alpha_{i/o}$-mediated inhibition is not a shared regulatory mechanism between all mAC isoforms, and inhibition of mAC activity has

only been documented for AC1, AC3, AC5, AC6 and AC8 (Chen and Iyengar, 1993; Steiner et al., 2005; Taussig et al., 1993a). Hence, to evaluate whether the HEK-ACΔ3/6 cellular model could also be used to characterize negative regulators of mACs, knockout cells were transiently co-transfected with the $G\alpha_{i/o}$-coupled dopamine D2 receptor (D2R) and Venus, AC1, AC2, AC3, AC4, AC5 or AC8. Cyclic AMP responses were examined in HEK-ACΔ3/6 cells in the presence of forskolin (Venus, AC3 and AC5), PMA (AC2), PGE-2 (AC4), or A23187 (AC1 and AC8) in combination with the D2R selective agonist, quinpirole **(Fig. 2.6a)**. Acute activation of the D2R reduced the cAMP responses to the corresponding stimulants of AC1, AC3 and AC5-expressing cells by 56%, 50%, and 84% respectively. No significant differences were observed between the cAMP levels of vehicle and quinpirole-induced responses of HEK-ACΔ3/6 cells expressing AC8. In addition, quinpirole potentiated the response to the corresponding stimulation conditions of AC2- and AC4-expressing cells by 70%. Activation of $G\alpha_i$-coupled receptors have also been implicated in another regulatory mechanism of mAC activity referred to as superactivation or heterologous sensitization. This adaptive cellular response developed after chronic activation of Gαi/o-coupled receptors, causes an enhancement of stimulated mAC activity, contrary to the inhibitory effects observed after acute receptor activation. Although the molecular mechanism underlying heterologous sensitization is not fully understood, it has been established that sensitization is a pertussis toxin(PTX)-sensitive event in which $G\alpha_s$ and $G\beta\gamma$ subunits are actively involved (Brust et al., 2015a). HEK-ACΔ3/6 transiently expressing the D2R receptor and Venus, AC1, AC2, AC3, AC4, AC5 or AC8 were treated for 2-hours with quinpirole followed by the stimulation of AC activity in the presence of the D2R antagonist, spiperone, to assess the isoform specific cAMP responses resulting from the sensitization paradigm **(Fig. 2.6b)**.

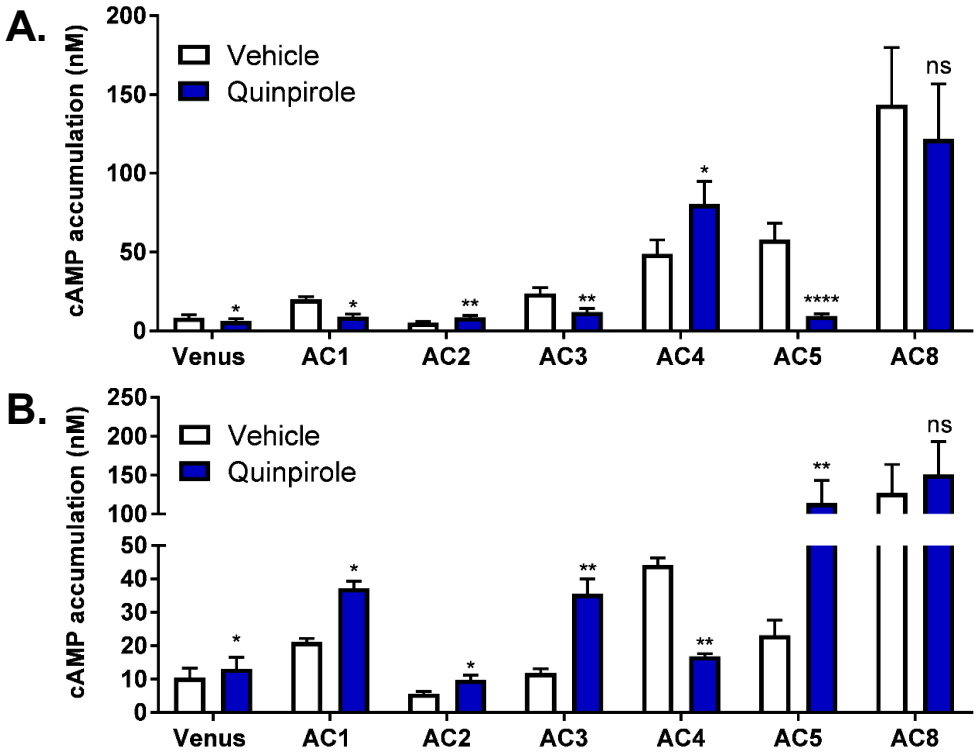

Figure 2.6 *Regulation of AC isoforms after acute and chronic activation of $G\alpha_i$-coupled receptor, D2R, in the HEK-ACΔ3/6 cell line.*

(A). HEK-ACΔ3/6 cells transiently coexpressing the $G\alpha_{i/o}$-coupled D2R, and the Venus control plasmid, AC1, AC2, AC3, AC4, AC5 or AC8 were treated with vehicle or 3 μM quinpirole in combination with an adenylyl cyclase activator. Cyclic AMP accumulation was induced in Venus and AC3-transfected cells with 10 μM forskolin; cells expressing AC2 and AC4 were activated with 1 μM PMA and 10 μM PGE-2, respectively; AC5-expressing cells were stimulated with 300 nM forskolin and cells expressing AC1 and AC8 were activated with 10 μM A23187. All transfection conditions were drug-treated for 1-hour, except for AC4-expressing cells that were treated with quinpirole and PGE-2 for 15 minutes prior cAMP accumulation was measured **(B).** Cotransfected HEK-ACΔ3/6 cells with the D2R and the corresponding AC were incubated with vehicle or 3 μM quinpirole for 2-hours prior to stimulation of AC activity in the presence of 1 μM spiperone to terminate the action of the D2R. Venus- and AC3-transfected cells were stimulated with 10 μM forskolin; AC2-transfected cells were stimulated with 1μM PMA and AC4-expressing cells were stimulated with 10 μM PGE-2; AC5-transfected cells were stimulated with 100 nM forskolin, and AC1- and AC8- transfected cells were stimulated with 3 μM A23187. Cyclic AMP accumulation was measured after the 1-hour incubation with the stimulants, except for AC4-expressing cells that were treated with PGE-2 for 15 minutes. Data represents the mean and SEM of at least three independent experiments conducted in duplicate. Statistical analysis was performed using paired t-test. *P < 0.05, **P < 0.01, ****P < 0.0001 compared to the cAMP levels of vehicle-treated cells.

Chronic activation of the D2R led to an enhancement of the cAMP responses of the AC isoforms, except for AC4 and AC8. PGE-2-mediated AC4 activity was inhibited after chronic activation of the D2R receptor in AC4-expressing HEK-ACΔ3/6 cells, even though the action of the D2R was blocked at the time of PGE-2 stimulation with spiperone (D2R antagonist). The lower response of AC4 also referred as "super inhibition" has been previously reported after chronic $G\alpha_i$-coupled receptor activation (Nevo et al., 1998).

2.3.6 Adenylyl cyclase activity in cellular membranes

In vitro studies of native or overexpressed membrane-bound ACs in cellular membranes of insect or mammalian cells have allowed the study of AC activity in a controlled environment providing valuable information about their pharmacology, regulatory mechanisms, and kinetic properties. Consequently, HEK-ACΔ3/6 pooled cell lines were generated that stably express AC1, AC2, AC5 or AC8 to isolate cellular membranes for *in vitro* studies. Forskolin and Gαs-mediated cAMP accumulation was examined on membrane preparations in the presence of the metal ion cofactor, Mg^{2+}, and the substrate ATP **(Fig. 2.7)**. An increase of catalytic activity with increasing concentrations of forskolin and $G\alpha_s$ was observed on cellular membranes overexpressing mACs, and these cAMP responses were significantly higher than the cAMP levels observed on the isolated membranes from untransfected HEK-ACΔ3/6 cells. Results with the cellular membranes of the HEK-ACΔ3/6 cell lines were in accordance with the cAMP responses observed with the intact cells. For instance, membranes isolated from HEK-ACΔ3/6-AC5 and HEK-ACΔ3/6-AC8 cells exhibited a markedly increased cAMP response to forskolin. The maximal extent of AC activation induced by forskolin or Gαs was similar on the membrane preparations overexpressing AC1, AC5, and AC8. In contrast, Gαs appeared to be more efficacious than forskolin in stimulating AC2.

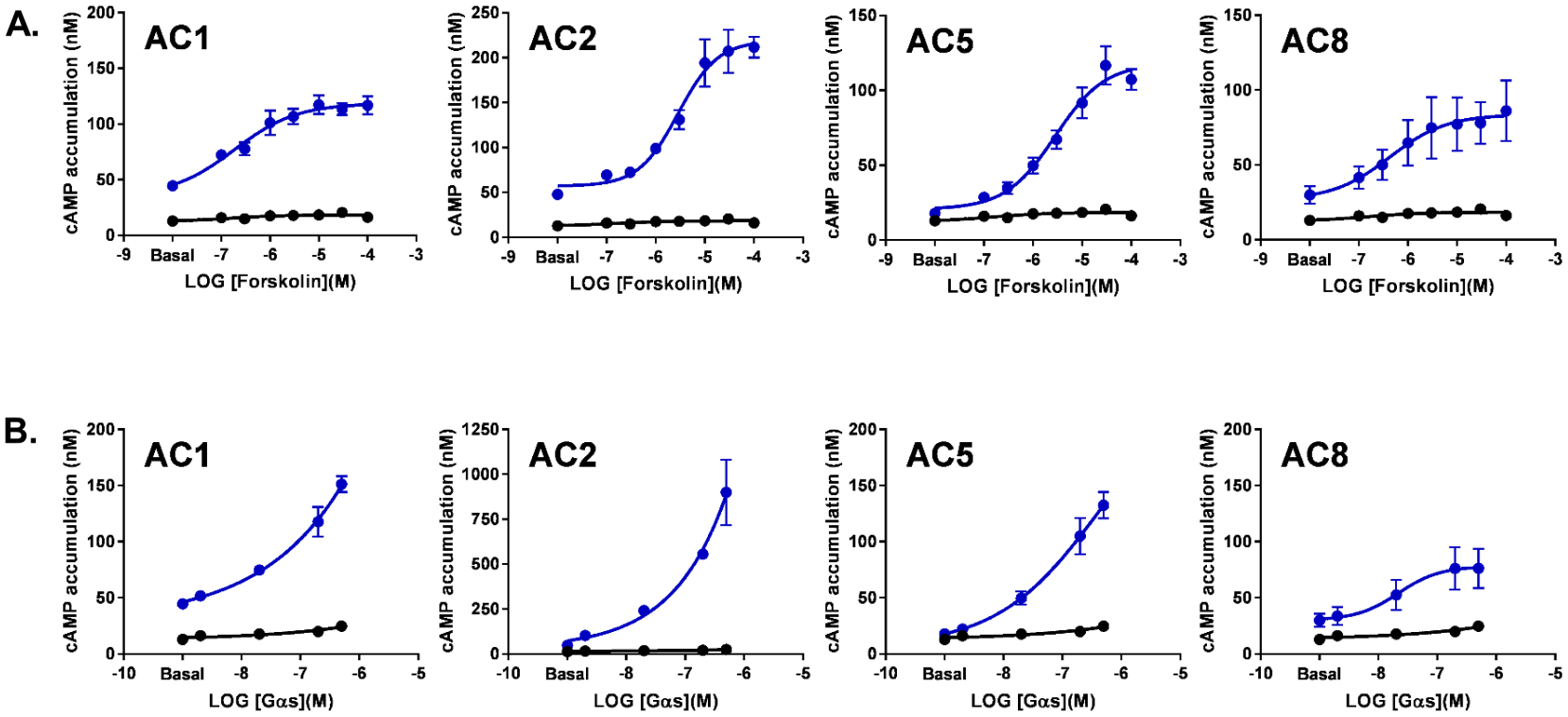

Figure 2.7 *Forskolin and Gα$_s$-induced cAMP responses of isolated membranes from HEK-ACΔ3/6 cells overexpressing mACs.*

Membranes isolated from HEK-ACΔ3/6 cells (black) or HEK-ACΔ3/6 cells stably expressing AC1, AC2, AC5, or AC8 (blue) were stimulated with increasing concentrations of **(A)** forskolin or **(B)** purified Gα$_s$, and cAMP accumulation was measured. Data represents the mean and SEM of at least three independent experiments conducted in duplicate.

2.3.7 HEK-ACΔ3/6 cellular model to study the activity of AC1 forskolin mutants

To further demonstrate that our HEK-ACΔ3/6 cell line is an improved cellular model to study ACs, the cAMP responses of several mutant AC1 constructs were examined in the HEK-ACΔ3/6 and HEK293 cells. The mutant AC1 constructs were designed to incorporate single amino acid mutations at the forskolin binding site. Mutants AC1-W419A, AC1-V423G and AC1-S924P intended to have impaired the response to forskolin taking into consideration that Trp^{419} and Val^{423} (AC1 numbering) in the C1 domain directly interact with forskolin, and Ser^{924} (AC1 numbering) in the C2 domain bridges a nearby water molecule with the diterpene. Mutant AC1-N878A was also included in our mutagenesis studies given that this Asn^{878} residue is located within the forskolin binding pocket of AC1, but it is not conserved across forskolin-sensitive isoforms (Tesmer et al., 1997). **Fig. 2.8** presents the location of the mutated amino acids within the forskolin binding site at the interface of the C1-C2 catalytic domains.

Adenylyl cyclase activity triggered by forskolin, A23187 or a combination of both was examined on transiently transfected HEK293 and HEK-ACΔ3/6 cells expressing Venus, AC1-WT and the mutant AC1 constructs: AC1-W419A, AC1-V423G, AC1-N878A or AC1-S924P **(Fig.2.9)**. Venus-transfected HEK293 cells displayed higher cAMP levels to forskolin-induced activation than the HEK-ACΔ3/6 cells as was expected. In the presence of the calcium ionophore, A23187, the forskolin response of the HEK293 cells was reduced compared to the responses mediated by forskolin alone. No difference was observed on forskolin activation of Venus-transfected HEK-ACΔ3/6 cells in the presence of A23187. At the highest concentration of forskolin (50 μM) a 3-fold difference between AC1-WT and mock-transfected cells was observed for HEK293 cells compared to a 20-fold difference between HEK-ACΔ3/6 expressing AC1-WT and Venus.

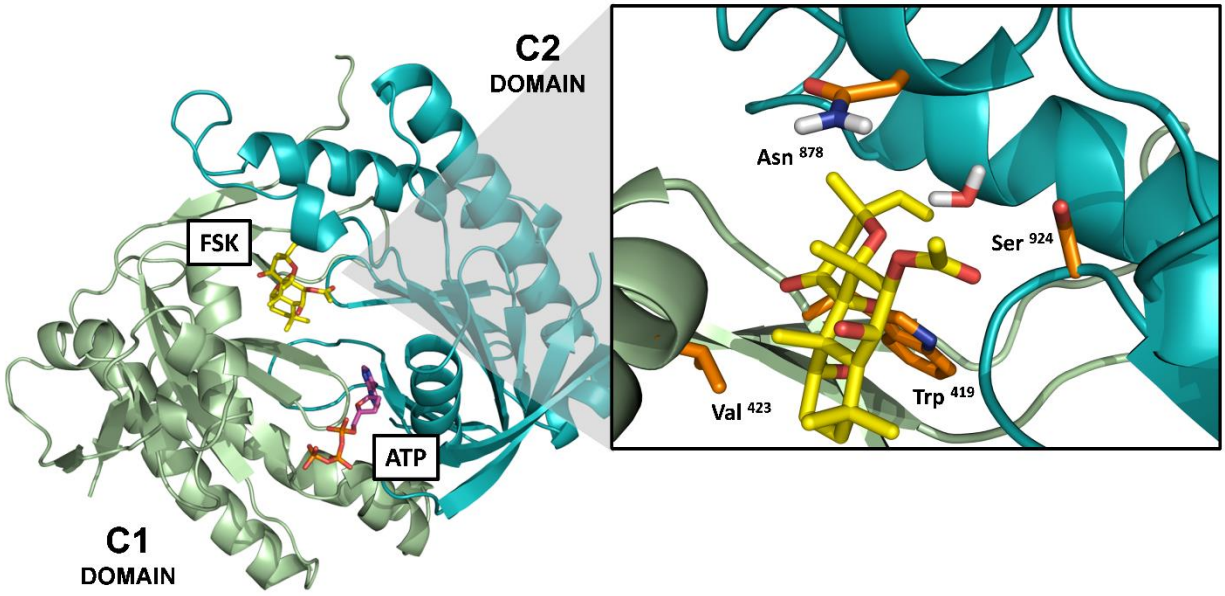

Figure 2.8. *Location of mutated amino acids on AC1 within the forskolin binding site.*

Model of the catalytic domains of AC1 based on the crystal structure of the C1(AC5)-C2(AC2) catalytic domains (PDB: 1AZS) (Tesmer et al., 1997). The model includes the ATP and forskolin (FSK) molecules bound at their pseudo symmetric binding sites within the interface of the C1-C2 catalytic domains. The enlarge panel corresponds to the forskolin binding site, and the side chains of the mutated amino acids on AC1 are represented in orange sticks. The amino acid numbering corresponds to the numbering of the full amino acid sequence for human AC1. *In the crystal structure, the Asn^{878} residue corresponds to Lys^{897} on the C2 domain of AC2.

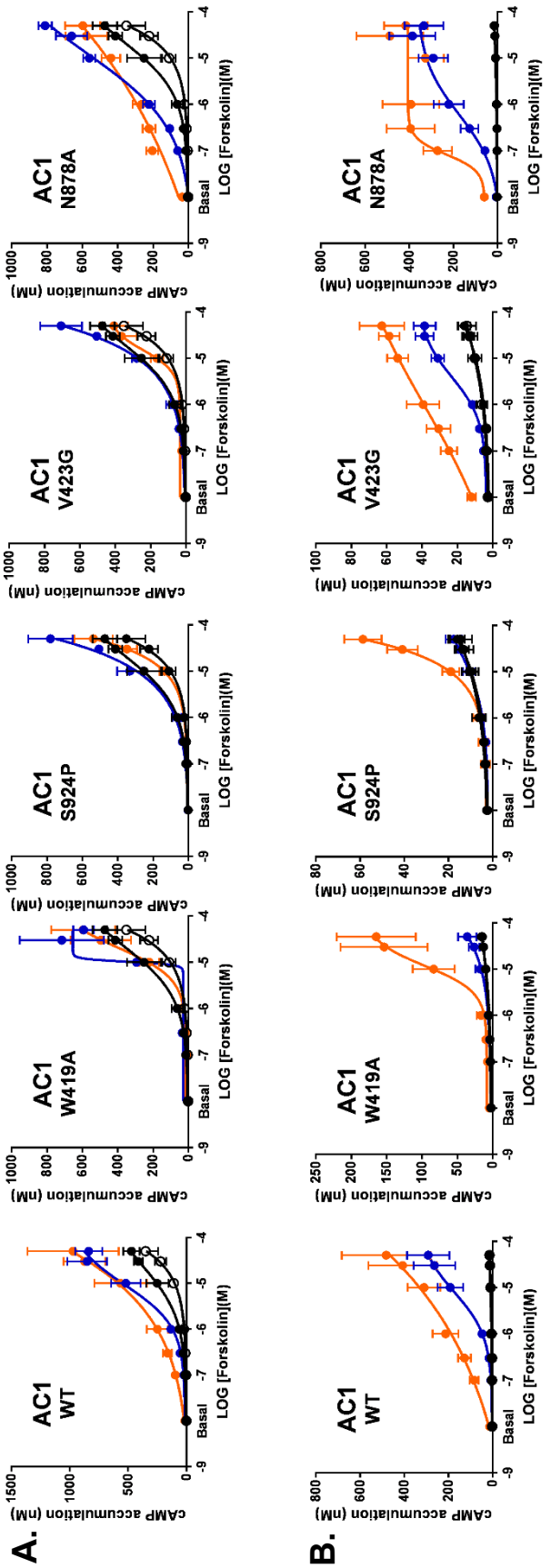

Figure 2.9 *Cyclic AMP responses to forskolin and A23187 of AC1 mutants expressed in HEK 293 and HEK-ACΔ3/6 cells.* HEK293 **(A)** or HEK-ACΔ3/6 cells **(B)** were transiently transfected with venus, AC1-wt or a AC1 mutant construct as indicated. After 40 hours, cAMP accumulation was stimulated with increasing concentrations of forskolin in the absence (blue) or presence (orange) of 3 µM A23187. Black and open circles represent the forskolin response of venus-transfected cells in the presence or absence of A23187, respectively. Data represents the mean and SEM of at least three independent experiments conducted in duplicate.

Although both cell models revealed A23187 potentiation of forskolin-stimulated cyclic AMP accumulation at lower forskolin concentrations, the response in the HEK-ACΔ3/6 cells was more robust. The interpretation of the AC responses of the HEK293 cells overexpressing the AC1 mutants was rather complicated. At first glance, AC1-W419A and AC1-S924P mutants appeared to be inactive in the HEK293 cells because neither forskolin, A23187, or a combination of both had an effect on cAMP accumulation. The AC1-V423G mutant seemed to be insensitive to forskolin but was responsive to A23187 **(Fig. S2)**. Surprisingly, the effects of forskolin and A23187 on the AC1-N878A mutant were substantially greater than those observed for AC1-WT in the HEK293 cells. In contrast to the HEK293 cells, the expression of the AC1 mutants in the HEK-ACΔ3/6 cells showed a more robust pharmacological profile.

AC1-W419A and AC1-S924P mutants showed little to no response when stimulated with forskolin or A23187, but the combination of the two was able to induce a distinguishable cAMP signal that was significantly higher than the control cells. In the case of the AC1-V423G mutant, expression in the HEK-ACΔ3/6 cellular model revealed that this mutant was responsive to forskolin, A23187, and a combination of both agents similar to AC1-WT. However, the extent of AC activation in response to forskolin was vastly reduced in the AC1-V423G mutant in comparison to AC1-WT. Although a stimulant-induced cyclic AMP response was observed for the AC1-N878A mutant in the HEK293 cells, the dose response curves of forskolin in the presence or absence of A23187 were shifted to the left in the HEK-ACΔ3/6 cells. Different cAMP responses were observed for AC1-WT and the AC1 forskolin-binding site mutants in response to A23187, but these distinct responses were the same when the AC1 constructs were either expressed in the parental HEK293 or the HEK-ACΔ3/6 cells **(Fig. S2)**.

2.4 Discussion

The cAMP signaling pathway is a dynamic interplay between GPCRs, ACs, phosphodiesterases, and downstream effectors, so a basic understanding of the individual roles of each signaling component is critical to unravel how cAMP is ultimately necessary for multiple cellular processes. In our continuing efforts to study AC function and regulation, we have developed a HEK293 cell line with a minimal background level of intracellular cAMP by using the CRISPR/Cas9 technology to disrupt the endogenous expression of AC3 and AC6. Functional characterization of the HEK-ACΔ6 and HEK-ACΔ3/6 cell lines revealed that the cAMP responses to forskolin and $G\alpha_s$-coupled receptor activation were mediated predominantly by AC6 in HEK293 cells. Differences in the cAMP responses elicited by β_2AR and EP_2R activation of these knockout cells also suggested that endogenous AC3 and AC6 contribute to a different extent to the overall cAMP accumulation in HEK293 cells. Although it has been determined *in vitro* that $G\alpha_s$ activates all AC isoforms (reviewed in Simonds, 1999), depending on the plasma membrane localization of the receptor and/or the AC, different AC isoforms might also couple to specific GPCRs (Johnstone et al., 2017). Thus, differences observed in the HEK-ACΔ6 and HEK-ACΔ3/6 cell lines might reflect subcellular localization of the receptors and ACs.

Our results indicate that in these knockout cells, the individual activity of the nine mAC isoforms could be characterized for general activators (forskolin and $G\alpha_s$-coupled receptors) given that the HEK-ACΔ3/6 cell line showed remarkably lower cAMP background levels for both stimulatory mechanisms. It is becoming more apparent that forskolin and $G\alpha_s$ evoke varying degrees of AC activation across the mAC isoforms even though their corresponding binding sites within the AC catalytic domains are highly conserved. For instance, it was reported for Sf9 membranes expressing AC1, AC2, and AC5 that the potency and efficacy of forskolin and forskolin analogs differs between isoforms (Pinto et al., 2008). Therefore, it was not surprising

that forskolin elicited different cAMP outcomes on AC isoform-expressing HEK-ACΔ3/6 isolated membranes and intact cells.

Activation of endogenous $G\alpha_s$-coupled receptors also revealed varying responses on AC isoform-expressing cells. The relative pattern of cAMP accumulation observed between isoforms was the same when cells were stimulated with either isoproterenol or PGE-2, and as observed in the parental HEK293 cell line, EP_2R activation in the transfected HEK-ACΔ3/6 cells led to higher cAMP levels than isoproterenol. All membrane-bound AC isoforms except for AC8 were stimulated by $G\alpha_s$-coupled receptor activation in the HEK-ACΔ3/6 cells. The absence of an AC8 response in cells was not explained by the inability of $G\alpha_s$ to bind or stimulate this isoform because *in vitro* studies with the HEKΔ36-AC8 membrane preparations demonstrated that the stimulatory Gα-subunit was able to activate AC8, and a the lack of a response in AC8-expressing cells to $G\alpha_s$-coupled receptor activation has been previously reported in HEK293 cells (Nielsen et al., 1996).

Selective regulatory properties of AC isoforms were also recapitulated in the HEK-ACΔ3/6 cells. Consistent with previous reports in the literature, Ca^{2+} influx stimulated Ca^{2+}/Calmodulin-regulated mACs, AC1 and AC8 (Tang et al., 1991). Likewise, our results with the AC1- and AC8-expressing cells for the cotreatments with the calcium ionophore, A23187, and PGE-2 were also in accordance with previous reports in intact cells, where only AC1 displayed an apparent synergistic response to Ca^{2+} stimulation in the presence of activated $G\alpha_s$ (Cumbay and Watts, 2001; Nielsen et al., 1996). In particular, by taking advantage of the unique regulatory properties of each mAC isoform, we ultimately demonstrated specific mechanisms to selectively activate all nine mACs with an improved signal window over basal levels.

Specifically, subtle cAMP responses were unmasked for AC isoforms such as AC7 or AC9 that did not display a robust cAMP response to various stimulatory mechanisms in the HEK-ACΔ3/6 cell model. Acute and chronic activation of the $G\alpha_i$-coupled receptor, D2R, elicited opposing effects on AC activity in the HEK-ACΔ3/6 cells, and these inhibitory or sensitized responses were AC isoform-dependent. Overall, the effects of acute and chronic $G\alpha_i$-coupled receptor activation in the D2R- and mAC-transfected HEK-ACΔ3/6 cells, were also consistent with previous studies (Chen and Iyengar, 1993; Taussig et al., 1993a; Watts and Neve, 2005), indicating that the HEK-ACΔ3/6 cell line can also be used to examine the unique inhibition or adaptive responses of adenylyl cyclase isoforms.

In vitro studies with isolated membranes from HEK-ACΔ3/6 cells overexpressing mACs also exhibited a suitable signal-to-background window for the characterization of isoform-specific basal and catalytic activities. The basal activity of the isolated membranes in the presence of Mg^{2+} and ATP was also significantly higher for isolated membranes overexpressing an AC isoform compared to the untransfected HEK-ACΔ3/6 cell membranes. Overall, the fold-change response to forskolin over the basal activity was significantly lower in the isolated membranes than that in cells, whereas the fold-change over the basal response triggered by purified $G\alpha_s$ was much higher in the membrane preparations. Particularly, these *in vitro* assays are a more direct approach to discern the effects of forskolin, $G\alpha_s$ and other modulators on AC activity. Therefore, our HEK-ACΔ3/6 cell line proved to be an adequate *in vitro* and *in vivo* cellular model to study mAC responses.

By disrupting the expression of AC3 and AC6 in the HEK293 cells, the enhancement of the signal window upon stimulation of AC activity in the knockout cells enable AC responses that previously were masked by the high cAMP levels, to become noticeable. The cAMP responses

detected for the uncharacterized AC1 constructs containing mutations within the forskolin-binding pocket were significantly different when these constructs were expressed in HEK293 or HEK-ACΔ3/6 cells. Mutation of the Trp^{419} or Ser^{924} residues were predicted to disrupt forskolin activity based on the binding interactions revealed by the crystal structure of the mAC catalytic domains (Tesmer et al., 1997). Interpretation of the data with the AC1-W419A and AC1-S924P mutants in the HEK293 cells suggested these two AC mutants were functionally inactive as indicated by the lack of a response over the cAMP levels of Venus-transfected cells. In contrast, expression of AC1-W419A and AC1-S924P in the HEK-ACΔ3/6 cells revealed a complete loss of forskolin sensitivity, but in combination with A23187 induced a distinct increase of cAMP accumulation higher than the drug-induced responses of the control-cells, demonstrating only a partial loss of function. An analogous mutation on Ser^{942} of AC2 (AC2-S942P) is forskolin insensitive in the absence or presence of $G\alpha_s$ despite showing similar $G\alpha_s$-mediated stimulation to AC2-WT (Brand et al., 2013), indicating that analogous mutations of conserved residues within the forskolin binding site of AC isoforms may affect the distinct responses to other stimulatory agents in different ways.

The crystal structure of the C1-C2 heterodimer also revealed that Val^{423} directly interacts with forskolin. However, mutating this residue did not abolished forskolin stimulation, and forskolin only showed diminished efficacy to activate AC1-V423G. No difference between the potency of forskolin for AC1-V423G and AC1-WT, also implies that the interaction between forskolin and Val^{423} is important to mediate its stimulatory effects but may not be essential for forskolin binding. That there were no significant effects of the mutation on the cAMP response mediated by A23187 alone also suggests that the AC1-WT and AC1-V423G constructs were expressed at similar levels.

The robust enhancement of cAMP accumulation detected for AC1-N878A in comparison to AC1-WT when the cells were stimulated with forskolin or/and A23187, was unanticipated. All the forskolin-sensitive mACs have a charged or polar residue at this position on the forskolin binding site, except for AC3 and AC8 (Seifert et al., 2012). By mutating Asn^{878} in AC1 to the counterpart Ala residue in AC8, it appears that the responses of AC1-N878A are comparable to the robust cAMP responses elicited by forskolin and A23187 on AC8-expressing cells. Even though the enhanced responses of the AC1-N878A construct were detected in both HEK293 and HEK-ACΔ3/6 cells, a shift to the left of the forskolin dose-response curves became apparent in the HEK-ACΔ3/6 cell model, besides the change in efficacy observed in both parental and knockout cells. In conclusion, the HEK-ACΔ3/6 cell line is a useful tool that has several advantages over the parental cell line for the study of mutant ACs with reduced catalytic activity and changes in forskolin sensitivity. Our knockout model not only allowed for functional characterization of AC mutants with diminished activity, but also revealed additional pharmacological effects on the AC1-N878A mutant that exhibited an enhanced cAMP response to stimulatory conditions.

For future applications, the HEK-ACΔ3/6 cellular system provides a more controlled environment for high throughput screening assays of selective AC modulators to ultimately lower false-positives rates (non-selective compounds) and simplify hit validation. Although the scope of the present work focused on mACs, our HEK-ACΔ3/6 cell line is also an appropriate cellular model to study function and regulation of soluble AC. Overexpression of sAC in HEK293 cells results in high cAMP levels in the presence of IBMX (Zippin et al., 2001) that reflects activity from sAC as well as the endogenous ACs (e.g. AC3 and AC6). The use of the HEK-ACΔ3/6 cells would presumably enhance the overall signal to noise window for evaluating modulators of AC10. An additional advantage of the new cell model is the human genetic background that readily allows

for a wider range of studies assessing cAMP signaling in intact cells. Our CRISPR/Cas-based cell line is a valuable human cellular system to study AC isoforms in an unbiased manner and is a tool that could simplify and aid future efforts to develop selective AC modulators.

CHAPTER 3. CHARACTERIZATION OF A PEPTIDE MODULATOR OF Gβγ SIGNALING DERIVED FROM AC2

Conditional stimulation by Gβγ subunits is the main regulatory property that characterizes adenylyl cyclases (AC) 2, 4, and 7. The objective of this study was to explore the modulatory properties on Gβγ-mediated signaling of an uncharacterized C2a domain adjacent to the membrane that displayed high degree of homology between Gβγ-stimulated cyclases. Surface plasmon resonance determined that a peptide derived from this juxta membrane C2a domain, C2-20, binds with high affinity to Gβγ subunits (K_D ~2 nM). Subsequently, a minigene strategy was used to characterize the activity of the C2-20 peptide on Gβγ-mediated conditional stimulation of AC2 activity. The minigene contained an N-terminal CD8 domain to localize the C2-20 peptide to the membrane. Expression of the CD8-C2-20 minigene inhibited completely Gβγ-mediated potentiation of AC2 following the activation of the dopamine D2 receptor (D2R). In addition, the specificity of the CD8-C2-20 minigene was explored with a series of mutant minigenes containing triple-alanine substitutions and their respective inhibitory activities suggested that the C2-20 domain interaction with Gβγ is mediated by multiple contact points given that none of the CD8-C2-20 mutants were sufficient to abolish its inhibitory action. Furthermore, the effects of the CD8-C2-20 minigene were evaluated on other Gβγ-mediated pathways such as ERK activation, β-arrestin recruitment, and heterologous sensitization of AC2 and AC5. Interaction of the C2-20 domain with Gβγ successfully blocked potentiation of AC2 activity induced by the Gβγ complex and attenuated β-arrestin recruitment to the D2R. However, it did not interfere with the role of Gβγ subunits in heterologous sensitization of AC2 and AC5 or Gβγ-mediated stimulation of the MAPK kinase cascade. The resulting studies suggest that specific regions of the C2a domain could be used

to selectively modulate Gβγ signaling. These studies highlight further the complexities associated with AC signaling and the unique ways in which isoforms are modulated by Gβγ subunits.

3.1 Introduction

Adenylyl cyclases (AC) play a vital role in many biological processes because they are the enzymes responsible for the conversion of ATP into the secondary messenger cAMP. Nine isoforms of membrane-bound ACs exist in mammals, and their structure consist of a cytosolic N-terminus, two helical membrane-spanning domains and two cytosolic regions (C1 and C2). The C1 and C2 domains of transmembrane ACs dimerize to form the catalytic core upon AC activation. Each cytosolic domain subdivides into a highly conserved region (C1a and C2a) that contains the essential residues for catalytic activity, and a less conserved domain (C1b and C2b) that contains several regulatory sites (Tang and Hurley, 1998).

Despite the high degree of structural and sequence homology of mAC isoforms, they exhibit differential regulatory mechanisms to stimulatory and inhibitory Gα-proteins, Gβγ subunits, protein kinases, and divalent cations. Thus, membrane-bound ACs are classified into 4 groups based on these regulatory properties. Calcium-stimulated cyclases, AC1, AC3, and AC8, belong to Group I, and Gβγ-stimulated AC2, AC4, and AC7 comprise Group II. Group III consists of AC5 and AC6 which are inhibited by sub micromolar concentrations of Ca^{2+}, while AC9 belongs to Group IV as the only mAC insensitive to the diterpene, forskolin (reviewed in Dessauer et al., 2017). Specific AC isoforms have been associated with various physiological and pathological conditions dictated by these isoform-specific regulatory properties and distinct tissue distribution patterns (Sadana and Dessauer, 2009). Therefore, AC isoforms have emerged as interesting drug targets for diseases ranging from cardiovascular disorders to pain and addiction (Dessauer et al., 2017; Pierre et al., 2009; Seifert et al., 2012).

The Gβγ complex is one of the mAC regulators that exerts either inhibitory or stimulatory actions depending on the AC isoform. Once released from the heterotrimeric G-protein complex after GPCR activation, the Gβγ dimer has the ability to conditionally stimulate AC2, AC4, and AC7 or inhibit AC1 and AC3 (Khan et al., 2013). Multiple binding domains have been characterized for Gβγ on the intracellular domains of the mAC isoforms. Unique sites have been reported for AC1 and AC3 within the C1 region, for AC2 on both C1 and C2 domains, and for AC5 and AC6 on the N-terminus (Boran et al., 2011; Brand et al., 2015; Wittpoth et al., 1999). In particular, five Gβγ-binding domains have been identified on AC2 (**Fig. 3.1**): the QEHA region in the C2 domain, the PFAHL region within the C1b domain, the KF loop—proximal to the QEHA region—and two additional sites in the C1 domain (339-360 and 578-602, AC2 numbering) (Boran et al., 2011; Chen et al., 1995; Diel et al., 2008; Diel et al., 2006). Several of these binding sites are homologous between the Gβγ-stimulated cyclases (AC2, AC4 and AC7; **Fig. 3.1**), and it appears, based on mutagenesis and domain swapping studies that the conditional stimulatory effect of Gβγ on AC2 is mediated by a complex interaction with several of those shared binding sites (Diel et al., 2006; Weitmann et al., 2001).

The involvement of the Gβγ complex in regulating important physiological processes (Khan et al., 2013) has motivated interest to elucidate the potential of Gβγ subunits as a therapeutic target (Smrcka et al., 2008). However, non-selectively inhibiting all Gβγ functions may cause unwanted side effects, so understanding the protein-protein interaction dynamics between Gβγ and its effectors is necessary to achieve selective modulation of Gβγ-mediated pathways. Gβγ subunits are localized to membranes by prenylation of the Gγ subunit (Smrcka, 2008).

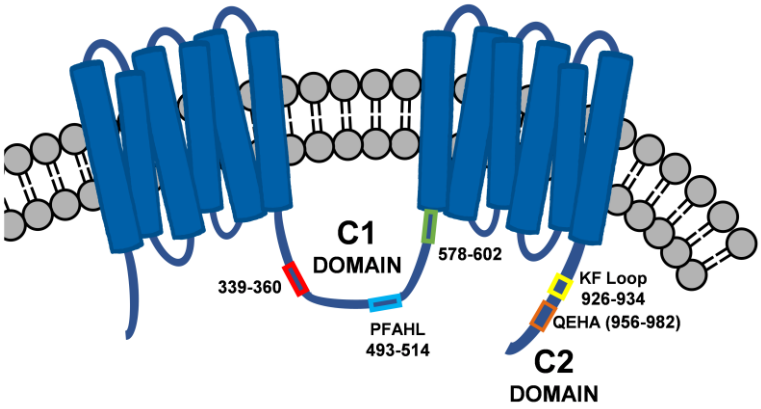

1. 339-360 Overall: 85 %

			Score
ADCY2	CYYCVSGLPISLPNHAKNCVKMG	339-360	
ADCY4	CYYCVSGLPLSLPDHAINCVRMG	323-345	85 %
ADCY7	CYYCVSGLPVSLPTHARNCVKMG	329-351	87 %

2. PFAHL Overall: 82 %

			Score
ADCY2	MTRYLESWGAAKPFAHLHHRDS	494-514	
ADCY4	MTRYLESWGAAKPFAHLSHGDS	478-499	91 %
ADCY7	MTRYLESWGAARPFAHLNHRES	484-505	85 %

3. 578-602 Overall: 35 %

			Score
ADCY2	LFYNKVLEKEYRATALPAFK	581-601	
ADCY4	YFREKEMEKEYRLSAIPAFK	565-585	60 %
ADCY7	IFLEKGFEREYRLAPIPRAR	574-594	35 %

4. KF Loop Overall: 89 %

			Score
ADCY2	LSKPKFSGV	926-934	
ADCY4	LSKPKFSGV	913-921	100 %
ADCY7	LLKPKFSGV	919-927	89 %

5. QEHA Overall: 44 %

			Score
ADCY2	QEHSQEPERQYMHIGTMVEFAFALVGK	956-982	
ADCY4	QDAQQDAERSCSHLGTMVEFAVALGSK	943-969	56 %
ADCY7	HE - NQELERQHAHIGVMVEFSIALMSK	949-975	59 %

Figure 3.1 *Sequence alignment between AC2, AC4, and AC7 of the Gβγ-binding sites*

The location of the Gβγ-binding sites identified on AC2 is indicated in the diagram by colored boxes. Amino acid sequences of human AC2 (ADCY2), AC4 (ADCY4), and AC7 (ADCY7) were aligned with the EMBL-EBI Clustal Omega software. For each corresponding Gβγ-binding site, the overall score represents the sequence homology between AC2, AC4 and AC7, and the scores reported for the AC4 and AC7 domains represent the sequence similarity between each AC and AC2. Identical amino acids and amino acids with similar properties between AC2, AC4 and AC7 are highlighted in grey and light blue, respectively.

Various strategies such as GPCR-derived pepducins—lipidated peptides corresponding to a juxtamembrane region of the receptor's intracellular loops—have emerged as novel mechanisms to modulate membrane-bound proteins (Zhang et al., 2015). For example, a juxtamembrane portion of an intracellular loop of the Glycine receptor (GlyR) interacts with the Gβγ complex, and a peptide derived from this domain, interferes with Gβγ-mediated activation of the G-protein-coupled inwardly rectifying K^+ channel (GIRK) (Guzman et al., 2009).

Consequently, the objective of this research was to determine whether juxtamembrane domains of AC2 could also modulate Gβγ activity. To do so, we first evaluated the homology between the cytosolic domains adjacent to the membrane of the Gβγ-stimulated cyclases: AC2, AC4 and AC7, and identified an uncharacterized juxtamembrane segment on the C2a domain that binds the Gβγ complex with high affinity. A minigene derived from this juxtamembrane C2a segment, blocked Gβγ-potentiation of AC2 activity in cells, and showed a biased profile for inhibition of AC2 potentiation over other Gβγ-mediated pathways.

3.2 Methods

3.2.1 Peptide synthesis

The C2-20 peptide (RQNEYYCRLDFLWKNKFKKE) and the scrambled version of the C2-20 peptide (LRNKEYRLDFKENYKFKWCQ) for the SPR experiments, were synthesized by Genscript Biotech (Piscataway, NJ).

3.2.2 Surface Plasmon Resonance

SPR was performed as described in (Seneviratne et al., 2011; Surve et al., 2014), with modifications. The C2-20 peptide or the scrambled peptide was immobilized on the surface of a polyethylene glycol-coated gold sensor chip (Reichert, NY) using N′-ethylcarbodiimide

hydrochloride (EDC) – N-Hydroxysuccinimide (NHS) chemistry, by injecting 10 μM C2-20 or the scrambled peptide in 50 mM HEPES, pH 7.6, 1 mM EDTA, 200mM NaCl, 0.1% polyoxyethylene 10 lauryl ether ($C_{12}E_{10}$), 1 mM dithiothreitol, and 0.1% DMSO. Gβγ was injected and its binding was observed for 2 minutes followed by dissociation for 5 minutes, at a flow-rate of 75 μL/min. After dissociation, the peptide surface was regenerated using 610 mM $MgCl_2$, 205 mM Urea, and 610mM Guanidine- HCl, followed by the second injection. The data was analyzed using Scrubber and the BIAevaluation software (Biacore), and the K_D was determined by globally fitting the binding curves determined at several concentrations of compound with a 1:1 binding model.

3.2.3 Constructs design

The pcDNA3.1$^+$/CD8-C2-20 construct was designed based on the pcDNA3/CD8-βARKct plasmid (Crespo et al., 1995). The CD8-C2-20 plasmid contains the transmembrane domain portion of the CD8 lymphocyte-specific receptor (residues 1-209), followed by the restriction site BamHI, and the C2-20 domain sequence: RQNEYYCRLDFLWKNKFKKE (residues 822-841, AC2 numbering). For the scrambled CD8-C2-20 construct, the C2-20 peptide sequence was randomly reorganized (LRNKEYRLDFKENYKFKWCQ), but charge distribution was maintained. CD8-C2-20 and scrambled CD8-C2-20 plasmids were synthesized, and codon optimized for human cell line expression by Genscript Biotech (Piscataway, NJ).

3.2.4 Site-directed mutagenesis of CD8-C2-20 minigene

Variants of the CD8-C2-20 minigene with triple alanine mutations or a C-terminal deletion were generated using the Q5® Site Directed Mutagenesis kit. First, primers were designed to replace in the C2-20 sequence a 9 bp segment that encodes for: RQN (*CD8 (RQN 1-3)*), EYY (*CD8 (EYY 4-6)*), CRL (*CD8 (CRL 7-9)*), DFL (*CD8 (DFL 10-12)*), or WKN (*CD8 (WKN 13-15)*),

with the codon sequence, *gcc gcc gcc*, that encodes for a triple AAA substitution (**Table S1**). In the case of the C-terminal deletion for the CD8 (C2-17) minigene, the primers designed flanked the 9bp codon sequence of the last three amino acids (KKE) of the C2-20 domain. PCR amplification of the entire pcDNA3.1^{+}/CD8-C2-20 plasmid using the corresponding forward and reverse set of primers for each CD8-C2-20 variant was performed according to the Q5 Site-Directed Mutagenesis protocol. The PCR products were further used to set up the KDL reactions of the Q5 Site-Directed Mutagenesis kit, and prior to bacterial transformation, each reaction was treated with DpnI for 1 hour at 37 ºC to remove the parental CD8 C2-20 PCR template. Once it was determined that the mutation was properly incorporated to the CD8-C2-20 constructs by Sanger sequencing, the CD8-C2-20 variant genes were cut with NheI and KpnI from the PCR generated constructs. The cut fragment was then cloned into an empty pcDNA3.1^{+} backbone to ensure that the CD8-C2-20 variant minigenes had no additional mutations outside the C2-20 sequence that could had been introduced during the PCR amplification.

3.2.5 Transfections

CHOwt cells or HEK293 cells were plated overnight to have cells at 70% confluency in a 12-well plate format for transfection the following day. Cells were transfected with Lipofectamine 2000 purchased from Life Technologies (Carlsbad, CA) or with XtremeGENE 9 from Roche (Basel, Switzerland) according to the manufacturer's recommendations. Lipofectamine 2000 was used for the transfection of HEK293 cells with the D2R, AC2 and CD8-C2-20, Scr-CD8-C2-20, CD8-βARKct or Venus constructs. A 1:2 DNA to Lipofectamine ratio and a 1:2:3 DNA ratio for the D2R, AC2, and Venus or CD8 minigene combinations, respectively, were the optimal parameters for these transfections. CHO cells were also transfected with Lipofectamine 2000 for the ERK phosphorylation experiments in a 1:2 DNA to Lipofectamine ratio and a 1:2 DNA ratio

of the D2R and Venus or CD8 minigene constructs. Xtreme GENE 9 was used instead for the transfection of the HEK 293 cells with D2R, AC2 or the CD8-C2-20 variants in a 1:2 DNA to XtremeGENE ratio and a 1:2:4 DNA ratio for the D2R, AC2, and Venus or CD8 minigene variant combinations, respectively. Transfection of the DiscoveRx CHO cells stably expressing the ProLink-tagged D2R and the enzyme acceptor-tagged β2-Arrestin (CHO-D2L) were also transfected with XtremeGENE 9 in a 1:2 DNA to XtremeGENE ratio.

3.2.6 Gβγ-mediated AC2 potentiation

After 48-hour transfection, transfected HEK293 cells were washed with PBS, harvested using cell dissociation buffer, and resuspended in serum-free Opti-MEM. The cells were centrifuged at 150 x g for 5 minutes, and the cell pellet was resuspended in Opti-MEM for a second centrifugation step. Transfected cells were then counted, and the volume of the cell suspension was adjusted to the desire cell concentration for plating in a low volume 384-well plate (Catalog # 784080) from Greiner Bio-One (Kremsmünster, Austria). After 1-hour incubation at 37 ºC in 5% CO_2, the cells were treated with vehicle or 3 μM quinpirole followed by 1 μM PMA in the presence of 500 μM 3-isobutyl-1-methylxanthine (IBMX). Cells were treated with the indicated drugs for 1-hour at room temperature before cAMP production was measured using the HTRF cAMP Gs assay kit from Cisbio (Bedford, MA). Fluorescence signals from each well were measured with a Cytation 3 plate reader at 330 nm excitation wavelength and 620/665 nm emission wavelengths. Cyclic AMP levels were determined by extrapolating the 620/665 fluorescence ratio from a cAMP standard curve ran in parallel.

3.2.7 Heterologous sensitization

Transfected D2R and AC2/AC5 cells were harvested and plated as described above for the Gβγ-mediated AC2 potentiation assays with the minigenes. After the 1-hour incubation at 37 ºC

in 5% CO_2, the cells were treated with 3 μM quinpirole for 2 hours prior the stimulation of AC2 or AC5 activity with 1 μM PMA or 30 nM forskolin (FSK), respectively, in the presence of 1 μM spiperone (D2R antagonist) and 500 μM IBMX. Cyclic AMP was measured as described above after 1-hour stimulation with the respective AC2 and AC5 activators.

3.2.8 β2-arrestin recruitment (PathHunter β2-arrestin assay)

After 24-hour transfection with XtremeGENE, DiscoveRx CHO-D2L cells were harvested and plated overnight in a low volume 384-well plate at 37 ºC in 5% CO_2. Next day, cells were incubated with increasing concentrations of quinpirole for 90 minutes at 37 ºC in 5% CO_2. To detect β2-arrestin recruitment after D2R activation, the PathHunter detection kit from DiscoveRx (Fremont, CA) was utilized. The detection reagent was prepared according to the PathHunter kit's protocol and was kept protected from light. The detection reagent was added and incubated for 1-hour at room temperature prior luminescence signal was measured with a Synergy4.

3.2.9 ERK Phosphorylation (AlphaLISA SureFire Ultra)

CHO cells transiently transfected with D2R and Venus, CD8-βARKct or CD8-C2-20 were harvested and centrifuged twice at 150 xg for 5 minutes. Cells were plated in a regular volume 384-well plate and after 2-hour incubation at 37 ºC in 5% CO_2, the cells were treated with 3 μM quinpirole or 1 μM PMA for 10 minutes at room temperature. Phosphorylated ERK 1/2 mediated by D2R and PKC activation was quantified using the AlphaLISA SureFire Ultra p-ERK1/2 (Thr202/Tyr204) assay kit. AlphaLISA SureFire Ultra lysis buffer was added to the wells and incubated for 10 minutes at room temperature while shaking on an orbital shaker. According to the kit's manual, the acceptor reagents beads were added to each well and incubated with the cell lysate for 1-hour protected from light followed by the addition of the donor beads.

The plate was incubated overnight before the AlphaScreen signal was detected using a Perkin Elmer EnSpire plate reader.

3.3 Results

3.3.1 An uncharacterized 20-mer segment derived from AC2 binds to Gβγ

Considering that Gβγ localizes at membranes and interacts with a large number of transmembrane proteins, we wanted to evaluate whether juxtamembrane domains on the N-terminus or the two catalytic domains of AC2 interact with the Gβγ complex. In previous studies, intracellular domains that display high degree of homology between AC2, AC4, and AC7, have shown to interact with Gβγ subunits (Boran et al., 2011). Therefore, we performed a sequence alignment between the 4 juxta membrane segments of the Gβγ-stimulated cyclases and determined their sequence homology **(Fig. 3.2)**. No significant sequence similarity was observed between the domains on the N-terminus or the C1a domain of AC2, AC4, and AC7. The juxtamembrane region on the C1b only showed strong homology between AC2 and AC4, and this shared binding domain (578-602, AC2 numbering) has been previously reported to bind Gβγ subunits with low affinity (Boran et al., 2011). Surprisingly, an uncharacterized juxtamembrane section on the C2a domain exhibited the highest overall degree of homology among the fragments evaluated. This section on the C2a domain displayed 65% identical and 85% similar sequence homology between AC2, AC4, and AC7.

To explore the relationship between the homology of the C2a juxtamembrane region and Gβγ's binding interactions with AC2, AC4, and AC7, a 20-mer peptide derived from the juxtamembrane region of the C2a domain of AC2 (C2-20) was synthesized for *in vitro* binding assays with Gβγ. Specifically, we used surface plasmon resonance (SPR) to determine whether this uncharacterized C2a segment interacts with Gβγ subunits.

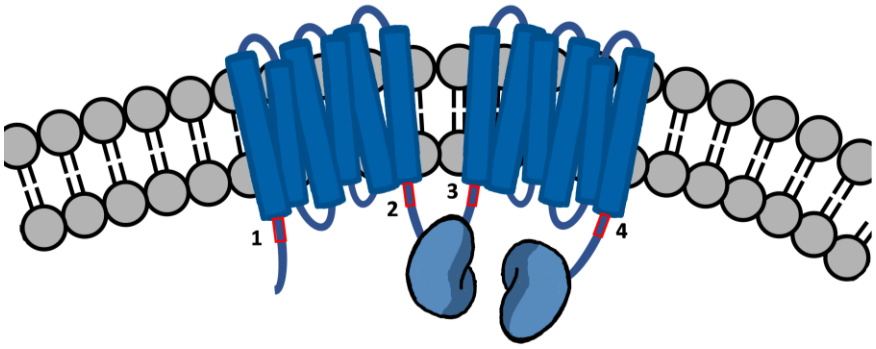

1. N-terminus	Overall: 35 %		**Score**
ADCY2	LPRSRDWLYESYYCMSQQHP	25-45	
ADCY4	PPPSEDLFYETYYSLSQQYP	8-28	55 %
ADCY7	EGPDQDALYEKYQLTSQHGP	13-33	35 %

2. C1a subdomain	Overall: 20 %		**Score**
ADCY2	HKHLMELALQQTYQDTCNCI	208-228	
ADCY4	HKALMERALRATFREALSSL	191-211	40 %
ADCY7	HKHQMQDASRDLFTYTVKCI	197-217	40 %

3. C1b subdomain	Overall: 35 %		**Score**
ADCY2	LFYNKVLEKEYRATALPAFK	581-601	
ADCY4	YFREKEMEKEYRLSAIPAFK	565-585	60 %
ADCY7	IFLEKGFEREYRLAPIPRAR	574-594	35 %

4. C2a subdomain	Overall: 65 %		**Score**
ADCY2	RQNEYYCRLDFLWKNKFKKE	822-842	
ADCY4	RQNEYYCRLDFLWKKKLRQE	808-828	85 %
ADCY7	RQIDYYCRLDCLWKKKFKKE	815-835	70 %

Figure 3.2 *Sequence alignment of juxta membrane cytosolic domains of AC2, AC4 and AC7.*

Amino acid sequences of the intracellular domains adjacent to the membrane of human AC2 (ADCY2), AC4 (ADCY4), and AC7 (ADCY7) were aligned with the EMBL-EBI Clustal Omega software. The location of the aligned domains is indicated in the diagram by the red boxes and the corresponding numbering. The overall score represents the sequence homology between AC2, AC4 and AC7, and the scores reported for the AC4 and AC7 domains represent the sequence similarity between each AC and AC2. Identical amino acids and amino acids with similar properties between AC2, AC4 and AC7 are highlighted in grey and light blue, respectively.

The C2-20 peptide was immobilized on the SPR chip and increasing concentrations of Gβγ were applied **(Fig. 3.3a)**. Kinetic analysis of the SPR binding curves indicated that the C2-20 peptide binds to Gβγ with a binding affinity of approximately 2 nM.

Compared to the K_D values reported by *Boran et al* for other Gβγ binding sites of AC2, the C2-20 peptide showed equal binding affinity to Gβγ as the PFAHL domain localized on the C1a domain, but it exhibited higher binding affinity than the QEHA domain and the other juxtamembrane 578-602 segment. Furthermore, the binding interaction between the C2-20 peptide and Gβγ was specific given that a sequence-scrambled C2-20 peptide failed to bind to Gβγ **(Fig. 3.3b),** and the C2-20 peptide did not bind to the $G\alpha_i$ subunit (data not shown).

3.3.2 Expression of a C2-20 peptide minigene inhibits Gβγ potentiation of AC2 activity

After having determined that the C2-20 peptide binds with high affinity to Gβγ, we examined the ability of the C2-20 domain to modulate Gβγ-mediated potentiation of AC2 activity. Using a minigene strategy, we designed a vector, CD8-C2-20, encoding for a N-terminal CD8 transmembrane domain—to localize the peptide at the membrane–followed by the C2-20 peptide sequence. Given that most of the stimulatory effects of Gβγ on ACs are mediated by the pertussis toxin-sensitive $G\alpha_{i/o}$-proteins (Smrcka, 2008), the effect of the CD8-C2-20 minigene on Gβγ signaling was examined in HEK293 cells transiently coexpressing AC2 and the $G\alpha_{i/o}$-coupled receptor, dopamine D2 receptor (D2R). Gβγ-mediated potentiation of AC2 activity also requires the simultaneous activation of the cyclase either by $G\alpha_s$-coupled receptors or by protein kinase C, so transfected HEK293 cells were treated with the phorbol ester, PMA, in the presence or absence of the D2R agonist, quinpirole (Watts and Neve, 1997).

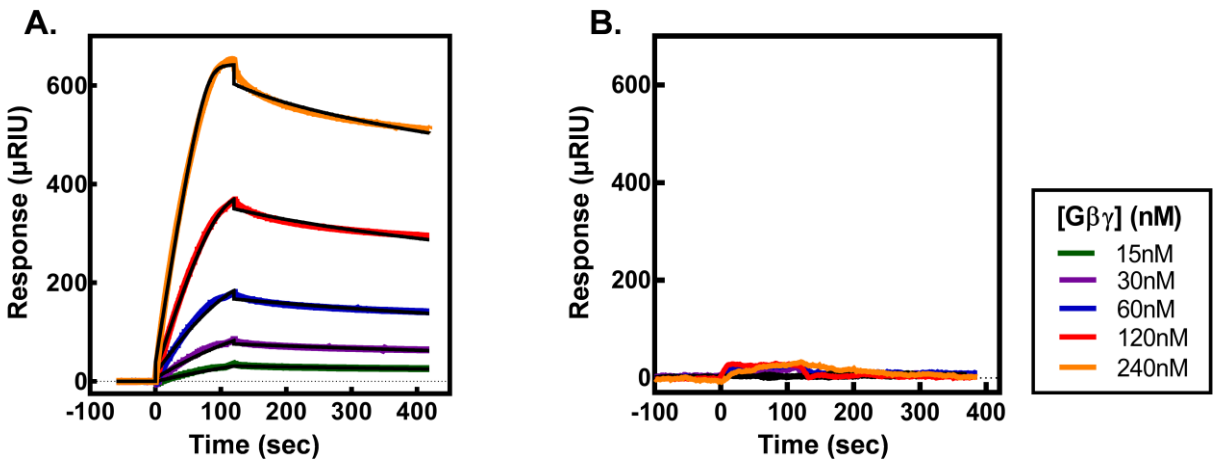

Figure 3.3 *The juxtamembrane C2a domain of AC2 binds to Gβγ*

Surface plasmon resonance curves of immobilized C2-20 **(A)** or a sequence-scrambled C2-20 peptide **(B)** binding to increasing concentrations of Gβγ subunit. Fitted curves (black lines) were calculated from the SPR data using Scrubber and the BIAevaluation software (Biacore). Data was generated and analyzed by Dr. Chinmay Surve in Dr. Alan Smrcka's lab.

Expression of the CD8-C2-20 minigene abolished Gβγ-mediated potentiation of AC2 activity **(Fig. 3.4)**, however, expression of a minigene with the scrambled amino acid sequence of the C2-20 peptide, CD8-Scr/C2-20, had no effect on potentiation of PMA-stimulated AC2 activity. In addition, the CD8-C2-20 minigene showed the same extent of inhibition of Gβγ-mediated AC2 potentiation as the positive control, the scavenger of Gβγ subunits, CD8-βARKct (Inglese et al., 1994; Koch et al., 1994). No major differences were observed on the cAMP response to PMA alone for the cells expressing CD8-C2-20, CD8-Scr/C2-20, or CD8-βARKct compared to the Venus-transfected cells, which suggests that the inhibition of AC2 activity by the CD8-C2-20 minigene was only limited to the conditional activation induced by the Gβγ complex.

3.3.3 Central residues of the C2-20 sequence are critical for the inhibitory activity of the CD8-C2-20 minigene

In order to identify the amino acids important for the inhibitory activity of the CD8-C2-20 minigene, several minigene variants were designed with triple-alanine mutations or a C-terminal truncation within the peptide sequence of the C2-20 segment **(Table 3.1)**. The ability of the CD8-C2-20 minigene variants to inhibit Gβγ potentiation of PMA-stimulated AC2 activity was examined in AC2 and D2R-transfected HEK293 cells, and the magnitude of Gβγ potentiation over the PMA response for each transfection condition was compared to the responses of wild-type CD8-C2-20 -expressing cells. Mutations within the central portion of the C2-20 sequence (EYY 4-6, CRL 7-9, and DFL 10-12) caused a substantial loss of the inhibitory activity of the CD8-C2-20 minigene by more than 50% **(Fig. 3.5)**. The bell-shaped distribution of the mutations' effects on the inhibitory activity of the CD8-C2-20 minigene with a peak at the intermediate residues, DFL 10-12, highlights the importance of this central portion for its inhibitory activity.

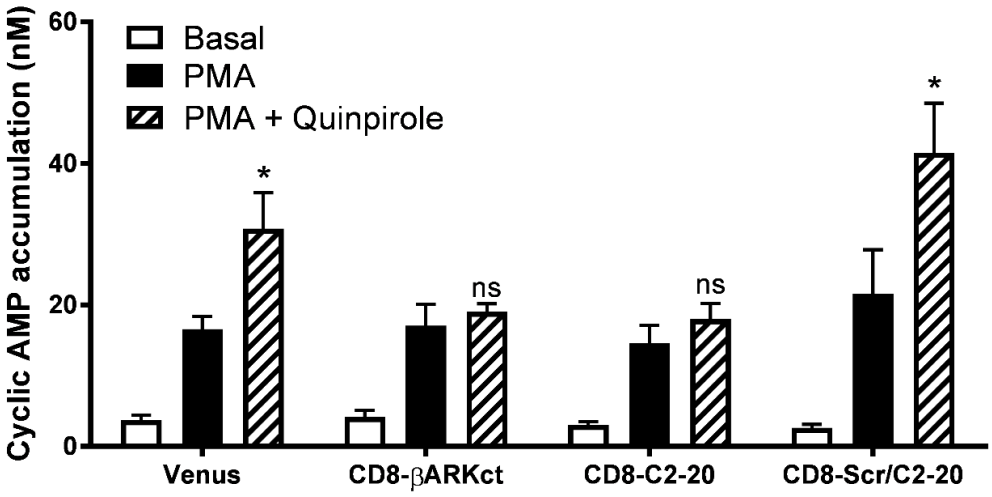

Figure 3.4 *Expression of a C2-20 minigene blocked the stimulatory effects of Gβγ on AC2 activity.* HEK293 cells were transiently transfected with human AC2, the D2R and Venus (transfection control), CD8-βARKct, CD8-C2-20 minigene or a scrambled version of the CD8-C2-20 minigene. After 48-hour transfection, cells were treated with 1μM PMA in the absence or presence of 3μM quinpirole to induce Gβγ-mediated potentiation of AC2 activity. Data represents the average and SEM of at least three independent experiments, each performed in triplicate. Statistical significance was calculated using unpaired student's t-test. ns, not significant, *P < 0.05 compared to the to the cAMP levels of the PMA alone.

Table 3.1 *Amino acid sequences of the CD8-C2-20 minigene variants and % inhibition of Gβγ-mediated potentiation of AC2 activity.*

The position within the C2-20 sequence of the triple alanine substitutions or the C-terminal truncation of the CD8-C2-20 minigene variants is highlighted in bold and underlined.
[a] Percentage inhibition of Gβγ potentiation of AC2 activity following PKC activation. First, fold-change over PMA response was calculated to determine relative magnitude of Gβγ-mediated potentiation for each transfection condition. Subsequently, percentage inhibition was calculated relative to the Gβγ-mediated potentiation (set as 0% inhibition) and PMA alone responses (set as 100% inhibition) of Venus-transfected cells.

Minigene	Sequence	% Inhibition[a] ± SEM
CD8-βARKct	CD8-(βARK residues)	79 ± 6
CD8-C2-20	CD8-(RQNEYYCRLDFLWKNKFKKE)	83 ± 10
RQN 1-3	CD8-(**AAA**EYYCRLDFLWKNKFKKE)	73 ± 8
EYY 4-6	CD8-(RQN**AAA**CRLDFLWKNKFKKE)	48 ± 8
CRL 7-9	CD8-(RQNEYY**AAA**DFLWKNKFKKE)	55 ± 14
DFL 10-12	CD8-(RQNEYYCRL**AAA**WKNKFKKE)	36 ± 13
WKN 15-17	CD8-(RQNEYYCRLDFL**AAA**KFKKE)	61 ± 5
CD8-C2-17	CD8-(RQNEYYCRLDFLWKNKF**- - -**)	75 ± 5

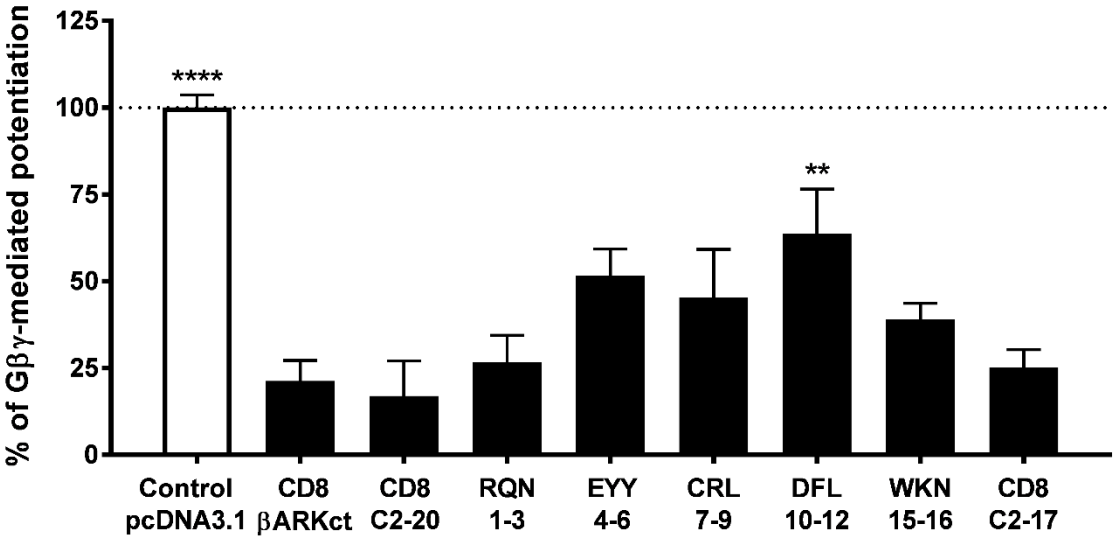

Figure 3.5 *CD8-C2-20 variants containing triple-alanine substitutions in the "middle" of the C2-20 domain displayed diminished inhibitory effects on Gβγ potentiation.*

HEK293 cells were transiently transfected with human AC2, D2R and Venus, CD8-βARKct, CD8-C2-20, or a CD8-C2-20 minigene variant containing a triple-alanine substitution or a c-terminus truncation. Transfected cells were treated with 1 μM PMA in the absence or presence of 3 μM quinpirole to induce Gβγ-mediated potentiation of AC2. Fold-change over PMA response was calculated to determine relative magnitude of Gβγ-mediated potentiation for each transfection condition, and Gβγ-mediated response was reported relative to the magnitude of Gβγ-mediated potentiation (set as 100%) and PMA alone responses (set as 0%) of Venus-transfected cells. Statistical analysis was performed using one-way ANOVA followed by a Dunnett's comparison. **P < 0.01, ****P < 0.0001 compared to the % of Gβγ-mediated potentiation of the CD8-C2-20-transfected cells.

However, no variant completely rescued Gβγ-mediated potentiation which indicates that more than one residue between Glu at position 4 and a Leu at position 12, are required for the inhibitory effects of the C2-20 domain. To ensure that the reduction of the inhibitory activity was not due to different expression levels of the CD8-C2-20 minigenes, protein expression levels of the CD8-C2-20 minigene variants and wild-type CD8-C2-20 were measured by Western blot using an anti-CD8 monoclonal antibody (data not shown). Surprisingly, the CD8-C2-20 variants that had a diminished ability to block Gβγ-mediated stimulatory effects on AC2 activity were generally more highly expressed compared to wild-type CD8-C2-20; thereby, the relative level of protein expression does not account for the decreased inhibitory effects of the CD8-C2-20 variants.

3.3.4 CD8-C2-20 fails to inhibit Gβγ-mediated pathways triggered by D2R activation

A large and diverse array of proteins are modulated by free Gβγ subunits (Khan et al., 2013). Several of these Gβγ effectors shared a common binding site (hot spot) on the top surface of Gβ subunit (Davis et al., 2005; Scott et al., 2001), so the effector specificity of the Gβγ and C2-20 interaction was examined. In order to explore how the interaction of the C2-20 peptide domain modulates Gβγ activity on other AC signaling events, the effects of the CD8-C2-20 minigene were studied on heterologous sensitization of AC2 and AC5. Heterologous sensitization of adenylyl cyclases is an adaptive cellular response developed after chronic activation of $G\alpha_{i/o}$-coupled receptors that causes an enhancement of AC activity (Brust et al., 2015a). The role of Gβγ subunits has been previously shown to be essential for heterologous sensitization (Conley and Watts, 2013; Ejendal et al., 2012; Nguyen and Watts, 2006), so the ability of the CD8 -C2-20 minigene to inhibit this adaptive mechanism was assessed in HEK293 cells expressing D2R and AC2 or AC5. As it had been previously shown, expression of CD8-βARKct completely abolished the sensitized response of both AC2 and AC5 after PMA or forskolin activation, respectively. Somewhat

surprisingly, expression of the CD8-C2-20 failed to suppress the enhancement of AC2 and AC5 activity (**Fig. 3.6**).

Next, the ability of the CD8-C2-20 minigene to interfere with the Gβγ activation of GRK2 and subsequent β-arrestin recruitment to the D2R was examined. DiscoveRx CHO-D2L cells stably expressing D2R and β2-arrestin tagged with the enzyme fragments of the β-galactosidase enzyme were transiently transfected with CD8-C2-20, CD8-βARKct, or Venus. Using the Path Hunter technology, β2-arrestin recruitment was readily detected after transfected cells were incubated with increasing concentrations of quinpirole **(Fig. 3.7)**. Expression of the CD8-C2-20 and CD8-βARKct minigene partially attenuated β2-arrestin recruitment when compared to Venus expression (**Fig. 3.7b**). The potency of quinpirole was similar for all transfection conditions **(Table 3.2)**, suggesting that neither CD8-βARKct or CD8-C2-20 altered the ability of the agonist to bind the receptor. The modest changes in the efficacy of quinpirole to recruit β2-arrestin when CD8-βARKct and CD8-C2-20 minigenes are expressed presumably reflect a decrease of Gβγ-mediated activation of GRK resulting in less β2-arrestin recruitment.

Another major signaling event initiated after GPCR activation is mitogen-activated protein kinase (MAPK) ERK1/2 phosphorylation. Activation of the MAPK cascade by $G\alpha_{i/o}$-coupled receptors has been shown to be mediated by Gβγ subunits via at least three different mechanisms (Khan et al., 2013). One pathway involves Gβγ-induced stimulation of the phosphatidylinositol 3-kinase (PI3K) and the Src family kinase. A second mechanism is mediated by recruited β-arrestin that functions as a scaffolding protein, and a third pathway occurs through transactivation of receptor tyrosine kinases (RTKs) **(Fig. 3.8a)**. The effects on Gβγ-induced ERK 1/2 phosphorylation were examined in CHO cells transiently expressing Venus, CD8-C2-20 or CD8-βARKct after 10-minute activation of the D2R by quinpirole.

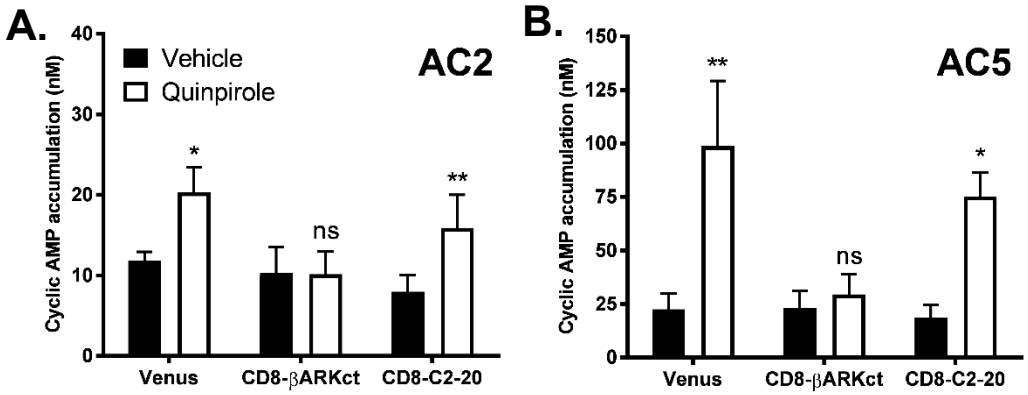

Figure 3.6 *CD8-C2-20 was unable to suppress heterologous sensitization of AC2 and AC5.*

HEK293 cells were transiently cotransfected with human AC2/AC5, the D2R and Venus (transfection control), CD8-βARKct or CD8-C2-20 minigene. After 48-hour transfection, cells were pretreated with 3 μM quinpirole for 2-hours followed by the activation of AC2 with PMA and AC5 with FSK in the presence of the D2R antagonist, spiperone. Data represents average and SEM of three independent experiments conducted in triplicate**.** Statistical significance was calculated using paired student's t-test. ns, not significant, *P < 0.05, **P < 0.01, compared to the cAMP levels of the vehicle-treated cells.

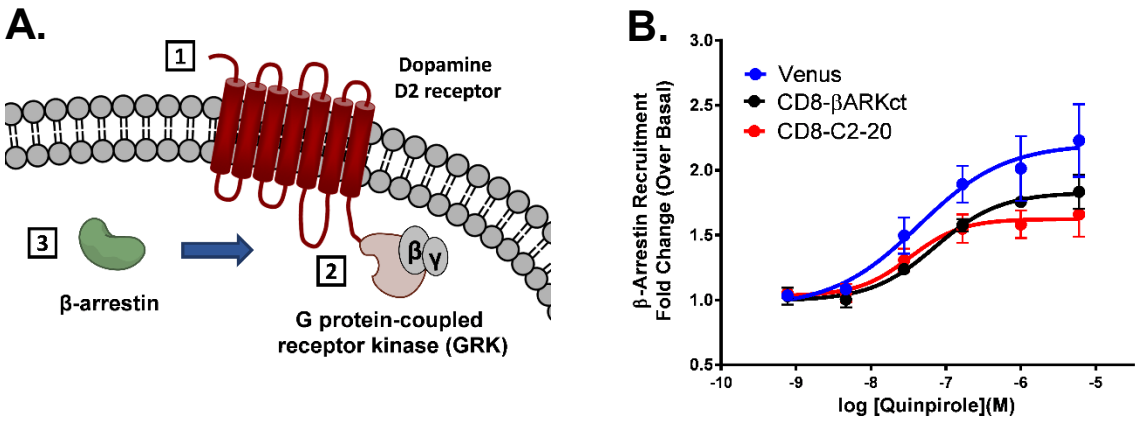

Figure 3.7 *CD8-C2-20 attenuated β-arrestin recruitment following D2R activation.*

(A) Schematic diagram of Gβγ-mediated recruitment of β-arrestin. After receptor activation **(1)**, Gβγ subunits recruit G-protein receptor kinases (GRKs) to the activated receptor **(2)** leading to subsequent recruitment of β-arrestin **(3)**. **(B)** PathHunter β-arrestin CHO cells from DiscoveRx stably expressing the D2R were transfected with Venus (blue), CD8-βARKct (black), or CD8-C2-20 (red). After 24 hours transfection, the cells were incubated in the presence of increasing concentrations of quinpirole, and β-arrestin recruitment was measured. Data is represented as mean and SEM of relative fold-change over basal levels of luminescence emission of each transfection condition. Fold change was calculated for at least four independent experiments conducted in duplicates.

Table 3.2 *EC_{50} and E_{max} values for β-arrestin recruitment to the D2R in the Path Hunter β-arrestin CHO cells.*

EC_{50} and E_{max} values were calculated from the curve fits of the quinpirole dose-response curves of **Fig. 3.7b**. [a] Relative fold-change of β-arrestin recruitment over the basal condition. Values reported in the table correspond to the average and SEM of the EC_{50} and E_{max} values calculated for at least four independent experiments.

Transfection	EC_{50} (nM) ± SEM	E_{max} (Fold change)[a]
Venus	51 ± 7	2 ± 0.2
CD8-βARKct	69 ± 24	1.8 ± 0.1
CD8-C2-20	40 ± 17	1.6 ± 0.1

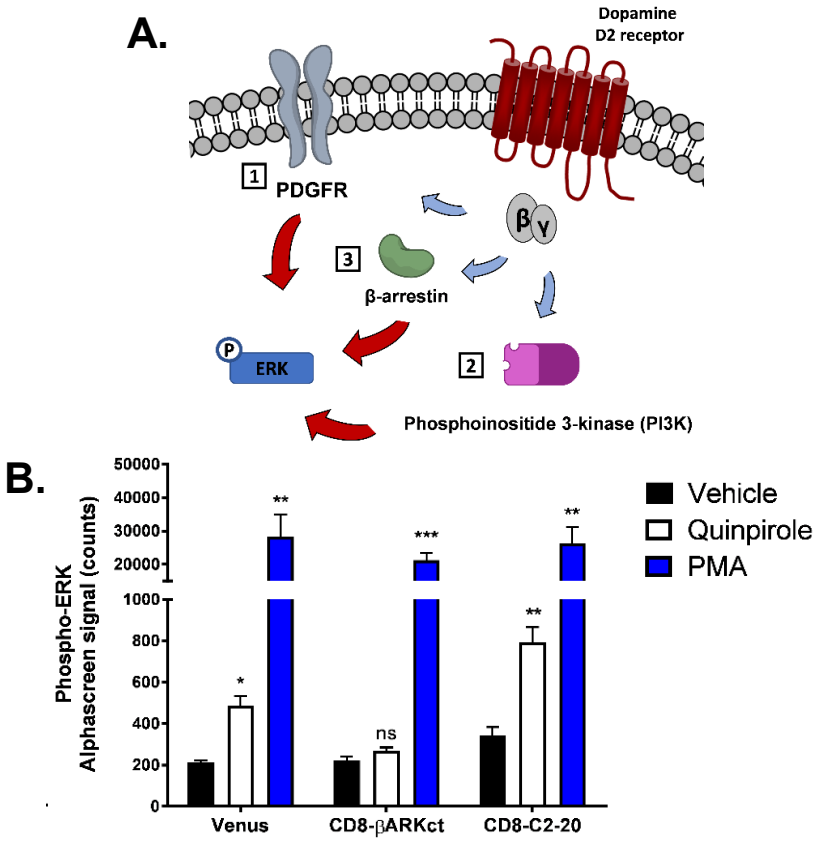

Figure 3.8 *CD8-C2-20 did not prevent Gβγ-mediated activation of ERK phosphorylation.*

(A) Gβγ subunits can promote ERK phosphorylation **(4)** by activating upstream effectors of the MAPK cascade such as platelet-derived growth factor receptor (PDGFR) **(1)** and phosphoinositide 3-kinase (PI3K) **(2)**, or by interacting with scaffold proteins such as β-arrestins **(3)** that also facilitate MAPK pathway activation. **(B)** CHOwt cells transiently expressed the dopamine D2 receptor in combination with Venus, CD8-βARKct, or CD8-C2-20. ERK phosphorylation was measured after 10-minute incubation with 3 μM quinpirole or 1 μM PMA (control) as indicated. Data represents the mean values and SEM of three independent experiments performed in duplicates. Statistical significance was calculated using paired student's t-test. ns, not significant, *P < 0.05, **P < 0.01, ***P < 0.001 compared to the pERK levels of the vehicle-treated cells.

Expression of CD8-βARKct completely blocked ERK 1/2 phosphorylation mediated by the D2R, but expression of CD8-C2-20 failed to halt the stimulatory effects mediated by Gβγ on phosphorylated ERK (**Fig. 3.8b**). However, no changes in total ERK levels (data not shown) or PKC-induced ERK phosphorylation levels were observed for the different transfection conditions.

3.4 Discussion

The Gβγ complex is a versatile modulator of adenylyl cyclase activity by having inhibitory or stimulatory effects depending on the AC isoform (Dessauer et al., 2017). Characterization of the specific binding interactions between Gβγ and AC isoforms suggest that multiple sites within the C1 and C2 domains of the cyclase cooperate to mediate the effects of the Gβγ complex (Diel et al., 2006). In the present work, an additional binding site for Gβγ on the C2 domain of AC2 was identified. This new Gβγ binding site on AC2, C2-20, resides next to the plasma membrane at the beginning of the C2a region. It displays high degree of homology between the related AC isoform family members that are conditionally activated by Gβγ subunits. SPR was to determine that the C2-20 domain binds to Gβγ with high affinity (K_D~2 nM)**.** Expression of a minigene encoding an N-terminal CD8 domain to localize the C2-20 peptide to the membrane reduced the stimulatory effects of Gβγ on PMA-stimulated AC2 activity. The effects of the minigene were specific to the C2-20 sequence considering that a scrambled version of the peptide sequence failed to abolish the Gβγ effects on AC2 activity. Alanine-scanning mutagenesis of the central portion of C2-20 diminished the inhibitory action of the CD8-C2-20 minigene on Gβγ-mediated AC2 potentiation. However, none of the variations incorporated were sufficient to abolish completely the inhibitory action on Gβγ stimulatory effects suggesting multiple contact points with Gβγ subunits. The effects of the C2-20 sequence display bias to Gβγ-mediated AC2 potentiation given that expression of the

CD8-C2-20 minigene only attenuated β-arrestin recruitment and had no effects on Gβγ-mediated heterologous sensitization of AC2 and AC5 activity or phosphorylation of ERK1/2.

The existence of multiple binding domains for Gβγ subunits on AC2 is particularly intriguing. Until now, five binding sites distributed across the C1 and C2 catalytic domains of AC2 have been reported. The C2-20 domain identified herein to interact with Gβγ is located upstream of the QEHA and KF loop binding regions also positioned within the C2 domain. From our results and the SPR analysis performed by *Boran et al.*, it appears that the C2-20 peptide has one of the highest binding affinities for the Gβγ complex compared to the peptides derived from the QEHA domain and the other three binding sites within the C1 domain. Similarly, the degree of homology of the C2-20 region (85%) among the Gβγ-stimulated ACs is very high, and it is of about the same extent as the sequence homology reported for the rest of the binding sites—except for the 578–602 region that is only shared between AC2 and AC4 (Boran et al., 2011).

Boran et al. also examined the ability of the Gβγ-binding peptides within the C1 domain to inhibit the effects on AC2 activity *in vitro*. Peptides derived from the 339-360 and 568-602 regions displayed inhibitory effects on $G\alpha_s$-mediated stimulation of AC2 activity (Boran et al., 2011). Expression of the CD8-C2-20 minigene did not alter the responses of AC2 to PMA. The C2-20 domain is distant from the $G\alpha_s$-binding sites and the PKC phosphorylation sites on AC2 (Berlot and Bourne, 1992; Shen et al., 2012), so the absence of effects on the stimulatory response to PKC activation implies that this region only interacts with the Gβγ complex. Considering that Gβγ effects are conditional to AC activation, and $G\alpha_s$ activates all AC isoforms, we used PMA to selectively activate AC2 activity in HEK293 cells. Previous studies examining the ability of the binding domains to inhibit the effects of the Gβγ complex on AC activity were done *in vitro* with Sf9 membranes, purified $G\alpha_s$ and Gβγ subunits. Hence, the degree of inhibition for the C2-20

peptide and the Gβγ binding domains on AC2 examined by *Boran et al.* cannot be adequately compared given that the stimulatory and assay conditions were significantly different. Nonetheless, our studies revealed that a minigene strategy could be used as an alternative approach to explore the activity of these inhibitory peptides on Gβγ in intact cells.

Gβγ subunits interact with a large set of proteins that are involved in diverse cellular processes (Khan et al., 2013). Protein-protein interaction studies on Gβγ and its effectors have revealed that various binding motifs on the effector proteins interact with a "hot spot" interface on the top surface of the Gβ subunit. Evidence to support the existence of the "hot spot" comes from the ability of synthetic peptides—either part of phage-display peptide library screens or derived from Gβγ effectors—to bind at the same surface of Gβ which prevents the interaction and inhibits the activity of more than one Gβγ-mediated pathway (Davis et al., 2005; Scott et al., 2001). For instance, when the QEHA domain of AC2 was characterized, it abolished potentiation of AC2 by Gβγ subunits, but it also inhibited other Gβγ-mediated effects on AC1, β-adrenergic receptor kinase (βARK), PLCβ3 and muscarinic K^+ channels (Chen et al., 1995). Consequently, a BLAST sequence similarity search was performed to determine whether other proteins contained similar regions to the C2-20 domain of AC2**.** As expected, the top three hits for the BLAST search were AC2, AC4 and AC7 (85% sequence similarity). They were followed by AC isoforms 5, 6 and 8, which was not totally surprising due to the high sequence homology of the AC cytosolic/catalytic domains. The juxtamembrane C2a domains of AC5, AC6 and AC8 displayed 50% sequence similarity with the C2-20 domain sequence of AC2 **(Fig. S3a)**. However, a closer evaluation of the sequence similarity revealed little conservation between AC5, AC6, and AC8 with the central portion of the C2-20 domain that based on our mutagenesis studies appears to be important for the inhibitory effects of the minigene on Gβγ. Thus, the absence of these residues may prevent or

disfavor the interaction of the juxtamembrane domains of AC5, AC6 and AC8 with Gβγ. No other known Gβγ effector was found among the hits of the BLAST sequence, but a domain near the membrane on the C-terminus of the orphan receptor GPR155 did show sequence homology (50% sequence similarity) with several amino acids of the C2-20 domain **(Fig. S3b)**. Although no interaction between Gβγ and GPR155 has been previously reported, it is curious that both homologous regions are positioned at similar locations on their respective membrane-bound proteins.

The location of the C2-20 domain is perhaps the most interesting feature of this new Gβγ-binding site. Analogous to the 564-602 domain within the C1b region of AC2, the C2-20 domain is adjacent to the membrane and precedes the C2 catalytic domain. The crystal structure of the mammalian AC catalytic domains in complex with $G\alpha_s$ and forskolin did not include the juxtamembrane cytosolic sections (Tesmer et al., 1997). However, a crystal structure recently solved for the cytosolic domains of a homologous membrane-bound mycobacterial AC indicates that the regions preceding the catalytic domains adopt a helical structure (Vercellino et al., 2017). Increasing evidence has emerged suggesting that these helical domains play an important role mediating the effects of AC regulators. For instance, polymorphisms identified in patients with familial dyskinesia and facial myokymia that are located within the helical domains of AC5 cause an enhancement of the catalytic activity in response to $G\alpha_s$ (Chen et al., 2012). Also, a recent study identified a 19-residue domain part of the juxtamembrane helical structure of adenylyl and guanylyl cyclases that appears to be important for the dimerization of the catalytic domains. This helical domain also referred as cyclase transducer element (CTE), exhibits high level of diversity and it can engage in protein-protein interactions with other AC/GC helical domains (Ziegler et al., 2017). Because the C2-20 domain is located N-terminally to the C2 catalytic domain of AC2, it

is possible that one of the mechanisms by which Gβγ mediates an enhancement of the catalytic activity in response to $G\alpha_s$ or PKC activation is by directly interacting with a helical element of AC2. Although intriguing, future structural studies of this domain in AC2 or other mammalian ACs and the catalytic core are required to support this hypothesis.

Expression of the CD8-C2-20 minigene did not have major effects on other Gβγ-mediated pathways downstream of $G\alpha_{i/o}$-coupled receptor activation. No inhibitory effects on heterologous sensitization of AC2 and AC5 or ERK activation suggested, that unlike CD8-βARKct, the CD8-C2-20 minigene does not sequester the Gβγ complex and arbitrarily nullify all Gβγ-mediated events. Although Gβγ is important to mediate the sensitization paradigm (Ejendal et al., 2012), the enhancement of AC activity after chronic $G\alpha_{i/o}$ coupled receptor activation does not appear to involve a direct AC-Gβγ interaction (Watts and Neve, 2005). Thus, the inability of the CD8-C2-20 minigene to modulate heterologous sensitization of AC2 activity was not surprising, despite the inhibitory effects on Gβγ-mediated potentiation of AC2 after acute activation of the D2R.

Following GPCR activation, the Gβγ complex plays a critical role in receptor desensitization and subsequent signal termination. Interaction of Gβγ subunits with G protein-coupled receptor kinases (GRK) promotes phosphorylation of the GPCR's C-terminus which leads to β-arrestin recruitment and internalization of the receptor (Benovic et al., 1986; DebBurman et al., 1996). CD8-C2-20 partially attenuated the efficacy of quinpirole to recruit β-arrestin, however our control CD8-βARKct showed only a minimal reduction in β-arrestin recruitment. The modest effects of CD8-βARKct were unexpected and without a positive control, the results for the CD8-C2-20 are difficult to reconcile. Alternatively, the β-arrestin recruitment observed in the PathHunter β-arrestin CHO cells could have been induced by other mechanisms besides Gβγ-mediated binding and recruitment of GRK2/3. Gβγ-independent translocation of GRK2 to the

receptor has also been reported via phosphoinositide 3-kinase (PI3K), and in those experiments GR2K-ct (βARKct) also failed to prevent receptor desensitization (Naga Prasad et al., 2001; Vasudevan et al., 2013). Thus, a more direct detection method is required to validate the negative effects of the C2-20 domain on the Gβγ-GRK interaction and subsequent β2-arrestin translocation to the plasma membrane.

In conclusion, we have identified a new Gβγ-binding site on the C2a domain of AC2 that is highly conversed between Gβγ-stimulated ACs, exhibited a high affinity for the Gβγ complex, and could be used to selectively modulate Gβγ signaling in intact cells. These studies highlight further the complexities associated with AC signaling and the unique ways in which AC isoforms are modulated by Gβγ subunits. Considering that the physiological relevance for Gβγ regulation of AC2 activity is not understood yet, the CD8-C2-20 minigene could be used as a tool to selectively characterize the stimulatory effects of Gβγ on AC2, AC4 and AC7 activity.

CHAPTER 4. STRUCTURE ACTIVITY RELATIONSHIP STUDIES FOR INHIBITORS OF TYPE 1 AND TYPE 8 ADENYLYL CYCLASE ISOFORMS

Ca^{2+}/calmodulin-stimulated adenylyl cyclase isoforms AC1 and AC8 are potential targets for treating chronic pain, opioid dependence, and anxiety. In an effort to develop selective and potent AC1 inhibitors, the objective of this study was to carry out a series of structure activity relationship (SAR) studies on existing and novel selective inhibitors of AC1 and/or AC8 activity. First, we performed SAR studies using both commercially available and novel synthesized analogs of the selective AC1 inhibitor, ST034307. The SAR for the ST034307 analogs revealed structural features that were important for the compound's inhibitory activity as well as for the selectivity at AC1. Several ST034307 analogs had inhibitory activity on both AC1 and AC8, and one ST034307 analog surprisingly showed modest selectivity for AC8 over AC1. Complementary to the SAR analysis for ST034307, a 10,000-compound screen was also completed searching for novel scaffolds with inhibitory activity on AC1. Two promising scaffolds were identified that had robust AC1 inhibitory activity with IC_{50} values in the low micromolar range (2-10 μM). These two novel scaffolds displayed AC1 selective or dual AC1/AC8 inhibition. Further SAR analysis for the class of compounds that had shown inhibitory activity at both AC1 and AC8, generated analogs with improved potency and efficacy at both Ca^{2+}/calmodulin-stimulated cyclases. However, no apparent trend was distinguished that would justify the improvement in selectivity or/and potency of the analogs. The inhibitory mode of action of these two scaffolds was also examined on different AC1 and AC8 stimulatory mechanisms (forskolin) using membrane preparations. In conclusion, we have identified potent inhibitors of AC1/AC8 activity, and the SAR results suggest that the

selectivity at AC1 or AC8 has a structural relationship; this information can be then applied to the design and synthesis of more potent and selective AC inhibitors with drug-like properties.

4.1 Introduction

Cyclic AMP and Ca^{2+} are major secondary messengers inside the cell that transmit signals intracellularly to coordinate various vital cellular responses. The understanding of the regulatory mechanisms of the cAMP and Ca^{2+} pathways have indicated that these two pathways are not independent, and cross-talk between them creates a dynamic signaling network that adds another level of complexity that the cells use to fine-tune a response (Bruce et al., 2003). Crosstalk between cAMP and Ca^{2+} is bidirectional, and it involves multiple different elements within each signaling pathway that directly or indirectly orchestrate a signaling event.

Adenylyl cyclases are the enzymes that synthesize cAMP and depending on the AC isoform, their catalytic activity is stimulated or inhibited by Ca^{2+} (Tang and Hurley, 1998). The major role of transmembrane ACs is to integrate GPCR signaling from receptors coupled to $G\alpha_s$ and $G\alpha_i$, but the differences in Ca^{2+} responsiveness among AC isoforms is also a major regulatory property that underlies isoform-specific cAMP responses (Sunahara et al., 1996). The structure of transmembrane ACs comprise a cytosolic N-terminus, two helical-spanning domains and the C1 and C2 catalytic domains. There are ten different mammalian AC isoforms, of which nine are membrane-bound (AC1-AC9), and one is cytosolic (sAC). The general mechanism of AC activation promotes the dimerization of the catalytic domains of the cyclase to create the active site of the enzyme at the C1-C2 interface (Tang and Hurley, 1998). Adenylyl cyclase isoforms 1 and 8 (AC1 and AC8) are stimulated by Ca^{2+} via the calcium-binding protein, calmodulin, whereas the soluble AC is directly activated by the divalent cation (Steegborn, 2014). On the contrary, AC2, AC4, AC7 and AC9 are Ca^{2+}-insensitive, and AC5 and AC6 are inhibited by micromolar

concentrations of Ca^{2+} (Dessauer et al., 2017). Thus, the direct and selective regulatory effects Ca^{2+} has on AC isoform activity is a major component that can modulate intracellular cAMP levels.

Ca^{2+} stimulation of AC1 and AC8 activity is mediated by the direct interaction of the cytosolic domains of the cyclase with calmodulin (Halls and Cooper, 2011). For AC1, the CaM binding site was found in the C1b domain, and for AC8, two binding sites were characterized: one at the N-terminus and the other at the C2 domain (Gu and Cooper, 1999; Levin and Reed, 1995). Although the precise mechanisms of AC1/AC8 activation by CaM have not been elucidated, it is clear that differential regulatory mechanisms coordinate the stimulatory effects of Ca^{2+}/Calmodulin on these two AC isoforms (Masada et al., 2012). Besides the difference in CaM-binding domains, the sensitivity to Ca^{2+} and the kinetics of catalytic activity in response to Ca^{2+}/Calmodulin also diverge between them. AC1 appears to be more sensitive to Ca^{2+} than AC8, but the amount of cAMP produced by AC8, as compared to AC1, is greater in response to Ca^{2+}/Calmodulin (Masada et al., 2009). Furthermore, the CaM domains that bind and regulate AC activity are not the same for AC1 and AC8 (Gu and Cooper, 1999; Macdougall et al., 2009; Vorherr et al., 1993). Consequently, Ca^{2+}/Calmodulin regulation of AC1 and AC8 activity does not appear to be functionally redundant.

The Ca^{2+}/Calmodulin-stimulated cyclases, AC1 and AC8, are highly expressed in the brain, so they represent a signal integration point of the cAMP and Ca^{2+} pathways in the central nervous system (Cali et al., 1994; Conti et al., 2007; Fagan et al., 1996). Indeed, AC1 and AC8 activity has been associated with memory and long-term potentiation. $AC1^{-/-}$ and $AC8^{-/-}$ double-knockout mice displayed memory deficits in passive avoidance and contextual learning assays, but single-knockout mice of either AC1 or AC8 exhibited modest or no impairment when performing the memory tasks (Ferguson and Storm, 2004; Wong et al., 1999). Studies with AC1 or AC8

single-knockout mice have also revealed that these two ACs also have isoform-specific functions. Studies with transgenic AC1-deficient mice suggested that AC1 plays a role in chronic pain, neurotoxicity, fragile-X syndrome and opioid dependence, whereas AC8-deficient mice showed that AC8 mediates anxiety-like behaviors (Bernabucci and Zhuo, 2016; Sethna et al., 2017; Vadakkan et al., 2006; Wei et al., 2002; Zachariou et al., 2008). Therefore, AC1 and AC8 have emerged as interesting targets for the treatment of various CNS disorders due to their isoform-specific physiological roles.

Particularly, the opioid crisis has driven the surge for novel druggable targets to treat chronic pain, whereby AC1 inhibitors represent a non-opioid based alternative option that bypasses Gαi inhibition through the opioid receptor to decrease cAMP levels. It was with the discovery of the first inhibitor of AC1 activity, NB001, that the active role of AC1 in pain mechanisms and the therapeutic potential of AC1 inhibitors was demonstrated (Zhuo, 2012). NB001, in accordance with the AC1 knockout studies, has elicited analgesic effects in various pain models and has reduced opioid dependence (Corder et al., 2013; Wang et al., 2011a). However, major limitations exist with this inhibitor since it lacks isoform-selectivity for AC1 over AC8, and its inhibitory effects appeared to be indirect given that in membrane preparations the inhibitor failed to reduce AC1 activity (Brand et al., 2013). Most recently, a selective AC1 inhibitor was identified that also exhibited antiallodynic effects in a mouse model of inflammatory pain (Brust et al., 2017). The ST034307 compound inhibited Ca^{2+}-mediated AC1 activity with a similar IC_{50} value as NB001 in the micromolar range, but it displayed much improved selectivity for AC1 over the rest of the membrane-bound AC isoforms. In addition, ST034307 appeared to engage the target since it displayed inhibitory effects on $G\alpha_s$ and calmodulin-mediated stimulation of AC1 activity in isolated membranes.

Hence, the objective of this research was to further optimize the pharmacological profile of the existing AC1 inhibitors by two approaches. In the first approach, a structure-activity relationship (SAR) analysis with commercially available and newly synthesized analogs of ST034307 was performed to determine whether the potency and overall selectivity of the AC1 inhibitor could be optimized. In the second approach toward identifying AC1 inhibitors, a high-throughput screen of a 10,000-compound library against AC1 was completed, and two promising scaffolds were identified that displayed robust AC1 inhibitory activity with IC_{50} values in the low micromolar range (0.5-10 μM). These novel and diverse scaffolds revealed both AC1-selective and dual AC1/AC8 inhibition. The AC1 and AC8 SAR analyses for ST034307 and the new scaffolds indicate that AC1 and AC8 selective inhibition has a structural relationship; this information can then be applied to the design and synthesis of more potent and selective AC inhibitors to create more drug-like compounds

4.2 Methods

4.2.1 Compounds

Commercially available analogs of the ST034307 compound were purchased as dry powders from Vitas-M laboratory (Champaign, IL), Enamine (Kiev, Ukraine), and TimTec (Newark, DE). The newly synthesized ST034307 analogs were designed and synthesized in the laboratory of Dr. Mingji Dai at the Department of Chemistry, Purdue University (West Lafayette, IN). Dry powders were resuspended in cell culture grade DMSO from Sigma-Aldrich (St. Louis, MO) to make 10 mM compound stocks. The compounds for the hit validation of the Life Chemical scaffolds and the counter-screen of the oxadiazole and pyrimidinone class of compounds were repurchased from Life Chemicals. Depending on the solubility of the compounds, dry powders were resuspended in DMSO to make a 10 mM or 50 mM stock solution. For the SAR analysis of the oxadiazole class

of compounds, analogs of the five lead compounds were designed and synthesized in the laboratory of Dr. Daniel Flaherty at the Department of Medicinal Chemistry and Molecular pharmacology, Purdue University (West Lafayette, IN). All the synthesized oxadiazole analogs were resuspended in DMSO to make 50mM stocks. The DMSO stock solutions were then aliquoted in microcentrifuge tubes that were stored in a -20°C freezer.

4.2.2 Compound screening

The compound screen was completed at the Biomolecular Screening and Drug Discovery Core Facility (BSDD), Purdue University (West Lafayette, IN) by Dr. Karin "Kaisa" Ejendal and Dr. Larisa Avramova. In a brief summary, cryopreserved HEK293 cells stably expressing AC1 (HEK-AC1) were counted and plated into a white opaque 384-well plate from Perkin Elmer (Waltham, MA). Cells were incubated for 1-hour in a 37°C incubator supplemented with 5% CO_2 to let the cells adhere to the plate prior incubation with the compounds. Subsequently, the positive control compound, ST034307, and the test compounds were added at a final concentration of 10 μM. Following a 30-minute incubation at room temperature with the compounds, the Ca^{2+} ionophore A23187 was added to the plates in the presence of the phosphodiesterase inhibitor, 3-isobutyl-1-methylxanthine (IBMX). After 1-hour incubation with A23187 at room temperature, cAMP accumulation was measured using the HTRF cAMP kit from Cisbio (Bedford, MA). The screen was carried out on three separate days and a total of 10,240 test compounds were screened. The percentage inhibition (%) was calculated by normalizing the cAMP levels of each of the compound wells to the mean cAMP levels of the positive control, ST034307 (100% inhibition) and vehicle (0% inhibition).

4.2.3 Cyclic AMP accumulation assays

Cryopreserved HEK cells overexpressing human AC1, AC2, AC5 or AC8 were transferred to a 15-mL Falcon tube and gently resuspended in prewarmed OptiMEM. The cells were centrifuged for 5 minutes at 150x g, then the supernatant was discarded, and the cell pellet was resuspended in 10 mL for a second centrifugation step. Then, the cells were counted, plated in a Perkin Elmer tissue culture–treated 384-well plate and incubated for 1-hour in a 37°C incubator supplemented with 5% CO_2. The test compound working solutions were prepared in prewarmed OptiMEM and the serial dilutions for the dose response curves were prepared using a Precision 2000 automated pipetting system. A 7-point dose response curve was generated for each test compound using a three-fold serial dilution starting at 30 μM concentration. After the 1-hour incubation at 37°C, the compounds were added and incubated for 30 minutes at room temperature. Next, in the presence of IBMX, AC1 and AC8 activity was stimulated with 3 μM A23187, AC2 activity was induced with 100nM PMA or AC5 activity was triggered with 1 μM forskolin. The Cisbio HTRF cAMP reagents, d2-labeled cAMP and the cryptate-labeled antibody, were added in equal parts to all the wells after 1-hour incubation with the stimulant at room temperature. Following 1-hour incubation with the cAMP detection reagents, fluorescence at 620nm and 665nm wavelengths were measured using a Synergy 4 or Cytation3 plate reader. Cyclic AMP accumulation per well was calculated by extrapolating the fluorescence 620/665 ratio from a cAMP standard curve.

4.2.4 Cell Toxicity assay

The cell toxicity assays were done in parallel with the cAMP accumulation assays on the HEK-AC1 cells at a single concentration of 30 μM compound, so the same protocol as the one described above was followed to plate and treat the cells. After 1-hour incubation with 3 μM A23187, cell viability was determined using the Cell-Titer GLO kit from Promega (Madison, WI) according to

the manufacturer's protocol. Following the addition of the Cell-Titer GLO reagent, the 384-well plate was protected from light and placed on an orbital shaker at a low shaking speed for 20 minutes. Luminescent signal was measured with a Synergy 4. Percentage viability was calculated by normalizing the luminescence counts of each of the compounds to the luminescence counts of the vehicle (100% viability) and the Triton X-100 (0% viability) treated wells.

4.2.5 Cyclic AMP Membrane assays

Membranes from the stable pool HEK-ACΔ3/6 cell lines overexpressing AC1 or AC8 were isolated as previously described (Brust et al., 2015b). The day of the assay, the cell membranes were thawed on ice and resuspended in washing buffer containing 2 mM Tris, 1mM EGTA and 1mg/mL of BSA. The membrane pellets were spun down at 10,000 x g for 10 minutes at 4°C, supernatant was discarded, and the centrifugation step was repeated two additional times. Following the final wash, the membrane pellet was resuspended in membrane buffer containing 33mM HEPES, 0.1% Tween 20, and 1mM EGTA. The Pierce BCA Protein assay kit was used to measure the protein concentration of the membrane suspension that was subsequently adjusted to 250 µg/mL for the AC1 membranes and 25µg/mL for the AC8 membranes. Membrane suspensions were plated in a white opaque 384-well plate at 10 µL/well, followed by the addition of 5 µL of compound at 120 µM (4x) concentration prepared in membrane buffer with no EGTA. Membrane suspensions were incubated for 20 minutes with the respective compound or vehicle prior the addition of 5 µL of increasing concentrations of forskolin prepared in stimulation buffer containing (4x): 33mM HEPES, 0.1% Tween 20, 10 mM $MgCl_2$, 1 mM ATP and 2mM IBMX at pH 7.4. Cellular membranes were incubated with the stimulants for 45 minutes at room temperature and cAMP accumulation was measured using the Cisbio HTRF cAMP detection kit as described above.

4.3 Results

4.3.1 Structure-Activity Relationship of ST034307 Analogs

ST034307 was discovered from the NDL-3000 natural derivatives library from TimTec as a selective inhibitor of the Ca^{2+}/calmodulin-stimulated cyclase AC1. ST034307 had no inhibitory activity on the other closely related and Ca^{2+}/calmodulin-stimulated cyclase AC8, but potentiated the cAMP responses of the Ca^{2+}-insensitive cyclase, AC2. To determine the functional groups important for the inhibitory activity and selectivity of ST034307, a structure–activity relationship (SAR) analysis for commercially available analogs of ST034307 was performed. HEK293 cells stably expressing human AC1 (HEK-AC1) or AC8 (HEK-AC8) were pretreated with increasing concentrations of the analogs prior to stimulation of AC1 and AC8 activity with the Ca^{2+} ionophore A23187. The IC_{50} and % inhibition values of each analog on AC1 and AC8-expressing cells is summarized in **Table 4.1.** All the ST034307 analogs that had a chromone scaffold but did not have trichloromethane at the 2-position of the ring, were inactive on AC1 and AC8. Also, the chloro substituent at position 6 of the chromone ring appeared to be irrelevant for the biological activity of the inhibitor since compound 307-1 had the same potency and efficacy as ST034307. Instead, analogs 307-2, 307-3 and 307-4 with substituents at position 6 and/or 7 of the ring displayed the same potency as ST034307, but partial inhibition of AC1 activity. Several compounds that had a flavone scaffold instead of the chromone showed inhibitory activity on both AC1 and AC8. Analogs 307-5, 307-6 and 307-7 with a flavone scaffold and a hydroxy substitution at the 3-position were less potent and efficacious on AC1 than ST034307, but inhibited AC8 activity by 50% at 30 μM concentration. Interestingly, analog 307-10 with two chloro substituents at the 6- and 8-position, inhibited by 50% both AC1 and AC8 activity at 30 μM, but showed modest selectivity for AC8 over AC1.

Table 4.1 *IC_{50} values and % inhibition of the commercially available ST034307 analogs.*

The IC_{50} values were calculated from the dose response curves generated for each corresponding compound in the HEK-AC1 and HEK-AC8 cells stimulated with the Ca^{2+} ionophore, A23187. The % inhibition values correspond to the normalized cAMP responses at 30 µM concentration of compound. Data represent the average of the calculated values of at least three independent experiments, each conducted in duplicate. NIO (no inhibition observed).

			HEK-AC1		HEK-AC8	
Compound ID	**Manufacturer's ID**	**Structure**	**IC50 - µM**	**% inhibition**	**IC50 - µM**	**% inhibition**
ST034307	ST034307	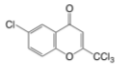	6.2 ± 0.3	101 ±1	NIO	-3 ± 3
307-1	ST034304	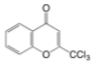	8.1	99	NIO	-1
307-2	STK806298	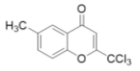	8.3	52	NIO	-9
307-3	STK020263	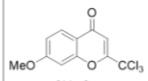	18	33	NIO	-17
307-4	STL298492	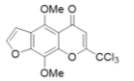	7.8	41	NIO	11
307-5	ST086622	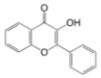	15	91	60 ± 28	57 ± 8
307-6	ST086116	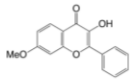	8.2	62	50 ± 34	38 ± 3
307-7	ST070866	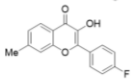	11	76	29 ± 15	43 ± 3
307-8	6-Chloro-7-methylflavone	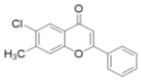	4.3	36	NIO	20
307-9	6-Chloroflavone	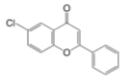	>100	44	>100	32
307-10	EN300-26779		>100	46	12 ± 2	56
307-11	6-Chlorochromone	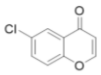	NIO	11	NIO	0
307-12	STK033957	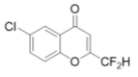	NIO	29	NIO	21
307-13	STK048907	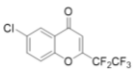	>100	37	NIO	26
307-14	BBL011926	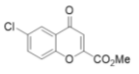	NIO	16	NIO	2
307-15	6-Bromo-2-methylchromone	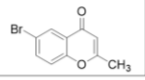	NIO	23	NIO	2

Further SAR studies were performed with ST034307 analogs that were designed based on the knowledge provided by the preliminary data with the commercially available compounds. The new ST034307 analogs primarily had substitutions at the 2-position of the chromone or had no hydroxy group at the 3-position of the flavone scaffold. **Table 4.2** summarizes the calculated IC_{50} and % inhibition values on AC1 and AC8 activity for the newly synthesized analogs. All the analogs were inactive or exhibited lower than 50% inhibitory activity at AC1 and AC8. The cell toxicity at 30 μM concentration was evaluated side-by-side with the cAMP assays for all the ST034307 analogs tested, and those that exhibited more than 30% cell toxicity were not included in the SAR comparisons/tables. Thus, the SAR studies revealed that the biological activity of ST034307 is strongly dependent on a trichloromethyl group at the 2-position of the chromone, and that ST034307 analogs also display a range of pharmacological profiles from partial inhibition of AC1 activity to AC8 selective inhibition (**Fig. 4.1**).

4.3.2 High-throughput screening for new AC1 inhibitors

The SAR analysis of the ST034307 analogs did not provide sufficient information to generate a strategy for lead optimization. Hence, a high-throughput screen of 10,000 compounds from the Life Chemicals library was completed to identify new AC1 inhibitor scaffolds. **Fig. 4.2** illustrates the flow from the high-throughput screen to the hit compound selection and validation. The Life Chemicals compounds were assayed at 10 μM concentration, and the ability of each to decrease A23187-mediated cAMP responses was assayed in the HEK-AC1 cells. The Z' value for the assay was 0.6. The cAMP levels detected for the negative control, DMSO, and the positive control, ST034307, were used as parameters to calculate the % inhibition of each compound. The % inhibition cut-off to defined hits was 90%, so 480 compounds met the criteria, representing approximately 5% of the whole library.

Table 4.2 *IC_{50} values and % inhibition of the newly synthesized ST034307 analogs.*

The IC_{50} values were calculated from the dose response curves generated for each corresponding compound in the HEK-AC1 and HEK-AC8 cells. The % inhibition values correspond to the normalized cAMP responses at 30 μM concentration of each compound. Data represent the average of the calculated values of at least three independent experiments, each conducted in duplicate. *Same IC_{50} value and % inhibition reported for ST034307 in Table 4.1. NIO (no inhibition observed).

			HEK-AC1		HEK-AC8	
Compound ID	Dai Lab's ID	Structure	IC50 - μM	% inhibition	IC50 - μM	% inhibition
ST034307 *	ST034307	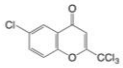	6.2 ± 0.3	101 ±1	NIO	-3 ± 3
307-16	KKB-2-026	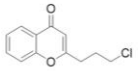	>100	49	NIO	27
307-17	KKB-2-015	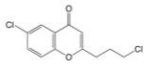	>100	49	>100	40
307-18	KKB-2-032	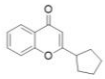	>100	36	NIO	27
307-19	KKB-2-033	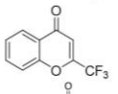	NIO	0	NIO	23
307-20	KKB-2-010	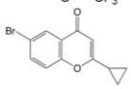	NIO	24	NIO	33
307-21	KKB-2-030	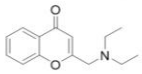	NIO	14	NIO	16
307-22	KKB-2-029	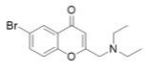	NIO	29	NIO	40
307-23	KKB-2-025	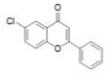	>100	62	>100	61
307-24	KKB-2-036	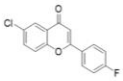	85 ±45	59	66 ± 20	80
307-25	KKB-2-037	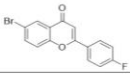	NIO	43	>100	52

	ST034307		307- 4		307- 3		307- 11		307- 7		307- 10	
	IC50 (µM)	% Inhibition	IC50 (µM)	% Inhibition	IC50 (µM)	% Inhibition	IC50 (µM)	% Inhibition	IC50 (µM)	% Inhibition	IC50 (µM)	% Inhibition
HEK-AC1	6.2	101	7.8	41	17.7	33	NIO	11	11	75	>100	46
HEK-AC8	NIO	- 3	NIO	-17	NIO	5	NIO	28	29	53	13	67

Figure 4.1 *ST034307 analogs displayed a range of pharmacological profiles from partial inhibition of AC1 activity to AC8 selective inhibition.*

IC_{50} values and percent (%) inhibition at 30µM concentration of a series of representative ST034307 analogs with different inhibitory activities on AC1 and/or AC8. The table values correspond to the mean of the calculated values already reported in Table 4.1. NIO (no inhibition observed).

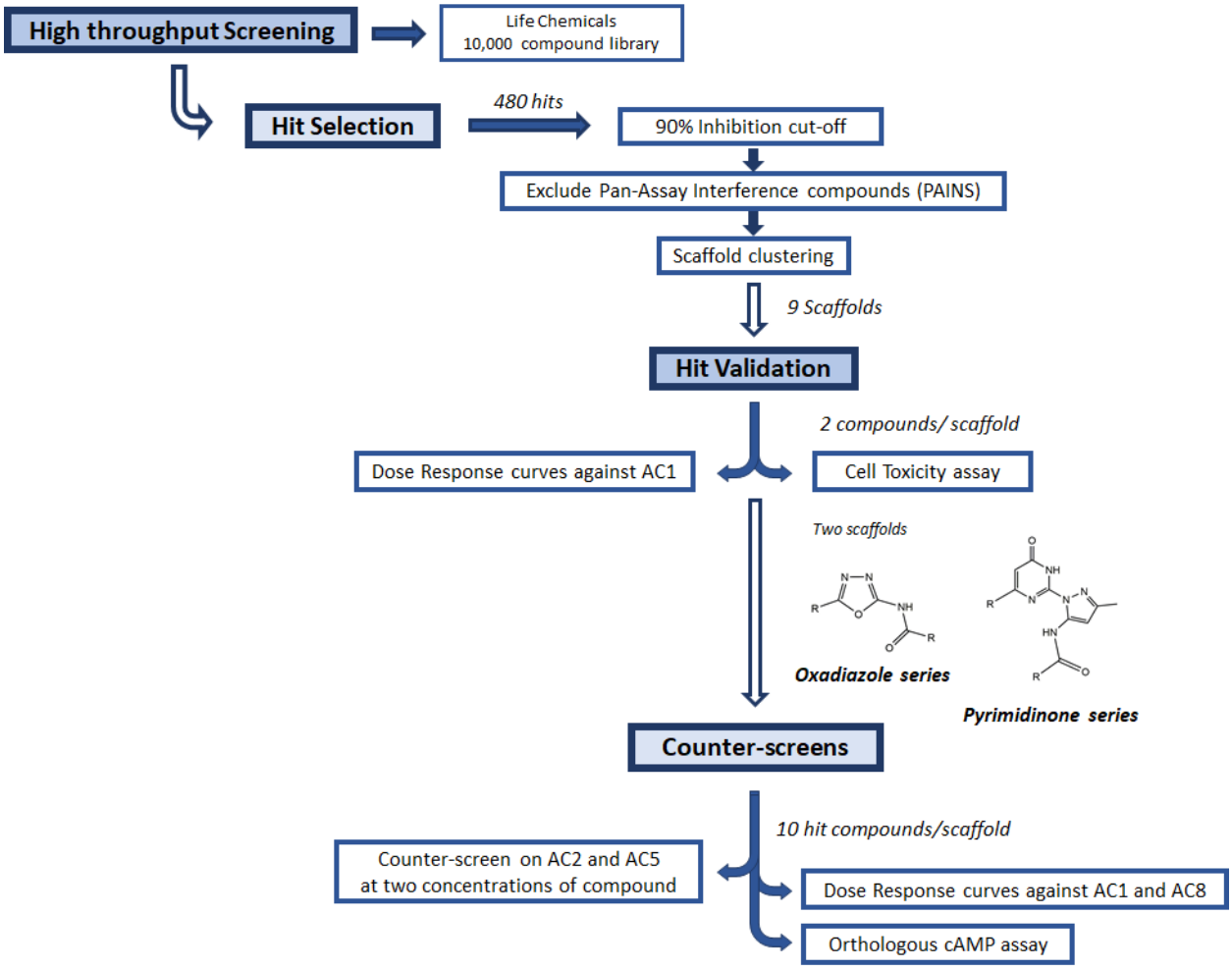

Figure 4.2 *Overview of the steps involved in the drug discovery process of the two novel AC1 inhibitor scaffolds.*

Additional parameters were considered to select the hit compounds taken forward due to the high hit rate. First, the list of 480 hit compounds was filtered for pan-assay interference compounds, or PAINS, and more than 200 apparent hits containing PAINS-like structures were excluded from further analysis (Baell and Walters, 2014; Baell and Nissink, 2018). Second, to prioritize and decrease the number of compounds for follow-up, hits that shared a similar scaffold were clustered and a total of nine groups were selected for further hit validation, each having at least 8 hit compounds (**Table 4.3**).

4.3.3 Hit Validation of AC1 Inhibitor Scaffolds

Dose response curves were generated in the HEK-AC1 cells for two "representative" compounds of each of the nine scaffolds. Cell toxicity of the compounds was also examined in parallel with the cAMP assays at a single concentration of 30 μM. IC_{50} and % inhibition values are reported in **Table 4.3** for those compounds that were not toxic to the cells. Out of the nine groups, five scaffolds were quickly discarded because they were either toxic to the cells (LC1, LC6, LC7 and LC8), or they interfered with the fluorescence of the cAMP detection technology (LC5). The compounds from the other 4 scaffolds, LC2, LC3, LC4 and LC7, showed IC_{50} values in the micromolar range and had no major effects on cell viability—except for one of the compounds of the LC4 group (F4385). Notably, the compounds from the LC2 and LC3 scaffolds had IC_{50} values in the single-digit micromolar range, displayed no toxic effects after 2-hour incubation period, and showed close to 100% inhibition of A23187-induced AC1 activity at 30 μM concentration. Hence, the LC2 and LC3 scaffolds also referred to as the oxadiazole and pyrimidinone series, respectively, were selected as the hit compound scaffolds for further validation and counter-screen.

Table 4.3 *IC_{50} values, % inhibition, and % viability of the two representative hit compounds from the nine clustered scaffolds.*

The IC_{50} values were calculated from the dose response curves generated for each corresponding compound in the HEK-AC1 cells. The % inhibition and % viability values correspond to the normalized cAMP responses (activity) or luminescence counts (viability) respectively at 30 μM concentration of compound. Data represent the average and ±SEM of the calculated values of at least three independent experiments, each conducted in duplicate. NIO (no inhibition observed).

				HEK-AC1		
GROUP	**# Hit compounds**	**Scaffold Structure**	**Compound ID**	**IC50 - μM (SEM)**	**% inhibition (SEM)**	**% Cell Viability**
LC1	28 compounds	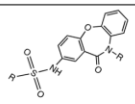	F2270-0225	ND	ND	≤ 30%
			F2270-0312	ND	ND	≤ 30%
LC2	42 compounds	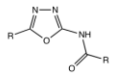	F0559-0097	4.7 ± 2	98 ± 1	125%
			F2289-0107	6.1 ± 0.4	96 ± 1	116%
LC3	22 compounds	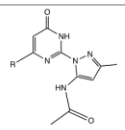	F2215-0216	2.1 ± 0.2	101 ± 0.3	98%
			F2215-0843	5.6 ± 2	99 ± 0.3	90%
LC4	13 compounds	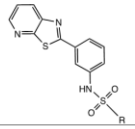	F0695-0056	14 ± 2	74 ± 1	58%
			F0695-0288	7 ± 3	92 ± 2	75%
LC5	8 compounds	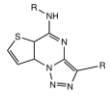	F2215-0216	Interferred with 620 nm and 665 nm fluorescence reads of the Cisbio HTRF cAMP assay		
			F2215-0843			
LC6	10 compounds	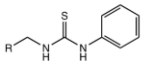	F0658-0069	ND	ND	≤ 30%
			F0667-0035	ND	ND	≤ 30%
LC7	8 compounds	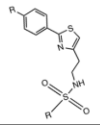	F2056-0011	ND	ND	≤ 30%
			F2056-0035	ND	ND	≤ 30%
LC8	8 compounds	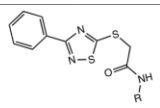	F0698-0027	5.6 ± 1	81 ± 3	80%
			F0698-0057	36 ± 3	54 ± 6	107%
LC9	7 compounds	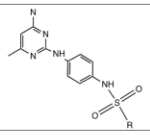	F2077-0633	ND	ND	≤ 50%
			F2078-0380	ND	ND	≤ 50%

4.3.4 Counter screen against AC isoforms

Having determined that the oxadiazole and pyrimidinone scaffolds inhibited Ca^{2+}/Calmodulin-stimulated AC1 activity in a dose-dependent manner, an additional set of 10 hit compounds per scaffold were repurchased as dry powders and included in the counter screen against the closely related AC8 isoform and other representative ACs (i.e. AC2 and AC5). Dose-response curves were generated for all hit compounds on AC1 and AC8-expressing cells to determine the selectivity of the inhibitory effects on the Ca^{2+}/Calmodulin-stimulated cyclases. The selectivity for other AC isoforms was examined at single concentrations of 10 μM and 30 μM of compound for the Ca^{2+}-insensitive and the Ca^{2+}-inhibited cyclase, AC2 and AC5 respectively. The results/effects on AC1, AC2, AC5 or AC8 activity of the oxadiazole and pyrimidinone class of compounds were summarized in **Table 4.4** and **Table 4.5,** respectively. The dose response curves on HEK-AC1 and HEK-AC8 cells indicated the oxadiazole compounds have dual AC1 and AC8 inhibitory activity on Ca^{2+}-mediated stimulation. The IC_{50} values of these set of compounds range on AC1 from 2 μM to 11 μM, and on AC8 from 5 μM to 60 μM. At the highest concentration tested (30 μM), the oxadiazole series inhibited AC1 activity close to 100% and AC8 activity by 70-80%. Compounds F9097, F3324, F4465, F8509, F9110 and F9189 were equipotent on AC1 and AC8, whereas the rest of the compounds showed modest selectivity for AC1 over AC8. The effect on AC5 of these compounds was comparatively much less on forskolin-stimulated AC5 activity, and only compound F8538 enhanced the AC5 response at 10 μM concentration. The structures of the 12 compounds of the oxadiazole series were significantly diverse, so no major conclusions could be drawn that would explain the differences in potency or selectivity. According to the dose response curves of the pyrimidinone series of compounds on AC1 and AC8, this scaffold appears to be selective for AC1.

Table 4.4 *IC_{50} values, % inhibition, and % viability of the oxadiazole hit compounds*

			HEK-AC1			HEK-AC8		HEK-AC2		HEK-AC5	
Compound ID	Life Chemicals ID	Structure	IC50 (μM) ± SEM	% Inhibition (30 μM) ± SEM	% Viability (30 μM)± SEM	IC50 (μM) ± SEM	% Inhibition (30 μM) ± SEM	% Inhibition (10 μM) ± SEM	% Inhibition (30 μM) ± SEM	% Inhibition (10 μM) ± SEM	% Inhibition (30 μM) ± SEM
F9097	F0559-0097	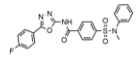	9.6 ± 2	98 ± 2	124 ± 0.2	11 ± 1	76 ± 11	5 ± 11	20 ± 1	(-)5± 20	20 ± 12
F9107	F2289-0107	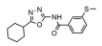	7.5 ± 2	99 ± 1	117 ± 1	57 ± 31	31 ± 12	(-)211 ± 95	(-)210 ± 65	(-)11 ± 15	(-)28 ± 33
F3324	F2273-0324	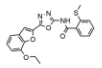	11 ± 2	94 ± 3	127 ±6	11 ± 4	76 ± 13	(-)23 ± 42	(-)34 ± 26	15 ± 9	18 ± 8
F4465	F1374-0465	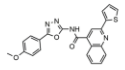	4.6 ± 1	101 ± 0.3	118 ± 3	5.6 ± 1	88 ± 9	(-)198 ± 96	(-)122 ± 57	(-)34 ± 18	(-)44 ± 12
F4036	F1374-1036	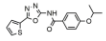	9.9 ± 1	97 ± 1	73± 3	NIO	24 ± 10	(-)95 ± 56	(-)122 ± 71	(-)15 ± 8	6 ± 26
F8011	F0608-0011	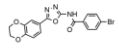	2 ± 0.2	101 ± 0.2	125 ± 3	18 ±2	79 ± 8	(-)168 ± 26	(-)7 ± 2	(-)48 ± 3	(-)10 ± 32
F8491	F0608-0491	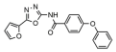	4.2 ± 0.4	100 ± 1	115 ± 3	19 ±4	78 ± 8	(-)175 ± 62	(-)103 ± 100	(-)42 ± 4	(-)24 ± 20
F8509	F0608-0509	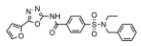	15 ± 2	87 ± 4	124 ± 1	11 ± 5	68 ± 13	8 ± 8	38 ± 6	13± 2	4 ± 8
F8538	F0608-0538	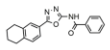	2.1 ± 0.4	101 ± 0.3	118 ± 6	21 ± 4	76 ± 8	(-)217 ± 120	(-)95 ± 69	(-)103 ± 36	(-)34 ± 12
F9110	F0559-0110	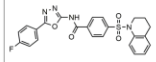	6.4 ± 1	98 ± 1	124 ± 3	5.3 ± 2	79 ± 13	(-)51 ± 32	(-)12 ± 11	(-)13 ± 3	14 ± 14
F9189	F0559-0189	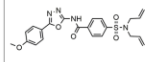	10 ± 3	89 ± 2	123 ± 2	7.9 ± 1	79 ± 13	(-)19 ± 22	5 ± 10	(-)6 ± 22	13 ± 1
F9346	F0559-0346	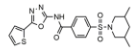	9.1 ± 2	99 ± 1	118 ± 2	17.7 ± 6	74 ± 13	(-)23 ± 7	(-)7 ± 16	(-)2 ± 7	4 ± 6

Table 4.5 *IC_{50} values, % inhibition, and % viability of the pyrimidinone hit compounds.*

			HEK-AC1			HEK-AC8		HEK-AC2		HEK-AC5	
Compound ID	Life Chemicals ID	Structure	IC50 (μM) ± SEM	% Inhibition (30 μM) ± SEM	% Viability (30 μM)± SEM	IC50 (μM) ± SEM	% Inhibition (30 μM) ± SEM	% Inhibition (10 μM) ± SEM	% Inhibition (30 μM) ± SEM	% Inhibition (10 μM) ± SEM	% Inhibition (30 μM) ± SEM
F5216	F2215-0216		1.8 ± 0.3	101 ± 0.4	103 ± 6	NIO	24 ± 14	(-)254 ± 144	(-)235 ± 124	(-)24 ± 22	(-)100 ± 29
F5843	F2215-0843		9.8 ± 0.3	98 ± 1	93 ± 1	NIO	8 ± 5	(-)123 ± 144	(-)210 ± 147	(-)10 ± 34	14 ± 14
F1003	F2181-0003	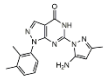	8.2 ± 1	98 ± 3	129 ± 6	38 ± 12	43 ± 8	10 ± 11	18 ± 14	38 ± 11	51 ± 2
F5053	F2215-0053		2.3 ± 1	101 ± 1	111 ± 1	NIO	22 ± 4	(-)173 ± 95	(-)95 ± 59	(-)24 ± 12	(-)39 ± 18
F5087	F2215-0087	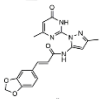	9.8 ± 1	90 ± 3	83 ± 2	30 ± 17	54 ± 6	(-)1 ± 2	(-)70 ± 40	5 ± 10	(-)7 ± 25
F5111	F2215-0111	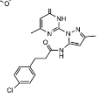	7.8 ± 2	100 ± 1	121 ± 0.2	NIO	25 ± 9	(-)84 ± 12	(-)177 ± 92	(-)9 ± 1	(-)17 ± 25
F5213	F2215-0213		0.5 ± 0.1	99 ± 1	101 ± 17	NIO	20 ± 18	(-)132 ± 59	(-)70 ± 68	(-)6 ± 12	9 ± 19
F5291	F2215-0291		1.1 ± 0.3	101 ± 0.3	109 ± 3	NIO	27 ± 12	(-)147 ± 56	(-)35 ± 18	(-)20 ± 14	8 ± 6
F5527	F2215-0527		2 ± 1	100 ± 1	95 ± 8	NIO	30 ± 9	(-)291 ± 143	(-)143 ± 107	(-)11 ± 10	(-)1 ± 25
F5600	F2215-0600		7.4 ± 0.3	98 ± 1	97 ± 7	NIO	23 ± 7	(-)71 ± 14	(-)303 ± 128	(-)4 ± 1	(-)13 ± 16
F5772	F2215-0772		0.9 ± 0.2	100 ± 0.2	81 ± 10	NIO	34 ± 7	(-)42 ± 10	32 ± 18	(-)2 ± 1	13 ± 24
F5954	F2215-0954		5.9 ± 0.4	99 ± 1	106 ± 14	NIO	35 ± 8	(-)39 ± 16	(-)185 ± 74	(-)7 ± 12	20 ± 8

Tables 4.4. and 4.5 continued

Tables 4.4. and 4.5 *IC_{50} values, % inhibition, and % viability of the oxadiazole and pyrimidinone hit compounds.*

The IC_{50} values were calculated from the dose response curves generated for each corresponding compound in the HEK-AC1 and HEK-AC8 cells stimulated with A23187. The % inhibition and % viability values correspond to the normalized cAMP responses (activity) or luminescence signal (viability) respectively. Negative % inhibition values indicate an enhancement of AC activity over the stimulant-induced cAMP responses. Data represent the average and ±SEM of the calculated values of at least three independent experiments, each performed in duplicate. NIO (no inhibition observed).

The IC_{50} values on AC1 activity range between 0.5 μM and 10 μM, and the maximum efficacy was 100% inhibition for all the pyrimidinone compounds at 30 μM concentration. The pyrimidinone scaffold showed less than 50% inhibition on AC8 activity at 30 μM concentration, and only for compounds F1003 and F5087 an IC_{50} value was calculated for AC8 inhibition. Compound F5213 is the most potent AC1 inhibitor of the two scaffolds with an IC_{50} value of 0.5 μM and at least 60-fold selectivity for AC1 over AC8. Similar to the oxadiazole series of compounds, the pyrimidinone scaffold exhibited mixed effects on AC2 and AC5, potentiating the activity of AC2 by 1 to 3-fold, but not having a significant effect on AC5 activity. Interestingly, compound F1003 seems to inhibit AC2 and AC5 activity, but with much lesser potency than AC1. The hit validation and counter screen with the oxadiazole and pyrimidinone class of compounds has confirmed the inhibitory activity of these two scaffolds on AC1 activity. Both scaffolds exhibit promising pharmacological profiles for AC1 or dual AC1/ AC8 inhibition. In addition, no other targets were found in the SciFinder Scholar and PubChem databases for the pyrimidinone scaffold, and only one study reported biological activity for the oxadiazole class of compounds as potential anti-prostate cancer agents (Mochona et al., 2016). Hence, the two scaffolds are suitable candidates for further hit expansion and lead optimization.

4.3.5 SAR analysis of the oxadiazole class of compounds

To understand the structural relationship of the dual AC1 and AC8 inhibition of the oxadiazole class of compounds, a SAR analysis was carried out with newly synthesized analogs. Five hit compounds, F8011, F8538, F9097, 9107 and F4036, were selected as the lead compounds to generate the SAR. The derivatives that were designed for each lead compound had modifications on the benzene substituent of the scaffold, whereas the direct substituents on the oxadiazole ring were kept consistent. The IC_{50} and % inhibition values for the analogs and lead compounds were

calculated from dose response curves generated on the HEK-AC1 and HEK-AC8 cells. In addition, the effects on AC2 activity and cytotoxicity of the compounds were also assessed at one or two high concentrations. **Supplementary Tables S2-6** report the biological activity of the oxadiazole derivatives and parent compounds at AC1, AC2, and AC8.

In general, the SAR studies with the derivatives of the lead compounds indicated that compounds with a naphthalene tetra hydro substituent at the 5-position of the oxadiazole ring, such as the parent compound F8538, tend to be more potent inhibiting AC1 activity than the other lead compounds that had a different functional group at the same position. Furthermore, substituents on the 3-, 4-, or 5-position of the benzene substituent increased the inhibitory activity of all the oxadiazole class of compounds at both AC1 and AC8. In particular, analogs that had a benzene ring or a trifluoromethyl group at the 2-position of the benzene substituent were more likely to be active at both AC1 and AC8.

For the set of analogs of the F9097 lead compound, IC_{50} values range from 1.4 μM to 29 μM for AC1, and 4 to 100 μM for AC8 (**Table S2**). No trend was observed for a position on the benzene ring substituent that would improve the potency or selectivity of the parent compound, however a substituent on the 2-position of the benzene ring (JK-246) was detrimental for the inhibitory activity on both AC1 and AC8. Various analogs showed improved potency against AC1 and a modest selectivity for AC1 over AC8 (7-fold), even though the parent compound appeared to be equipotent. An interesting feature of the F9097 hit compound was its reduced stimulatory activity on AC2; however, all analogs potentiated the activity of AC2 to the same extent that it was observed for the other hit compounds.

Adding substituents to the benzene ring considerably improved the inhibitory activity of the F8538 parent compound on AC8 (**Table S3**). For instance, compound JK-251 was equipotent for

both Ca^{2+}/calmodulin-stimulated cyclases with IC_{50} values of 1.2 μM (AC1) and 2 μM (AC8), and it displayed almost complete inhibition of the AC activity at 30 μM concentration. The analogs of the F8538 lead compound had IC_{50} values for AC1 between 1 μM to 26 μM, and for AC8 between 2 μM to 46 μM. Also, the resynthesized F8538 compound (DF-180) recapitulated the inhibitory activity of F8538, showing only a 2-fold difference in the IC_{50} values. Almost all the analogs of the F8538 series showed selectivity for AC1 over AC8, except for compound JK-265 that exhibited a 5-fold selectivity for AC8 over AC1. Unfortunately, all the analogs potentiated AC2 activity, and those that were the most potent at AC1 also strongly potentiated PMA-stimulated AC2 activity.

The resynthesized F9107 compound (DF-188) displayed the same IC_{50} value for AC1 but the IC_{50} value for AC8 was 3-fold less potent. The inhibitory activity of the F9107 derivatives was improved at both AC1 and AC8 compared to the parent compound (**Table S4**). Compound JK-252 exhibited equipotent activity on both Ca^{2+}/calmodulin-stimulated cyclases with an IC_{50} value of 1.4 μM, and together with the JK-251 analog are the most potent AC1 and AC8 inhibitors of the oxadiazole class of compounds. Compared to the other lead compounds and their corresponding analogs, the F9107 set of derivatives displayed consistently the highest selectivity for AC1 over AC8. Again, no major changes or trends were observed on the stimulatory effects of the analogs on AC2 activity compared to the F9107 parental compound.

The analogs for F8011 and F4036 did not exhibit significant differences in activity with the parental compounds, and resynthesized F8011(AK303) and F4036 (LH2-01) were slightly less potent than the hit compounds repurchased from Life Chemicals (**Table S5 and S6**). Thus, the efforts of the medicinal chemists were focused on the previously described lead compounds due to the little information drawn from the preliminary set of F8011 and F4036 analogs.

A total of 70 newly synthesized oxadiazole compounds were included in the SAR studies. **Fig. 4.3** exemplifies the most potent derivatives on AC1 from the five lead compounds evaluated. The SAR analysis established that the oxadiazole scaffold has dual inhibitory activity on AC1 and AC8, and depending on the substituents on the benzene ring, various ranges of IC_{50} values for AC1 and AC8 were observed. Furthermore, the SAR analysis indicated that the selectivity of the scaffold was predominantly for AC1 over AC8, but few analogs were equipotent or showed a modest selectivity for AC8.

4.3.6 Inhibitory activity of the new AC1 scaffolds is selective to Ca^{2+}/calmodulin-stimulated AC activity

To further characterize the inhibitory properties of the oxadiazole and pyrimidinone scaffolds, the ability to inhibit forskolin-mediated stimulation of AC1 and AC8 was examined in membrane preparations. Given that forskolin stimulates AC activity of all membrane-bound isoforms except for AC9, we used isolated membranes from a stable pool HEK-ACΔ3/6 cell line overexpressing AC1 or AC8 to ensure that the changes in cAMP levels were only from the overexpressed cyclase. Membranes were treated with increasing concentrations of forskolin in the presence or absence of the inhibitors (**Fig. 4.4**). The selective AC1 inhibitor ST034307 reduced the efficacy of forskolin-mediated activity in AC1 membranes but had no effect on the forskolin-induced cAMP responses of the AC8 membranes. Instead, the oxadiazole compound JK-211 and the pyrimidinone compound F5213 failed to inhibit forskolin-mediated responses in the AC1 and AC8 membranes, suggesting that the inhibitory action of both scaffolds in cells is selective on Ca^{2+}/calmodulin-stimulated AC activity.

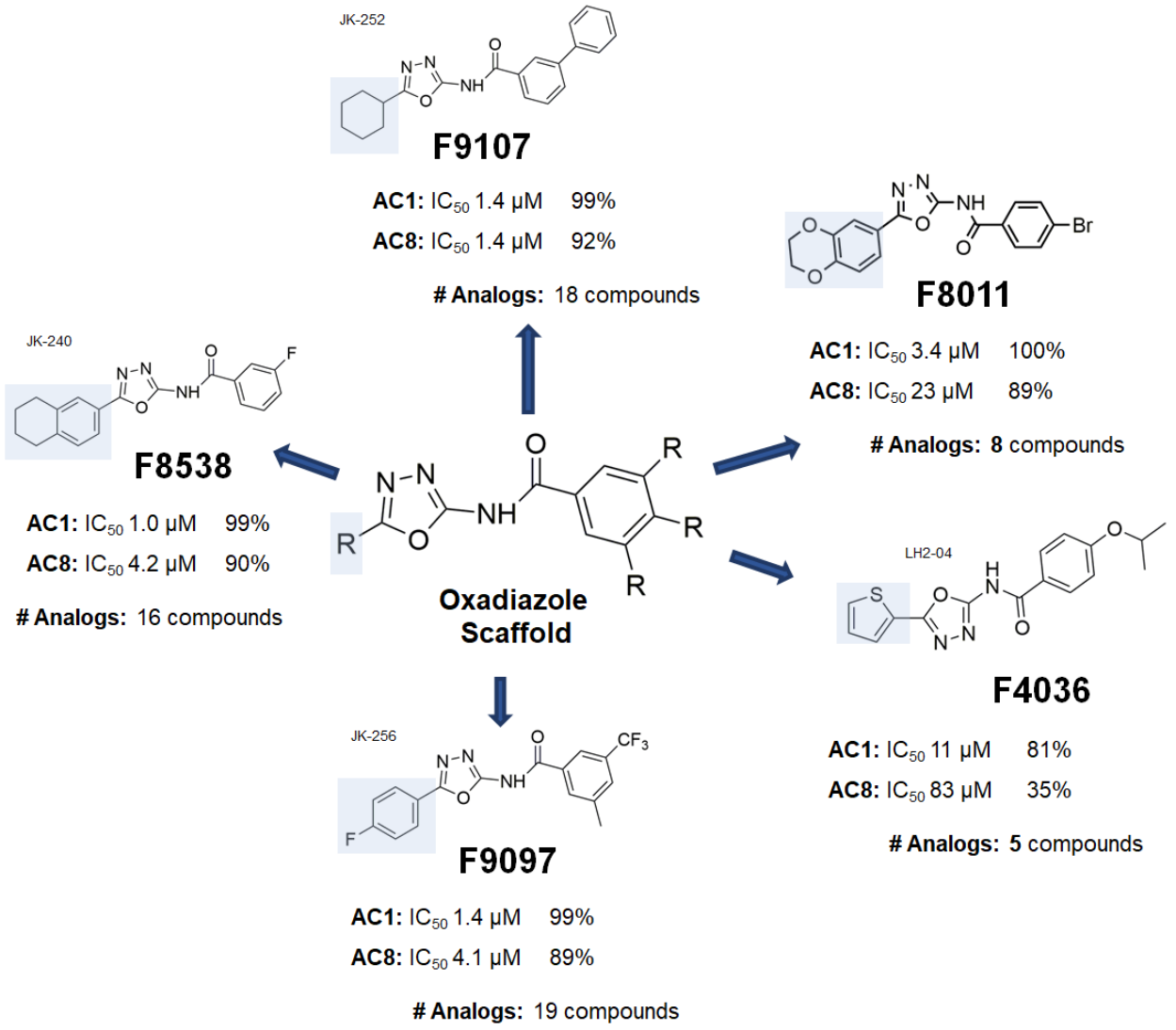

Figure 4.3 *Summary of the SAR analysis for the oxadiazole lead compounds*

On the oxadiazole scaffold structure, an R indicates the sites that were modified on the benzene ring substituent and/or the oxadiazole ring. The blue color structures designate the substituent on the 5-position of the oxadiazole ring that was unmodified on the parent compound and its respective analogs. The structure shown for each lead compound, corresponds to the most potent analog at AC1, and the % values correspond to the inhibitory activity on AC1 or AC8 at 30 µM concentration.

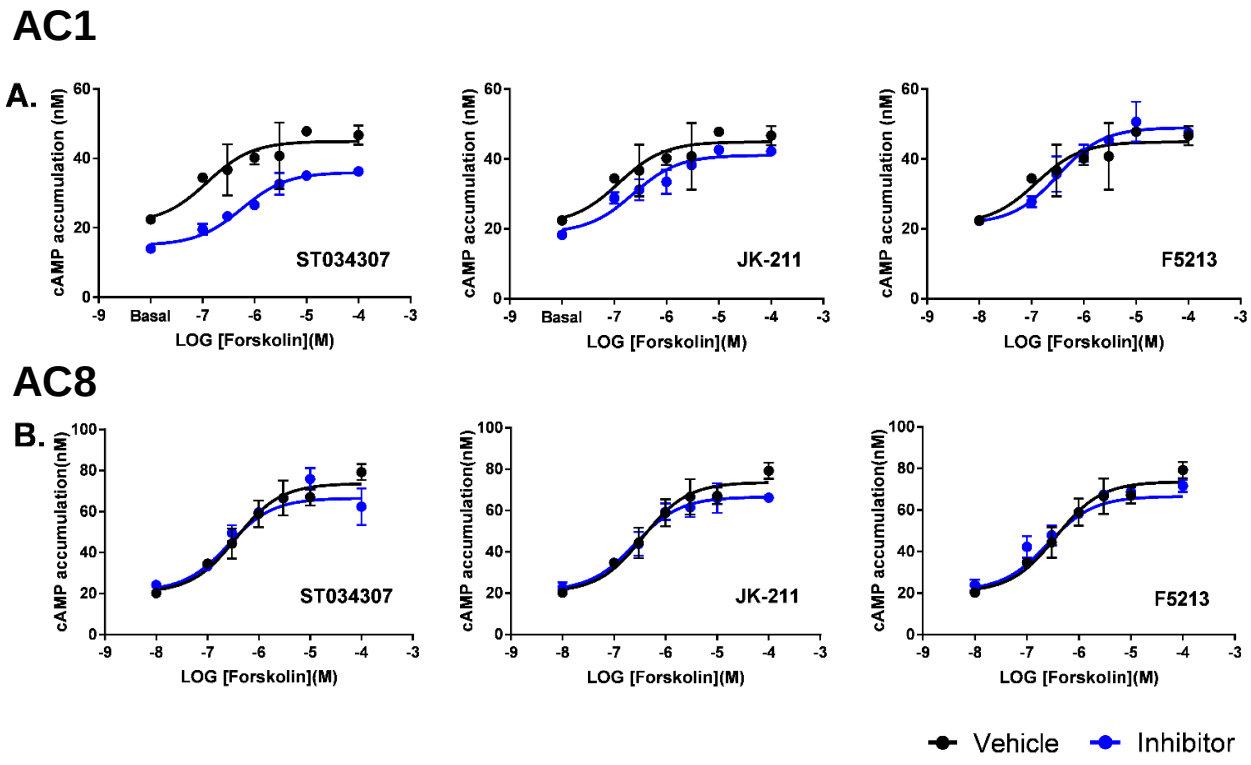

Figure 4.4 *Effects of AC1 inhibitors on forskolin-stimulated AC1 and AC8 activity in membrane preparations.*

Membranes isolated from HEK-ACΔ3/6 cells stably expressing AC1**(A)** or AC8 **(B)** were incubated with vehicle (black) or 30 μM inhibitor (blue) for 20 minutes prior the stimulation with increasing concentrations of forskolin in the presence of IBMX. After 1-hour incubation with the stimulant, cAMP accumulation was measured. Data represents the mean and SEM of at least two independent experiments conducted in duplicate.

4.4 Discussion

The specific physiological roles of Ca^{2+}/calmodulin-stimulated ACs, AC1 and AC8, have motivated the development of selective AC1 inhibitors for the treatment of chronic pain and opioid dependence. The discovery of AC1 inhibitors such as NB001 and ST034307 has demonstrated that AC1 is a druggable target with high potential to be an alternative method other than opioids for the effective treatment of chronic pain.

To further improve the potency and selectivity of ST034307, the starting point of the SAR analysis was by obtaining commercially available ST034307 analogs. The broad spectrum of inhibitory activities at both AC1 and/or AC8 of the analogs tested were the first indication that the selectivity of ST034307 for AC1 over AC8 had a structural-basis. Notably, these limited set of analogs revealed the crucial role of the trichloromethane group at the 2-position of the chromone ring for the biological activity and selectivity of ST034307 at AC1. Further expansion of the SAR with newly synthesized analogs also provided compelling data supporting the critical role of the trichloromethane substituent. In addition, the SAR analysis suggested that substitutions at positions 6 and 7 of the chromone ring affected the efficacy of the ST034307 analogs to inhibit AC1 activity. Interestingly, the ST034307 analogs with a benzene ring substituent at the 2-position of the chromone ring and a hydroxy group at position 3 displayed dual AC1 and AC8 inhibitory activity. In particular, the hydroxy substituent appeared to improve the biological activity of these chromone derivatives—also referred as flavones—at both AC1 and AC8. It is also worth noting that compound 307-10 stood out from the rest of the ST034307 analogs because it displayed modest selectivity for AC8 over AC1. The lack of activity at both AC1 and AC8 of the 307-11 compound with only a chloro substitution at position 6, suggests that the additional chloro modification at position 8 may be responsible for the selectivity of compound 307-10 at AC8. Hence, the preliminary SAR studies for the ST034307 analogs indicated that the inhibitory activity

of the chromone scaffold on Ca^{2+}/calmodulin-stimulated ACs has a structural relationship that can be modified for tuning selectivity between AC1 and AC8. Nonetheless, further characterization of the binding site for the ST034307 compound and its active analogs is also required to provide more compelling data that confirms the structure-selectivity relationship.

The strong dependence of the inhibitory activity on the trichloromethane moiety of the ST034307 compound and the limited evidence provided by the SAR to improve the potency and selectivity of the chromone scaffold, motivated the search for new scaffolds with improved AC1 inhibitory activity. Two promising scaffold clusters, oxadiazole and pyrimidinone class of compounds, were identified from the Life Chemicals library of 10,000 compounds that showed either selective inhibitory activity at AC1 or displayed dual inhibitory activity at AC1 and AC8. Despite the high hit rate (~5%) for the screen, reevaluation of the hit list by filtering to exclude compounds with PAINS-like structures, considerably reduced the number of initial hits. Likewise, clustering hit compounds with similar scaffolds enabled a fast validation of the promising scaffolds and provided certain confidence on the scaffold's activity. All the compounds part of the screening library that had an oxadiazole or pyrimidinone scaffold showed up as hits, and these two scaffold clusters contained the largest number of hit compounds among the nine scaffolds examined. Even though the 12 compounds tested per scaffold in the counter screen displayed a wide range of activities against AC1, AC2, AC5 and AC8, no SAR could be derived from the hit compounds due to their structural diversity. The different pharmacological profiles of the oxadiazole class of compounds suggest also a structural relationship between AC1 and AC8 selectivity—similar to the one observed for the chromone scaffold. Additionally, structural features were identified among the hit compounds that diminished the off-target effects on AC2 activity (i.e. F9097, F9110, F9189, and F9346). Furthermore, F5213—a pyrimidinone derivative—with sub micromolar

potency against AC1 coupled with its 60-fold selectivity for AC1 over AC8, makes it the most potent inhibitor to date of Ca^{2+}/calmodulin-stimulated AC1 activity.

The SAR campaign for the five lead compounds of the oxadiazole scaffold successfully led to the identification of several analogs with improved potency and inhibitory efficacy than the parent compound. The oxadiazole analogs, in general, were more potent on AC1 than AC8, however no trend was observed for a functional group or a given position on the benzene ring that would determine the potency and selectivity for either AC1 or AC8. Indeed, the effects a respective substituent on the benzene ring had on the inhibitory activity of the analog, differed depending on the functional group of the lead compound on the 5-position of the oxadiazole ring. For instance, the ethyl substitution on the 4-position of the benzene ring had opposite effects on the F8538 and F9097 lead compounds. For the F8538 analog, JK-251, the ethyl group improved the potency at AC8, but for the F9097 analog, JK-235, the same substituent reduced the potency against AC8 by 5-fold. Several analogs derived from the lead compounds are worth noting. For example, the JK-252 compound was equipotent against AC1 and AC8 with an IC_{50} value of 1.4 μM, whereas its parent compound, F9107, was 5x more potent at AC1 than AC8 with IC_{50} values of 6 μM and 27μM respectively. Conversely, the F9097 parent compound was equipotent at Ca^{2+}/calmodulin-stimulated ACs, but several of its analogs displayed selectivity for AC1 over AC8. Additionally, the reduced activity on AC2 of F9097 was not recapitulated by its analogs, suggesting that the sulfamoyl moiety at position 4 of the benzene ring is potentially responsible for the diminished activity on AC2 of hit compounds F9097, F9110, F9189 and F9346. Considering that the oxadiazole compounds were consistently more selective for AC1 over AC8, the F8538 analog, JK-265, is also particularly interesting because it appeared to be more selective for AC8 than AC1 (5-fold). Overall, the oxadiazole class of compounds displayed dual activity at AC1 and AC8, and

the modifications evaluated in the SAR analysis indicated that substitutions at the 3-, 4- and 5-positions of the benzene ring could modulate the activity/selectivity at AC1 or AC8.

Examining the inhibitory activity of the scaffolds on forskolin-mediated activity in HEK-ACΔ3/6-AC1 and HEK-ACΔ3/6-AC8 membrane preparations provided insightful information about the mechanisms of action of the scaffolds. In a general overview, compounds inhibiting cAMP production by competing with ATP for the active site should inhibit catalytic activity regardless of the stimulatory mechanism, or those compounds that bind to the transition state such as P-site inhibitors, their efficacy improves as the activity of the cyclase increments (Seifert et al., 2012). Thus, the inability of the oxadiazole and pyrimidinone scaffolds to inhibit forskolin-triggered cAMP responses in the isolated membranes indicate that the scaffolds are not P-site inhibitors, do not bind to the active site of the cyclase or compete for the forskolin-binding site.

The lack of inhibitory activity on forskolin-mediated activation at first would imply that the mechanism of inhibitory action of the two scaffolds is selective on Ca^{2+}/calmodulin-mediated stimulation of AC1 and/or AC8 activity. However, it also suggests that the inhibitory effects on AC1 and AC8 activity are indirect, and the target of the scaffolds is calmodulin and not the cyclase. A recent screen for inhibitors that would disrupt the protein-protein interaction between AC8 and calmodulin, identified a set of FDA-approved small molecules that inhibited AC1 and AC8 activity, but were ultimately calmodulin-binders (Hayes et al., 2017). Considering the potential indirect effects on calmodulin, a set of preliminary studies with the oxadiazole and pyrimidinone scaffolds were recently completed to determine whether the compounds were binding CaM. Comparison of the NMR spectra of ^{15}N-labeled calmodulin in the presence and absence of the scaffolds revealed that surprisingly both compounds directly bind calmodulin. The chemical shift perturbations observed for the two scaffolds were significantly different, indicating the scaffolds

have different binding mechanisms. Due to the dual inhibitory activity of the oxadiazole series, calmodulin was a potential target for this series of compounds, but it was unexpected that the pyrimidinone scaffold would be mediating its inhibitory effects via calmodulin since it exhibited potent and selective inhibitory activity at AC1 over AC8. Hence, further characterization of the AC1/8-CaM interactions is still required in order to establish the mechanism of action of the inhibitors and potentially elucidate how calmodulin inhibition mediate selective effects on AC1 over AC8 activity.

CHAPTER 5. CONCLUSIONS AND FUTURE DIRECTIONS

Adenylyl cyclases are key integrators of extracellular and intracellular signal inputs. The diverse mechanisms that regulate the catalytic activity of the membrane-bound ACs, together with the distinct subcellular localization of the AC isoforms, enable the control of distinct cAMP signaling events in an organized and dynamic manner (Arora et al., 2013).

To develop novel tools to characterize isoform-specific AC responses the work reported herein first accomplished the development of a CRISPR/Cas9-based cell line with remarkably low cAMP levels. Functional characterization of the HEK-ACΔ3/6 cell line demonstrated that all the stimulatory and inhibitory mechanisms previously described in the literature for the membrane-bound ACs can be recapitulated in this cell model (Dessauer et al., 2017). The improved signal window of the knockout cell line enabled the detection of distinct cAMP responses from all mAC isoforms by different stimulatory mechanisms, which was particularly exciting for AC7 and AC9 given that they do not show robust enough responses in the parental HEK293 cells (Brust et al., 2017). It also became more apparent with the HEK-ACΔ3/6 cells that AC isoforms don't exhibit the same cAMP responses to general activators of AC activity such as forskolin or $G\alpha_s$, so by having a cell model with low cAMP background, the specific isoform responses to forskolin and $G\alpha_s$ can be appropriately evaluated and distinguished in HEK-ACΔ3/6 intact cells or membranes. This becomes quite handy when trying to develop selective AC modulators because the HEK-ACΔ3/6 cell model, besides offering a platform to counter screen against all AC isoforms, it also enables the evaluation of AC inhibitors' activity on various stimulatory mechanisms. Furthermore, the human genetic background and the capability to examine cAMP accumulation in live-cells of our HEK-ACΔ3/6 cells, present some advantages to our knockout cellular model over the widely used Sf9 insect system that also exhibits low cAMP background levels.

Thus, the use of the HEK-ACΔ3/6 cells in combination with cAMP biosensors would be another interesting approach to further assess AC isoform specific responses as a result of subcellular localization or specific coupling with a GPCR or anchoring protein (Paramonov et al., 2015).

The comparison of the cAMP responses of the AC1wt and AC1 mutant constructs in the HEK293 cells and the HEK-ACΔ3/6 cell line, demonstrated that the HEK-ACΔ3/6 cell model is not only beneficial for ACs with low catalytic activity, but also for overactive ones. As it was evidenced with the AC1-N878A mutant, the forskolin dose response curves in the absence and presence of A23187 were different in the knockout and the parental HEK293 cell lines. Most recently a set of AC3 variants were identified that linked loss in AC3 activity with obesity (Grarup et al., 2018). Therefore, it would be interesting to pharmacologically characterize the responses to various stimulatory mechanisms in the knockout cells of these insensitive AC3 variants as well as other variants with enhanced AC3 activity to correlate the genetic findings with pharmacological data that potentially could provide insightful information for the development of novel therapies (Pitman et al., 2014).

For the work on chapter 3, it was startling to identify a sixth Gβγ binding site on AC2. SPR analysis confirmed the interaction of Gβγ with the highly conserved C2a domain shared between AC2, AC4, and AC7. Likewise, a minigene expressing an N-terminal CD8 membrane-anchoring domain followed by the C2-20 peptide, blocked Gβγ-mediated potentiation of AC2 activity. The identification of the C2-20 domain adds a third Gβγ binding site on the C2 catalytic domain. The high binding affinity and degree of sequence homology between AC2, AC4, and AC7 of the C2a region is similar to the one reported for the PFAHL domain (Boran et al., 2011). Considering that the PFAHL region is critical for Gβγ's stimulatory effects, and it requires an additional binding site on the C2 domain in order to be functional, the C2-20 domain could be the other binding

domain required to mediate with PFAHL the stimulatory effects of Gβγ (Diel et al., 2006). Mutagenesis studies based on the CD8-C2-20 variants or domain swapping for instance with the 50% homologous C2a domain of the Gβγ-inhibited AC8, may allow to disrupt the role of the C2a region on AC2 without affecting much the activity of the cyclase. However, it is important to keep in mind that not all domains that interact with Gβγ mediate its stimulatory effects. QEHA binds Gβγ, and it can inhibit various Gβγ-mediated signaling events, but it is not a required binding domain for conditional stimulation of AC2 given that a chimera of AC2 that does not have the QEHA binding site still gets stimulated by the Gβγ complex (Chen et al., 1995; Weitmann et al., 2001). Therefore, the role of the C2-20 domain may be important for the AC2-Gβγ interaction, but not to transduce the stimulatory effects of Gβγ on AC2 activity.

Our studies with the minigene are the first to examine the ability of Gβγ binding sites to prevent Gβγ-mediated potentiation of PMA-stimulated AC2 activity in intact cells. All of the rest of the studies with the other five Gβγ binding sites have evaluated *in vitro* the inhibitory effects of the peptide domains on $G\alpha_s$ stimulation in isolated membranes (Boran et al., 2011). Therefore, now that the HEK-ACΔ3/6 cell model was developed, it could be used to examine the inhibitory effects of the minigene on $G\alpha_s$-mediated activation of AC2, AC4, or AC7 activity, and to determine whether it can block the Gβγ effects on AC4 and AC7. Evaluating the Gβγ-mediated effects on both PMA and $G\alpha_s$ stimulation could provide insightful information that could justify the existence of multiple binding sites. Depending on the stimulatory mechanism and the corresponding induced-conformation of the catalytic domains, Gβγ by having multiple binding sites on AC2 may recognize multiple conformations of activated AC2.

Targeting the AC isoform regulatory mechanisms mediated by G-proteins, Ca^{2+} or protein kinases appears to be a reasonable strategy to develop selective AC isoform modulators.

Ca^{2+}/calmodulin-stimulated cyclases have emerged as potential targets for several CNS disorders, driving ongoing efforts to identify selective AC1 and/or AC8 inhibitors (Brust et al., 2017; Hayes et al., 2017). Hence, it was the goal of the work done in chapter 4 to improve the current pharmacological profiles of the known AC1 inhibitors. In a first approach, a SAR analysis was carried out for analogs of the selective AC1 inhibitor, ST034307. The limited set of commercially available analogs immediately indicated that the trichloromethane at the 2-position of the chromone ring is the functional group that determines the activity of the compound on AC1. The inability to identify other substitutions that were comparable to ST034307 discouraged us to keep expanding the SAR campaign for ST034307, so the Life Chemicals screen was our second strategy to improve the current chemical moieties acting on AC1. Out of 10,000 compounds, two scaffolds stood out after hit compound validation and counter-screens. The pyrimidinone series of compounds displayed AC1 selective activity and are to-date the most potent inhibitors of Ca^{2+}/calmodulin-stimulated AC1 activity. The other scaffold, the oxadiazole class of compounds, are dual inhibitors of AC1/AC8 and displayed a wide range of IC_{50} values, however they were mostly AC1 selective.

Unfortunately, after a preliminary evaluation of the inhibitory activity of the scaffolds in membranes and subsequent testing for calmodulin binding, it was determined that both scaffolds were not engaging the target and the inhibitory effects on AC1/8 activity were indirect and mediated by calmodulin inhibition. Further characterization at this point is required to determine whether the calmodulin inhibition is selective for AC activation or if there any other calmodulin targets that are also inhibited. Calmodulin is a small and flexible protein that interacts with more than 300 proteins including critical kinases and phosphatases that modulate various cellular processes. In order to take the oxadiazole and pyrimidinone scaffolds forward it is critical to

determine potential off-target effects on primary CaM effectors such as CaMKII or calcineurin. As it is the case for Gβγ, calmodulin might have distinct mechanisms of activation for various of its targets, so selectivity could still be achieved.

The chemical shift observed for the oxadiazole series resembles the NMR spectra detected for the calmodulin inhibitors identified in the screen of FDA-approved small molecules (Hayes et al., 2017). Interestingly, the NMR spectra of the F5213 compound suggested a single and definite interaction with CaM, so collaborators at the University of Iowa are in the process of assigning peaks to the calmodulin residues on the F5213 spectra in order to determine the binding site of the scaffold on the protein. Identifying the binding site and structure determination of the F5213 and CaM interaction is key in the process of designing the analogs for the future SAR campaign of the pyrimidinone class of compounds. Initially we thought unlikely that the pyrimidinone scaffold could bind calmodulin since the scaffold displayed a 60-fold selectivity for AC1 over AC8. However, the pyrimidinone scaffold could still achieve selectivity by targeting the distinct mechanisms of activation or by disrupting the unique calmodulin binding sites that mediate the interaction between CaM-AC1 and CaM-AC8. Consequently, further characterization of the mechanism by which the pyrimidinone scaffold prevents AC1 activity without having a major effect on AC8 needs to be explored. Protein-protein interaction studies with the catalytic domains of AC1 and CaM could be employed to determine whether the inhibitors disrupt the AC1-CaM interaction. Additionally, the action of both scaffolds on calmodulin might also explain the off-target effects of the compounds on AC2 activity. AC2 is activated by protein kinase C which in turn, is inhibited by the calmodulin-effector, CaMKII. Inhibition of calmodulin could inhibit CaMKII and subsequently disinhibit PKC. Therefore, we are evaluating whether in the presence of a PKC and CaMKII inhibitors the scaffolds still potentiate AC2 activity. Failure to potentiate

AC2 activity in the presence of the inhibitors would support the hypothesis that the target of the scaffold is calmodulin and the modulation of AC activity by these scaffolds are result of indirect effects.

APPENDIX A. SUPPLEMENTARY FIGURES

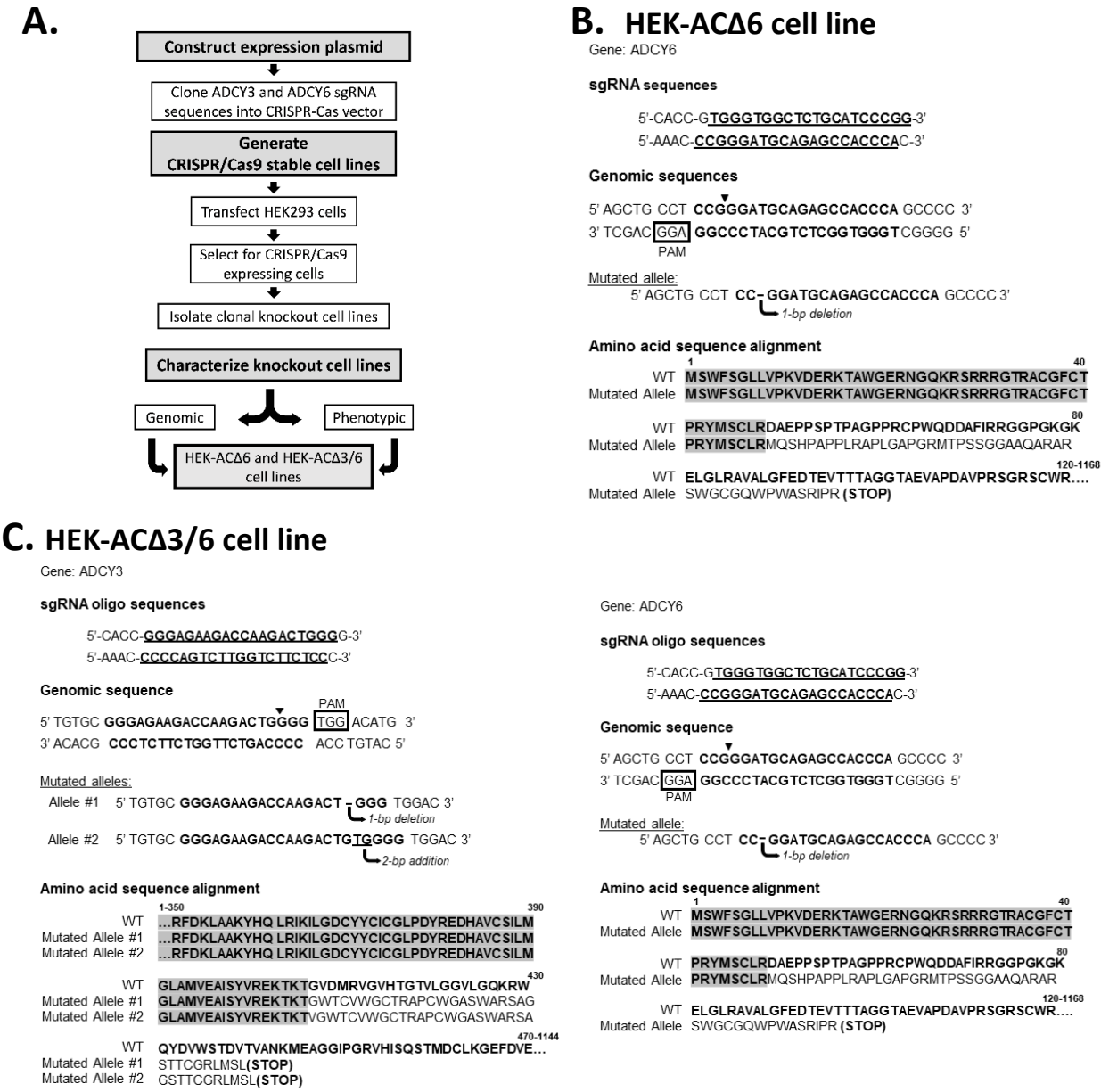

Supplementary Figure 1. *Genotypic characterization of HEK-ACΔ6 and HEK-ACΔ3/6 cell lines*

Schematic for the generation and characterization of the CRISPR/Cas9-based cell lines **(A)**. Genomic sequencing and predicted protein sequence alignment for the ADCY3 and/or ADCY6 edited genes in the HEK-ACΔ6 **(B)** and the HEK-ACΔ3/6 **(C)** cell lines. The sgRNA target sequences are in bold, and the black triangles indicate the Cas9-mediated cleavage site upstream of the PAM (box) sequence.

Supplementary Figure 1 continued

The resulting indels for the ADCY6 and/or ADCY3 genes were determined by sequencing a PCR product that contained the nuclease cleavage site from the genomic DNA of the clonal cell lines. The black arrows show the mutation (deletion/insertion) introduced for each allele of the targeted genes and the deleted/inserted base pairs are underlined. These indels caused a frame-shift on both ADCY3 and ADCY6 genes that introduced a premature STOP codon as illustrated by the amino acid sequence alignment between wild-type AC3 or AC6 and the predicted protein sequences of the mutated genes. Amino acid sequence for the wild-type genes are in bold and aligned regions with 100% identity are shaded in grey.

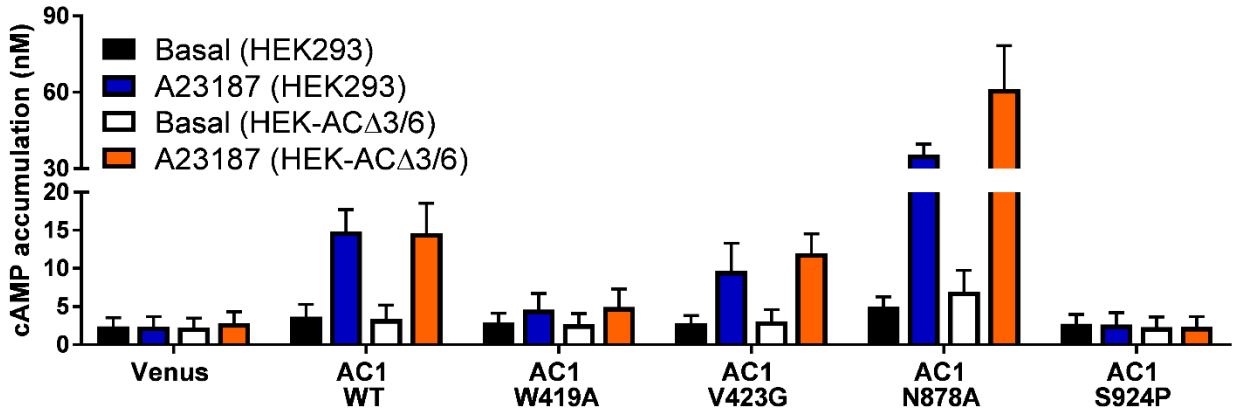

Supplementary Figure 2. *Cyclic AMP responses of AC1 mutants expressed in HEK293 and HEK-ACΔ3/6 cells elicited by the calcium ionophore, A23187.*

Cyclic AMP responses of HEK293 and HEK-ACΔ3/6 cells transiently transfected with Venus, AC1-WT, or a AC1 mutant constructs stimulated with 3 μM A23187 for 1-hour. Data represents the mean and SEM of at least three independent experiments conducted in duplicate.

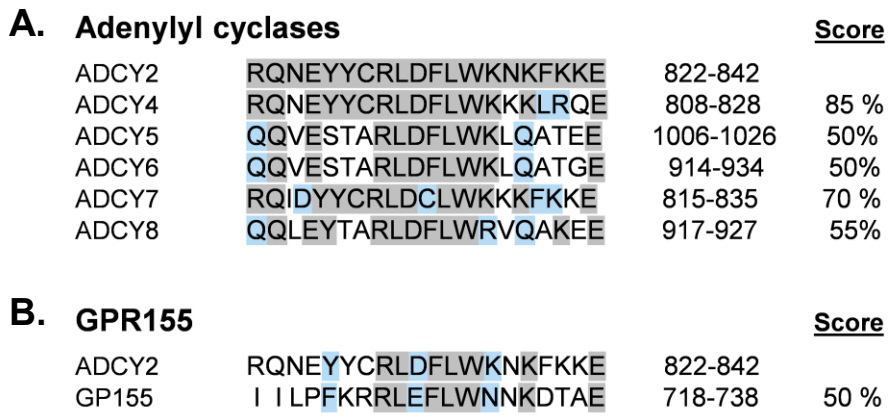

Supplementary Figure 3. *Sequence alignment between C2-20 sequence from AC2 and top hits of the BLAST search*

Amino acid sequences of **(A)** human AC2 (ADCY2), AC4 (ADCY4), AC5 (ADCY5), AC6 (ADCY6), AC7 (ADCY7) and AC8 (ADCY8) or **(B)** human AC2 (ADCY2) and GPR155 (GP155) were aligned with the EMBL-EBI Clustal Omega software. The scores reported represent the sequence similarity between each AC/receptor and AC2. Identical amino acids and amino acids with similar properties are highlighted in grey and light blue, respectively.

APPENDIX B. SUPPLEMENTARY TABLES

Supplementary Table S1. *Primer sequences for site-directed mutagenesis of CD8 (C2-20) variants*

Forward and reverse primer sequences designed for Q5 Site-Directed Mutagenesis using the NEBaseChanger tool from New England BioLabs. Lowercase letters indicate the base mismatches incorporated to introduce the desired mutation.

CD8-C2-20 Variants	Primer Sequence (5'→ 3')
RQN 1-3	**Fwd**-*cgcc* GAATATTACTGTAGGTTAGACTTCTTATG **Rev**-*gcggc* GGATCCCCTGTGGTTGCA
EYY 4-6	**Fwd**-*cgcc* TGTAGGTTAGACTTCTTATGG **Rev**-*gcggc* ATTCTGTCTGGATCCCCTG
CRL 7-9	**Fwd**-cgccGACTTCTTATGGAAGAACAAATTC **Rev**-gcggcGTAATATTCATTCTGTCTGGATC
DFL 10-12	**Fwd**-cgccTGGAAGAACAAATTCAAAAAAGAG **Rev**-gcggcTAACCTACAGTAATATTCATTCTG
WKN 15-17	**Fwd**-cgccAAATTCAAAAAAGAGTGAATGGC **Rev**-gcggcTAAGAAGTCTAACCTACAGTAATATTC
CD8-C2-17	**Fwd**-TGAGTAGACTCGAGCGGC **Rev**-GAATTTGTTCTTCCATAAGAAGTCTAAC

Supplementary Table S2. *IC_{50} values, % inhibition, and % viability of the F9097 analogs.*

			HEK-AC1			HEK-AC8			HEK-AC2	
Compound ID	Flaherty Lab ID	Structure	IC50 (μM) ± SEM	% Inhibition (30 μM) ± SEM	% Viability (30 μM) ± SEM	IC50 (μM) ± SEM	% Inhibition (30 μM) ± SEM	% Viability (30 μM) ± SEM	% Inhibition (10 μM) ± SEM	% Inhibition (30 μM) ± SEM
F9097	NA	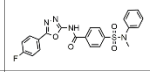	7.6 ± 1	94 ± 1	129 ± 14	10 ± 2	80 ± 2	111 ± 3	(-) 64 ± 11	(-) 32 ± 10
JK-256	JK2-AC1-056	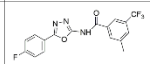	1.4 ± 0.2	99 ± 0.5	102 ± 10	4.1 ± 0.4	89 ± 2	71 ± 5	(-) 235 ± 41	(-) 158 ± 43
JK-255	JK2-AC1-055	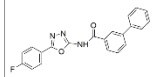	2.3 ± 0.4	98 ± 1	71 ± 8	7 ± 1	84 ± 3	31 ± 6	(-) 164 ± 25	(-) 102 ± 19
JK-257	JK2-AC1-057	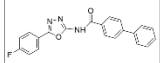	2.8 ± 0.6	97 ± 1	114 ± 4	7.5 ±1	90 ± 10	91 ± 3	(-) 204 ± 30	(-) 140 ± 16
JK-258	JK2-AC1-058	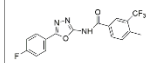	4.6 ± 2	93 ± 5	133 ± 26	9 ±5	75 ± 12	72 ± 8	(-) 182 ± 39	(-) 157 ± 33
JK-259	JK2-AC1-059	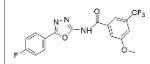	5 ±1	97 ± 1	108 ± 15	6 ± 1	80 ± 9	51 ± 3	(-) 191 ± 31	(-) 227 ± 72
JK-212	JK2-AC1-012	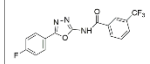	5 ± 1	99 ± 2	108 ± 20	29 ±1	58 ± 1	76 ± 11	(-) 339 ± 47	(-) 282 ± 76
JK-216	JK2-AC1-016	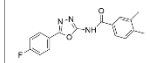	6.5 ±1	93 ± 4	95 ± 23	46 ±7	42 ± 4	99 ± 7	(-)301 ± 36	(-)347 ± 32
JK-220	JK2-AC1-020	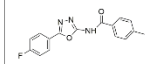	7.3 ± 2	80 ± 10	104 ± 1	61 ± 33	31 ± 6	89 ± 5	(-)237 ± 67	(-)341 ± 58
JK-235	JK2-AC1-035	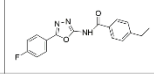	8.2 ± 2	88 ± 4	95 ± 12	51 ± 7	32 ± 12	86 ± 5	(-)180 ± 35	(-)236 ± 42

Supplementary Table S2 continued

			HEK-AC1			HEK-AC8			HEK-AC2	
Compound ID	Flaherty Lab ID	Structure	IC50 ± SEM	% Inhibition (30 µM) ± SEM	% Viability (30 µM) ± SEM	IC50 (µM) ± SEM	% Inhibition (30 µM) ± SEM	% Viability (30 µM) ± SEM	% Inhibition (10 µM) ± SEM	% Inhibition (30 µM) ± SEM
F9097	NA	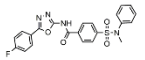	7.6 ± 1	94 ± 1	129 ± 14	10 ± 2	80 ± 2	111 ± 3	(-) 64 ± 11	(-) 32 ± 10
JK-244	JK2-AC1-044	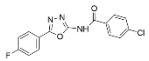	8.9 ± 1	76 ± 1	84 ± 5	ND	11 ± 9	85 ± 6	(-)163 ± 30	(-)194 ± 5
DF-167	DF1-167-AC1	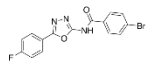	10 ± 1	78 ±3	103 ±1	71 ±18	33 ±3	98 ±8	(-)150 ±26	(-)221 ±14
JK-238	JK2-AC1-038	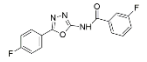	10.6 ±3	81 ± 7	104 ± 6	69 ± 11	35 ± 1	91 ± 5	(-)117 ± 19	(-)186 ± 13
JK-232	JK2-AC1-032	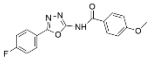	13 ±3	73 ± 4	82 ±5	ND	20 ± 6	NA	(-)76 ± 18	(-)97 ± 25
JK-223	JK2-AC1-023	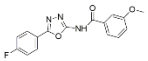	15 ± 4	79 ± 9	99 ± 10	101 ± 14	23 ± 5	106 ± 5	(-)134 ± 22	(-) 204 ± 42
JK-224	JK2-AC1-024	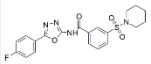	16 ± 4	83 ± 6	119 ± 14	39 ± 16	38 ± 7	122 ± 14	(-) 156 ± 32	(-)302 ± 52
JK-242	JK2-AC1-042	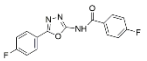	17 ± 2	64 ± 1	100 ± 7	ND	14 ± 3	92 ± 2	(-) 41 ± 28	(-) 86 ± 26
DF-164	DF1-164-AC1	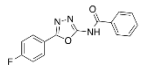	29 ±10	65 ±8	88 ±2	ND	8 ±2	94 ±10	(-)22 ±18	(-)129 ±28
JK-246	JK2-AC1-046	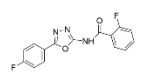	ND	12 ±4	87 ± 9	ND	13 ± 7	87 ± 2	3 ± 6	(-) 14 ± 8

Supplementary Table S3. *IC_{50} values, % inhibition, and % viability of the F8538 analogs.*

			HEK-AC1			HEK-AC8			HEK-AC2	
Compound ID	**Flaherty Lab ID**	**Structure**	**IC50 (μM) ± SEM**	**% Inhibition (30 μM) ± SEM**	**% Viability (30 μM) ± SEM**	**IC50 (μM) ± SEM**	**% Inhibition (30 μM) ± SEM**	**% Viability (30 μM) ± SEM**	**% Inhibition (10 μM) ± SEM**	**% Inhibition (30 μM) ± SEM**
F8538	NA	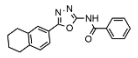	1.4 ± 0.2	101 ± 0.3	117 ± 9	12 ± 2	80 ± 3	87 ± 13	(-) 302 ± 32	(-) 255 ± 34
JK-240	JK2-AC1-040	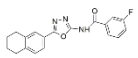	1.0 ± 0.3	99 ±0.4	94 ± 9	4.2 ± 0.2	90 ± 1	57 ± 7	(-)362 ± 26	(-)276 ± 34
JK-211	JK2-AC1-011	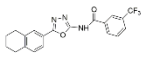	1.6 ± 0.2	100 ±1	84 ± 4	7.9 ±3	82 ±7	83 ±4	(-)571 ± 101	(-)449 ± 73
JK-251	JK2-AC1-051	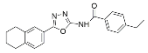	1.2 ± 0.2	98 ±1	114 ± 5	2 ± 0.4	88 ± 2	90 ± 2	(-)187 ± 32	(-)191 ± 59
JK-248	JK2-AC1-048	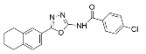	1.5 ± 1	99 ±1	97 ± 2	3.6 ± 0.4	90 ± 0.4	61 ± 5	(-) 204 ± 39	(-) 170 ± 26
DF-187	DF1-187-AC1	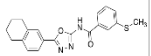	1.7 ±0.7	97 ± 4	137 ± 20	9.4 ±2	68 ±5	NA	(-)278 ± 18	(-)231 ±75
DF-180	DF1-180-AC1	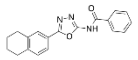	3.4 ±1	100 ±1	107 ±5	19.1 ±5	80 ±6	100 ±8	(-)214 ± 50	(-)196 ±8
JK-221	JK2-AC1-021	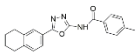	3.4 ± 1	100 ± 1	107 ± 27	25 ± 6	60 ± 8	113 ± 14	(-) 292 ± 39	(-) 275 ± 51
LH2-03	LH2-003	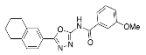	3.1 ± 0.4	99 ±0	111 ±46	25 ±4	55 ±3	NA	(-)358 ± 143	(-)283 ±97
JK-247	JK2-AC1-047	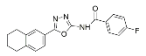	5.9 ± 1	98 ± 1	110 ±3	22 ± 4	74 ±8	88 ± 2	(-)222 ± 24	(-)244 ± 22

Supplementary Table S3 continued

			HEK-AC1			HEK-AC8			HEK-AC2	
Compound ID	Flaherty Lab ID	Structure	IC50 (μM) ± SEM	% Inhibition (30 μM) ± SEM	% Viability (30 μM) ± SEM	IC50 (μM) ± SEM	% Inhibition (30 μM) ± SEM	% Viability (30 μM) ± SEM	% Inhibition (10 μM) ± SEM	% Inhibition (30 μM) ± SEM
F8538	NA	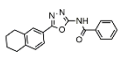	1.4 ± 0.2	101 ± 0.3	117 ± 9	12 ± 2	80 ± 3	87 ± 13	(-) 302 ± 32	(-) 255 ± 34
JK-234	JK2-AC1-034	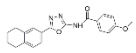	6.4 ±1	94 ± 2	121 ± 14	46 ±13	34 ± 11	NA	(-)246 ± 31	(-)305 ± 30
JK-265	JK2-AC1-065	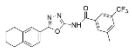	9.1 ±3	85 ±4	169 ±14	2.4 ± 0.02	78 ± 13	104 ±6	(-)89 ±18	(-)93 ±9
JK-267	JK2-AC1-067	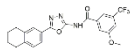	9.4 ±1	85 ±3	121 ±20	10 ±0.4	79 ±6	98 ±3	(-)42 ±14	(-)18 ±14
LH2-02	LH2-002	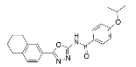	9.9 ±7	77 ±13	129 ±24	12.6 ±6	63±7	NA	(-)148 ±50	(-)118 ±1
DF-182	DF1-182-AC1	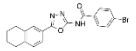	12.2 ±3	74±4	113 ±6	27 ±8	64±13	100 ±6	(-)217 ±24	(-)160 ±23
JK-266	JK2-AC1-066	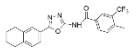	26 ±11	64±8	115 ±42	13 ±2	65 ±12	107 ±4	(-)137 ±36	(-)103 ±20

Supplementary Table S4. *IC_{50} values, % inhibition, and % viability of the F9107 analogs.*

			HEK-AC1			HEK-AC8			HEK-AC2	
Compound ID	Flaherty Lab ID	Structure	IC50 (μM) ± SEM	% Inhibition (30 μM) ± SEM	% Viability (30 μM) ± SEM	IC50 (μM) ± SEM	% Inhibition (30 μM) ± SEM	% Viability (30 μM) ± SEM	% Inhibition (10 μM) ± SEM	% Inhibition (30 μM) ± SEM
F9107	NA	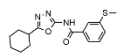	6.0 ± 1	96 ± 2	113 ± 3	27 ± 3	65 ± 4	97 ± 8	259 ± 30	(-) 305 ± 27
JK-252	JK2-AC1-052	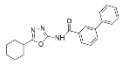	1.4 ± 0.2	99 ± 1	115 ± 7	1.4 ± 0.4	92 ± 1	86 ± 6	(-)388 ± 44	(-) 339 ± 74
JK-262	JK2-AC1-062	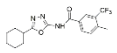	3.7 ± 1	100 ± 1	139 ± 8	7 ± 1	83 ± 7	77 ± 6	(-)341 ± 52	(-) 279 ± 56
JK-261	JK2-AC1-061	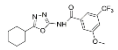	4.8± 1	90 ± 2	113 ±5	9 ±1	79 ±11	64 ±2	(-)180 ± 15	(-)203 ± 35
JK-210	JK2-AC1-010	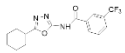	6 ±0.6	99 ±1	102 ±9	33 ±8	62 ±8	70 ±12	(-)414 ± 78	(-)570 ± 86
DF-188	DF1-188-AC1	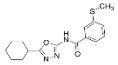	6.6 ±3	77 ±8	137 ±25	61 ±22	43 ±6	NA	(-)202 ±49	(-)216 ±46
JK-236	JK2-AC1-036	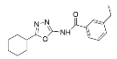	7.3 ± 3	91 ± 4	119 ± 5	71 ± 14	44 ± 7	96 ± 2	(-)279 ± 46	(-) 388 ± 36
JK-204	JK2-AC1-004	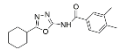	8.1 ±2	85 ±4	112 ±5	44 ±6	57 ±7	94 ±2	(-)557 ± 92	(-)684 ± 98
DF-166	DF1-166-AC1	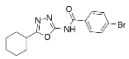	8.6 ±3	82 ±7	108 ±4	25 ±8	71 ±11	98 ±7	(-)188 ±35	(-)229 ±37

Supplementary Table S4 continued

			HEK-AC1			HEK-AC8			HEK-AC2	
Compound ID	Flaherty Lab ID	Structure	IC50 (μM) ± SEM	% Inhibition (30 μM) ± SEM	% Viability (30 μM) ± SEM	IC50 ± SEM	% Inhibition (30 μM) ± SEM	% Viability (30 μM) ± SEM	% Inhibition (10 μM) ± SEM	% Inhibition (30 μM) ± SEM
F9107	NA	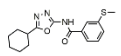	6.0 ± 1	96 ± 2	113 ± 3	27 ± 3	65 ± 4	97 ± 8	259 ± 30	(-) 305 ± 27
JK-260	JK2-AC1-060	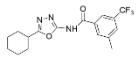	9.6 ±1	96 ±1	125 ±19	15 ±2	83 ±7	84 ±7	(-)136 ±21	(-)330 ±67
LH2-07	LH2-007	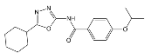	10.1 ±1	86 ±7	103 ±4	53 ±21	35 ±8	80 ±16	(-)193 ± 56	(-)496 ± 75
JK-239	JK2-AC1-039	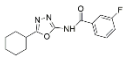	10.5 ± 2	79 ± 8	112 ± 5	ND	11 ± 3	94 ± 1	(-)124 ± 33	(-) 229 ± 30
JK-243	JK2-AC1-043	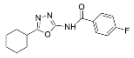	12.8 ±1	74 ±3	95 ±7	ND	7 ± 4	91 ± 4	(-)117 ± 10	(-)228 ± 19
JK-245	JK2-AC1-045	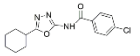	13.5 ± 2	71 ± 5	89 ± 11	ND	10 ± 12	88 ± 3	(-)122 ± 7	(-) 157 ± 18
JK-219	JK2-AC1-019	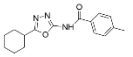	15.8 ± 2	78 ± 4	111 ± 9	ND	1 ± 12	94 ± 5	(-)276 ± 38	(-)411 ± 63
JK-233	JK2-AC1-033	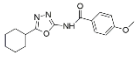	22 ±3	73 ± 1	80 ±2	ND	6 ± 16	NA	(-)65 ±13	(-)203 ± 39
DF-181	DF1-181-AC1	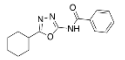	24.5 ±2	65 ±4	87 ±1	ND	3 ±6	93 ±11	(-)43 ±22	(-)199±43

Supplementary Table S5. *IC_{50} values, % inhibition, and % viability of the F8011 analogs.*

			HEK-AC1			HEK-AC8			HEK-AC2	
Compound ID	**Flaherty Lab ID**	**Structure**	**IC50 (μM) ± SEM**	**% Inhibition (30 μM) ± SEM**	**% Viability (30 μM) ± SEM**	**IC50 (μM) ± SEM**	**% Inhibition (30 μM) ± SEM**	**% Viability (30 μM) ± SEM**	**% Inhibition (10 μM) ± SEM**	**% Inhibition (30 μM) ± SEM**
F8011	NA	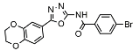	1.9 ± 0.2	101 ± 0.2	127 ± 7	12 ± 2	68 ± 3	106 ± 6	(-) 210 ± 32	(-)70 ± 26
AK303	AK3-003	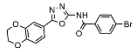	3.4 ± 0.6	101 ± 0.4	121 ± 1	23 ± 3	68 ± 0.5	117 ± 13	(-) 194 ± 35	(-)198 ± 49
JK-215	JK2-AC1-015	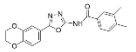	5.3 ± 0.4	100 ± 1	113 ±19	14 ± 3	61 ± 1	116 ± 14	(-) 401 ± 56	(-) 301 ± 58
JK-209	JK2-AC1-009	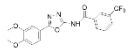	5.1 ± 0.7	100 ± 0.2	116 ±7	32 ±12	60 ±8	76 ±19	(-)283 ± 56	(-)339 ± 44
JK-230	JK2-AC1-030	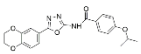	7.5 ± 0.7	88 ± 3	160 ±18	56 ± 23	39 ± 7	NA	(-)154 ± 16	(-)164 ± 21
JK-218	JK2-AC1-018	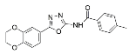	11.5 ±4	86 ± 11	98 ± 1	83 ±47	25 ± 6	90 ± 4	(-) 102 ± 35	(-)218 ± 32
DF-186	DF1-186	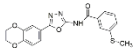	9.5 ±1	88 ± 5	109 ±3	76 ±39	37 ±9	72 ±17	(-)146 ± 26	(-)360 ± 59
JK-231	JK2-AC1-031	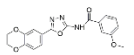	9.6 ± 3	84 ± 5	103 ±11	115 ±43	18 ± 10	NA	(-)178 ± 25	(-)283 ± 64
DF-178	DF1-178-AC1	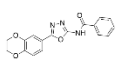	31 ± 3	60 ± 3	87 ± 8	102 ±26	24 ±7	94 ± 5	(-)276 ± 38	(-)411 ± 63

Supplementary Table S6. *IC_{50} values, % inhibition, and % viability of the F4036 analogs.*

			HEK-AC1			HEK-AC8			HEK-AC2	
Compound ID	Flaherty Lab ID	Structure	IC50 ± SEM	% Inhibition (30 µM) ± SEM	% Viability (30 µM) ± SEM	IC50 ± SEM	% Inhibition (30 µM) ± SEM	% Viability (30 µM) ± SEM	% Inhibition (10 µM) ± SEM	% Inhibition (30 µM) ± SEM
F4036	NA	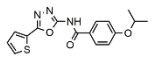	7.7 ± 1	93 ± 2	70 ± 3	33 ± 8	48 ± 4	49 ± 7	(-) 209 ± 49	(-) 247 ± 39
LH2-04	LH2-004	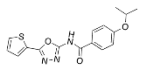	10.7 ±2	84 ±5	81 ±19	83 ±22	35±4	NA	(-)148 ±81	(-)214 ±38
LH2-01	LH2-001	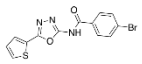	7.7 ±1	81 ±1	110 ±1	55 ±20	41 ±9	90 ±20	(-)167 ±46	(-)165 ±5
DF-189	DF1-189-AC1	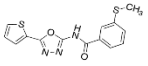	11 ±2	84 ±5	110 ±3	66 ±2	34 ±1	NA	(-)138 ±1	212 ±49
DF-191	DF1-191	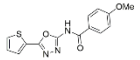	15 ±2	80 ±5	84 ±2	ND	10 ±7	55 ±19	(-)65 ±22	(-)209 ± 55
DF-178	DF1-183-AC1	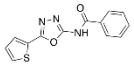	29 ±3	56 ±5	97 ±11	101 ±3	18 ±2	98 ±5	(-)134 ±35	(-)94 ±45

REFERENCES

Aldehni F, Tang T, Madsen K, Plattner M, Schreiber A, Friis UG, Hammond HK, Han PL and Schweda F (2011) Stimulation of renin secretion by catecholamines is dependent on adenylyl cyclases 5 and 6. *Hypertension* **57**:460-468.

Andressen KW, Norum JH, Levy FO and Krobert KA (2006) Activation of adenylyl cyclase by endogenous G(s)-coupled receptors in human embryonic kidney 293 cells is attenuated by 5-HT(7) receptor expression. *Mol Pharmacol* **69**:207-215.

Antoni FA, Wiegand UK, Black J and Simpson J (2006) Cellular localisation of adenylyl cyclase: a post-genome perspective. *Neurochem Res* **31**:287-295.

Arora K, Sinha C, Zhang W, Ren A, Moon CS, Yarlagadda S and Naren AP (2013) Compartmentalization of cyclic nucleotide signaling: a question of when, where, and why? *Pflugers Arch* **465**:1397-1407.

Atwood BK, Lopez J, Wager-Miller J, Mackie K and Straiker A (2011) Expression of G protein-coupled receptors and related proteins in HEK293, AtT20, BV2, and N18 cell lines as revealed by microarray analysis. *BMC Genomics* **12**:14.

Baell J and Walters MA (2014) Chemistry: Chemical con artists foil drug discovery. *Nature* **513**:481-483.

Baell JB and Nissink JWM (2018) Seven Year Itch: Pan-Assay Interference Compounds (PAINS) in 2017-Utility and Limitations. *ACS Chem Biol* **13**:36-44.

Bakalyar HA and Reed RR (1990) Identification of a specialized adenylyl cyclase that may mediate odorant detection. *Science* **250**:1403-1406.

Baldwin TA and Dessauer CW (2018) Function of Adenylyl Cyclase in Heart: the AKAP Connection. *J Cardiovasc Dev Dis* **5**.

Bauman AL, Soughayer J, Nguyen BT, Willoughby D, Carnegie GK, Wong W, Hoshi N, Langeberg LK, Cooper DM, Dessauer CW and Scott JD (2006) Dynamic regulation of cAMP synthesis through anchored PKA-adenylyl cyclase V/VI complexes. *Mol Cell* **23**:925-931.

Bayewitch ML, Avidor-Reiss T, Levy R, Pfeuffer T, Nevo I, Simonds WF and Vogel Z (1998) Inhibition of adenylyl cyclase isoforms V and VI by various Gbetagamma subunits. *FASEB J* **12**:1019-1025.

Beazely MA and Watts VJ (2005) Activation of a novel PKC isoform synergistically enhances D2L dopamine receptor-mediated sensitization of adenylate cyclase type 6. *Cell Signal* **17**:647-653.

Beazely MA and Watts VJ (2006) Regulatory properties of adenylate cyclases type 5 and 6: A progress report. *Eur J Pharmacol* **535**:1-12.

Bender AT and Beavo JA (2006) Cyclic nucleotide phosphodiesterases: molecular regulation to clinical use. *Pharmacol Rev* **58**:488-520.

Benovic JL, Strasser RH, Caron MG and Lefkowitz RJ (1986) Beta-adrenergic receptor kinase: identification of a novel protein kinase that phosphorylates the agonist-occupied form of the receptor. *Proc Natl Acad Sci U S A* **83**:2797-2801.

Berlot CH and Bourne HR (1992) Identification of effector-activating residues of Gs alpha. *Cell* **68**:911-922.

Bernabucci M and Zhuo M (2016) Calcium activated adenylyl cyclase AC8 but not AC1 is required for prolonged behavioral anxiety. *Mol Brain* **9**:60.

Bishop GA, Berbari NF, Lewis J and Mykytyn K (2007) Type III adenylyl cyclase localizes to primary cilia throughout the adult mouse brain. *J Comp Neurol* **505**:562-571.

Bogard AS, Adris P and Ostrom RS (2012) Adenylyl cyclase 2 selectively couples to E prostanoid type 2 receptors, whereas adenylyl cyclase 3 is not receptor-regulated in airway smooth muscle. *J Pharmacol Exp Ther* **342**:586-595.

Bogard AS, Xu C and Ostrom RS (2011) Human bronchial smooth muscle cells express adenylyl cyclase isoforms 2, 4, and 6 in distinct membrane microdomains. *J Pharmacol Exp Ther* **337**:209-217.

Bol GF, Gros C, Hulster A, Bosel A and Pfeuffer T (1997) Phorbol ester-induced sensitisation of adenylyl cyclase type II is related to phosphorylation of threonine 1057. *Biochem Biophys Res Commun* **237**:251-256.

Boran AD, Chen Y and Iyengar R (2011) Identification of new Gbetagamma interaction sites in adenylyl cyclase 2. *Cell Signal* **23**:1489-1495.

Brand CS, Hocker HJ, Gorfe AA, Cavasotto CN and Dessauer CW (2013) Isoform selectivity of adenylyl cyclase inhibitors: characterization of known and novel compounds. *J Pharmacol Exp Ther* **347**:265-275.

Brand CS, Sadana R, Malik S, Smrcka AV and Dessauer CW (2015) Adenylyl Cyclase 5 Regulation by Gbetagamma Involves Isoform-Specific Use of Multiple Interaction Sites. *Mol Pharmacol* **88**:758-767.

Bruce JI, Straub SV and Yule DI (2003) Crosstalk between cAMP and Ca2+ signaling in non-excitable cells. *Cell Calcium* **34**:431-444.

Brust TF, Alongkronrusmee D, Soto-Velasquez M, Baldwin TA, Ye Z, Dai M, Dessauer CW, van Rijn RM and Watts VJ (2017) Identification of a selective small-molecule inhibitor of type 1 adenylyl cyclase activity with analgesic properties. *Sci Signal* **10**.

Brust TF, Conley JM and Watts VJ (2015a) Galpha(i/o)-coupled receptor-mediated sensitization of adenylyl cyclase: 40 years later. *Eur J Pharmacol* **763**:223-232.

Brust TF, Hayes MP, Roman DL, Burris KD and Watts VJ (2015b) Bias analyses of preclinical and clinical D2 dopamine ligands: studies with immediate and complex signaling pathways. *J Pharmacol Exp Ther* **352**:480-493.

Buck J, Sinclair ML, Schapal L, Cann MJ and Levin LR (1999) Cytosolic adenylyl cyclase defines a unique signaling molecule in mammals. *Proc Natl Acad Sci U S A* **96**:79-84.

Cabrera-Vera TM, Vanhauwe J, Thomas TO, Medkova M, Preininger A, Mazzoni MR and Hamm HE (2003) Insights into G protein structure, function, and regulation. *Endocr Rev* **24**:765-781.

Calebiro D and Maiellaro I (2014) cAMP signaling microdomains and their observation by optical methods. *Front Cell Neurosci* **8**:350.

Cali JJ, Zwaagstra JC, Mons N, Cooper DM and Krupinski J (1994) Type VIII adenylyl cyclase. A Ca2+/calmodulin-stimulated enzyme expressed in discrete regions of rat brain. *J Biol Chem* **269**:12190-12195.

Cao H, Chen X, Yang Y and Storm DR (2016) Disruption of type 3 adenylyl cyclase expression in the hypothalamus leads to obesity. *Integr Obes Diabetes* **2**:225-228.

Chen-Goodspeed M, Lukan AN and Dessauer CW (2005) Modeling of Galpha(s) and Galpha(i) regulation of human type V and VI adenylyl cyclase. *J Biol Chem* **280**:1808-1816.

Chen J, DeVivo M, Dingus J, Harry A, Li J, Sui J, Carty DJ, Blank JL, Exton JH, Stoffel RH and et al. (1995) A region of adenylyl cyclase 2 critical for regulation by G protein beta gamma subunits. *Science* **268**:1166-1169.

Chen J and Iyengar R (1993) Inhibition of cloned adenylyl cyclases by mutant-activated Gi-alpha and specific suppression of type 2 adenylyl cyclase inhibition by phorbol ester treatment. *J Biol Chem* **268**:12253-12256.

Chen X, Cao H, Saraf A, Zweifel LS and Storm DR (2015) Overexpression of the type 1 adenylyl cyclase in the forebrain leads to deficits of behavioral inhibition. *J Neurosci* **35**:339-351.

Chen Y, Harry A, Li J, Smit MJ, Bai X, Magnusson R, Pieroni JP, Weng G and Iyengar R (1997) Adenylyl cyclase 6 is selectively regulated by protein kinase A phosphorylation in a region involved in Galphas stimulation. *Proc Natl Acad Sci U S A* **94**:14100-14104.

Chen YZ, Matsushita MM, Robertson P, Rieder M, Girirajan S, Antonacci F, Lipe H, Eichler EE, Nickerson DA, Bird TD and Raskind WH (2012) Autosomal dominant familial dyskinesia and facial myokymia: single exome sequencing identifies a mutation in adenylyl cyclase 5. *Arch Neurol* **69**:630-635.

Cheng HC, Qi RZ, Paudel H and Zhu HJ (2011) Regulation and function of protein kinases and phosphatases. *Enzyme Res* **2011**:794089.

Cheng X, Ji Z, Tsalkova T and Mei F (2008) Epac and PKA: a tale of two intracellular cAMP receptors. *Acta Biochim Biophys Sin (Shanghai)* **40**:651-662.

Chester JA and Watts VJ (2007) Adenylyl cyclase 5: a new clue in the search for the "fountain of youth"? *Sci STKE* **2007**:pe64.

Chien CL, Wu YS, Lai HL, Chen YH, Jiang ST, Shih CM, Lin SS, Chang C and Chern Y (2010) Impaired water reabsorption in mice deficient in the type VI adenylyl cyclase (AC6). *FEBS Lett* **584**:2883-2890.

Choi EJ, Xia Z and Storm DR (1992) Stimulation of the type III olfactory adenylyl cyclase by calcium and calmodulin. *Biochemistry* **31**:6492-6498.

Clapham DE (2007) Calcium signaling. *Cell* **131**:1047-1058.

Conley JM, Brand CS, Bogard AS, Pratt EP, Xu R, Hockerman GH, Ostrom RS, Dessauer CW and Watts VJ (2013) Development of a high-throughput screening paradigm for the discovery of small-molecule modulators of adenylyl cyclase: identification of an adenylyl cyclase 2 inhibitor. *J Pharmacol Exp Ther* **347**:276-287.

Conley JM and Watts VJ (2013) Differential effects of AGS3 expression on D(2L) dopamine receptor-mediated adenylyl cyclase signaling. *Cell Mol Neurobiol* **33**:551-558.

Conti AC, Maas JW, Jr., Muglia LM, Dave BA, Vogt SK, Tran TT, Rayhel EJ and Muglia LJ (2007) Distinct regional and subcellular localization of adenylyl cyclases type 1 and 8 in mouse brain. *Neuroscience* **146**:713-729.

Corder G, Doolen S, Donahue RR, Winter MK, Jutras BL, He Y, Hu X, Wieskopf JS, Mogil JS, Storm DR, Wang ZJ, McCarson KE and Taylor BK (2013) Constitutive mu-opioid receptor activity leads to long-term endogenous analgesia and dependence. *Science* **341**:1394-1399.

Crespo P, Cachero TG, Xu N and Gutkind JS (1995) Dual effect of beta-adrenergic receptors on mitogen-activated protein kinase. Evidence for a beta gamma-dependent activation and a G alpha s-cAMP-mediated inhibition. *J Biol Chem* **270**:25259-25265.

Cumbay MG and Watts VJ (2001) Heterologous sensitization of recombinant adenylate cyclases by activation of D(2) dopamine receptors. *J Pharmacol Exp Ther* **297**:1201-1209.

Cumbay MG and Watts VJ (2005) Galphaq potentiation of adenylate cyclase type 9 activity through a Ca2+/calmodulin-dependent pathway. *Biochem Pharmacol* **69**:1247-1256.

Davis TL, Bonacci TM, Sprang SR and Smrcka AV (2005) Structural and molecular characterization of a preferred protein interaction surface on G protein beta gamma subunits. *Biochemistry* **44**:10593-10604.

DebBurman SK, Ptasienski J, Benovic JL and Hosey MM (1996) G protein-coupled receptor kinase GRK2 is a phospholipid-dependent enzyme that can be conditionally activated by G protein betagamma subunits. *J Biol Chem* **271**:22552-22562.

Defer N, Best-Belpomme M and Hanoune J (2000) Tissue specificity and physiological relevance of various isoforms of adenylyl cyclase. *Am J Physiol Renal Physiol* **279**:F400-416.

Defer N, Marinx O, Stengel D, Danisova A, Iourgenko V, Matsuoka I, Caput D and Hanoune J (1994) Molecular cloning of the human type VIII adenylyl cyclase. *FEBS Lett* **351**:109-113.

Desrivieres S, Pronko SP, Lourdusamy A, Ducci F, Hoffman PL, Wodarz N, Ridinger M, Rietschel M, Zelenika D, Lathrop M, Schumann G and Tabakoff B (2011) Sex-specific role for adenylyl cyclase type 7 in alcohol dependence. *Biol Psychiatry* **69**:1100-1108.

Dessauer CW (2009) Adenylyl cyclase--A-kinase anchoring protein complexes: the next dimension in cAMP signaling. *Mol Pharmacol* **76**:935-941.

Dessauer CW, Chen-Goodspeed M and Chen J (2002) Mechanism of Galpha i-mediated inhibition of type V adenylyl cyclase. *J Biol Chem* **277**:28823-28829.

Dessauer CW, Tesmer JJ, Sprang SR and Gilman AG (1998) Identification of a Gialpha binding site on type V adenylyl cyclase. *J Biol Chem* **273**:25831-25839.

Dessauer CW, Watts VJ, Ostrom RS, Conti M, Dove S and Seifert R (2017) International Union of Basic and Clinical Pharmacology. CI. Structures and Small Molecule Modulators of Mammalian Adenylyl Cyclases. *Pharmacol Rev* **69**:93-139.

Diel S, Beyermann M, Llorens JM, Wittig B and Kleuss C (2008) Two interaction sites on mammalian adenylyl cyclase type I and II: modulation by calmodulin and G(betagamma). *Biochem J* **411**:449-456.

Diel S, Klass K, Wittig B and Kleuss C (2006) Gbetagamma activation site in adenylyl cyclase type II. Adenylyl cyclase type III is inhibited by Gbetagamma. *J Biol Chem* **281**:288-294.

DiRocco DP, Scheiner ZS, Sindreu CB, Chan GC and Storm DR (2009) A role for calmodulin-stimulated adenylyl cyclases in cocaine sensitization. *J Neurosci* **29**:2393-2403.

Duan B, Davis R, Sadat EL, Collins J, Sternweis PC, Yuan D and Jiang LI (2010) Distinct roles of adenylyl cyclase VII in regulating the immune responses in mice. *J Immunol* **185**:335-344.

Ejendal KF, Dessauer CW, Hebert TE and Watts VJ (2012) Dopamine D(2) Receptor-Mediated Heterologous Sensitization of AC5 Requires Signalosome Assembly. *J Signal Transduct* **2012**:210324.

Exton JH (1996) Regulation of phosphoinositide phospholipases by hormones, neurotransmitters, and other agonists linked to G proteins. *Annu Rev Pharmacol Toxicol* **36**:481-509.

Fagan KA, Mahey R and Cooper DM (1996) Functional co-localization of transfected Ca(2+)-stimulable adenylyl cyclases with capacitative Ca2+ entry sites. *J Biol Chem* **271**:12438-12444.

Feinstein PG, Schrader KA, Bakalyar HA, Tang WJ, Krupinski J, Gilman AG and Reed RR (1991) Molecular cloning and characterization of a Ca2+/calmodulin-insensitive adenylyl cyclase from rat brain. *Proc Natl Acad Sci U S A* **88**:10173-10177.

Ferguson GD and Storm DR (2004) Why calcium-stimulated adenylyl cyclases? *Physiology (Bethesda)* **19**:271-276.

Fredriksson R, Lagerstrom MC, Lundin LG and Schioth HB (2003) The G-protein-coupled receptors in the human genome form five main families. Phylogenetic analysis, paralogon groups, and fingerprints. *Mol Pharmacol* **63**:1256-1272.

Gao BN and Gilman AG (1991) Cloning and expression of a widely distributed (type IV) adenylyl cyclase. *Proc Natl Acad Sci U S A* **88**:10178-10182.

Gao MH, Lai NC, Giamouridis D, Kim YC, Tan Z, Guo T, Dillmann WH, Suarez J and Hammond HK (2016) Cardiac-Directed Expression of Adenylyl Cyclase Catalytic Domain Reverses Cardiac Dysfunction Caused by Sustained Beta-Adrenergic Receptor Stimulation. *JACC Basic Transl Sci* **1**:617-629.

Gao MH, Tang T, Lai NC, Miyanohara A, Guo T, Tang R, Firth AL, Yuan JX and Hammond HK (2011) Beneficial effects of adenylyl cyclase type 6 (AC6) expression persist using a catalytically inactive AC6 mutant. *Mol Pharmacol* **79**:381-388.

Gao X, Sadana R, Dessauer CW and Patel TB (2007) Conditional stimulation of type V and VI adenylyl cyclases by G protein betagamma subunits. *J Biol Chem* **282**:294-302.

Garelick MG, Chan GC, DiRocco DP and Storm DR (2009) Overexpression of type I adenylyl cyclase in the forebrain impairs spatial memory in aged but not young mice. *J Neurosci* **29**:10835-10842.

Gille A, Lushington GH, Mou TC, Doughty MB, Johnson RA and Seifert R (2004) Differential inhibition of adenylyl cyclase isoforms and soluble guanylyl cyclase by purine and pyrimidine nucleotides. *J Biol Chem* **279**:19955-19969.

Goupil E, Laporte SA and Hebert TE (2012) Functional selectivity in GPCR signaling: understanding the full spectrum of receptor conformations. *Mini Rev Med Chem* **12**:817-830.

Grarup N, Moltke I, Andersen MK, Dalby M, Vitting-Seerup K, Kern T, Mahendran Y, Jorsboe E, Larsen CVL, Dahl-Petersen IK, Gilly A, Suveges D, Dedoussis G, Zeggini E, Pedersen O, Andersson R, Bjerregaard P, Jorgensen ME, Albrechtsen A and Hansen T (2018) Loss-of-function variants in ADCY3 increase risk of obesity and type 2 diabetes. *Nat Genet* **50**:172-174.

Gu C and Cooper DM (1999) Calmodulin-binding sites on adenylyl cyclase type VIII. *J Biol Chem* **274**:8012-8021.

Guillou JL, Nakata H and Cooper DM (1999) Inhibition by calcium of mammalian adenylyl cyclases. *J Biol Chem* **274**:35539-35545.

Guzman L, Moraga-Cid G, Avila A, Figueroa M, Yevenes GE, Fuentealba J and Aguayo LG (2009) Blockade of ethanol-induced potentiation of glycine receptors by a peptide that interferes with Gbetagamma binding. *J Pharmacol Exp Ther* **331**:933-939.

Hacker BM, Tomlinson JE, Wayman GA, Sultana R, Chan G, Villacres E, Disteche C and Storm DR (1998) Cloning, chromosomal mapping, and regulatory properties of the human type 9 adenylyl cyclase (ADCY9). *Genomics* **50**:97-104.

Halls ML and Cooper DM (2011) Regulation by Ca2+-signaling pathways of adenylyl cyclases. *Cold Spring Harb Perspect Biol* **3**:a004143.

Halls ML and Cooper DM (2017) Adenylyl cyclase signalling complexes - Pharmacological challenges and opportunities. *Pharmacol Ther* **172**:171-180.

Hammond HK, Penny WF, Traverse JH, Henry TD, Watkins MW, Yancy CW, Sweis RN, Adler ED, Patel AN, Murray DR, Ross RS, Bhargava V, Maisel A, Barnard DD, Lai NC, Dalton ND, Lee ML, Narayan SM, Blanchard DG and Gao MH (2016) Intracoronary Gene Transfer of Adenylyl Cyclase 6 in Patients With Heart Failure: A Randomized Clinical Trial. *JAMA Cardiol* **1**:163-171.

Hanoune J and Defer N (2001) Regulation and role of adenylyl cyclase isoforms. *Annu Rev Pharmacol Toxicol* **41**:145-174.

Hanson PI and Schulman H (1992) Neuronal Ca2+/calmodulin-dependent protein kinases. *Annu Rev Biochem* **61**:559-601.

Harry A, Chen Y, Magnusson R, Iyengar R and Weng G (1997) Differential regulation of adenylyl cyclases by Galphas. *J Biol Chem* **272**:19017-19021.

Hayes MP, Soto-Velasquez M, Fowler CA, Watts VJ and Roman DL (2017) Identification of FDA-Approved Small Molecules Capable of Disrupting the Calmodulin-Adenylyl Cyclase 8 Interaction through Direct Binding to Calmodulin. *ACS Chem Neurosci*.

Hill J, Howlett A and Klein C (2000) Nitric oxide selectively inhibits adenylyl cyclase isoforms 5 and 6. *Cell Signal* **12**:233-237.

Ho D, Zhao X, Yan L, Yuan C, Zong H, Vatner DE, Pessin JE and Vatner SF (2015) Adenylyl Cyclase Type 5 Deficiency Protects Against Diet-Induced Obesity and Insulin Resistance. *Diabetes* **64**:2636-2645.

Huang B, Zhao J, Lei Z, Shen S, Li D, Shen GX, Zhang GM and Feng ZH (2009) miR-142-3p restricts cAMP production in CD4+CD25- T cells and CD4+CD25+ TREG cells by targeting AC9 mRNA. *EMBO Rep* **10**:180-185.

Huang KP (1989) The mechanism of protein kinase C activation. *Trends Neurosci* **12**:425-432.

Hurley JH (1999) Structure, mechanism, and regulation of mammalian adenylyl cyclase. *J Biol Chem* **274**:7599-7602.

Inglese J, Luttrell LM, Iniguez-Lluhi JA, Touhara K, Koch WJ and Lefkowitz RJ (1994) Functionally active targeting domain of the beta-adrenergic receptor kinase: an inhibitor of G beta gamma-mediated stimulation of type II adenylyl cyclase. *Proc Natl Acad Sci U S A* **91**:3637-3641.

Ishikawa Y, Katsushika S, Chen L, Halnon NJ, Kawabe J and Homcy CJ (1992) Isolation and characterization of a novel cardiac adenylylcyclase cDNA. *J Biol Chem* **267**:13553-13557.

Iwami G, Kawabe J, Ebina T, Cannon PJ, Homcy CJ and Ishikawa Y (1995) Regulation of adenylyl cyclase by protein kinase A. *J Biol Chem* **270**:12481-12484.

Iwamoto T, Okumura S, Iwatsubo K, Kawabe J, Ohtsu K, Sakai I, Hashimoto Y, Izumitani A, Sango K, Ajiki K, Toya Y, Umemura S, Goshima Y, Arai N, Vatner SF and Ishikawa Y (2003) Motor dysfunction in type 5 adenylyl cyclase-null mice. *J Biol Chem* **278**:16936-16940.

Jacobowitz O, Chen J, Premont RT and Iyengar R (1993) Stimulation of specific types of Gs-stimulated adenylyl cyclases by phorbol ester treatment. *J Biol Chem* **268**:3829-3832.

Jacobowitz O and Iyengar R (1994) Phorbol ester-induced stimulation and phosphorylation of adenylyl cyclase 2. *Proc Natl Acad Sci U S A* **91**:10630-10634.

Jacobson KA (2015) New paradigms in GPCR drug discovery. *Biochem Pharmacol* **98**:541-555.

Ji TH, Grossmann M and Ji I (1998) G protein-coupled receptors. I. Diversity of receptor-ligand interactions. *J Biol Chem* **273**:17299-17302.

Johnstone TB, Agarwal SR, Harvey RD and Ostrom RS (2017) cAMP Signaling Compartmentation: Adenylyl Cyclases as Anchors of Dynamic Signaling Complexes. *Mol Pharmacol*.

Kapiloff MS, Rigatti M and Dodge-Kafka KL (2014) Architectural and functional roles of A kinase-anchoring proteins in cAMP microdomains. *J Gen Physiol* **143**:9-15.

Katritch V, Cherezov V and Stevens RC (2012) Diversity and modularity of G protein-coupled receptor structures. *Trends Pharmacol Sci* **33**:17-27.

Katsushika S, Chen L, Kawabe J, Nilakantan R, Halnon NJ, Homcy CJ and Ishikawa Y (1992) Cloning and characterization of a sixth adenylyl cyclase isoform: types V and VI constitute a subgroup within the mammalian adenylyl cyclase family. *Proc Natl Acad Sci U S A* **89**:8774-8778.

Kaupp UB and Seifert R (2002) Cyclic nucleotide-gated ion channels. *Physiol Rev* **82**:769-824.

Kawabe J, Iwami G, Ebina T, Ohno S, Katada T, Ueda Y, Homcy CJ and Ishikawa Y (1994) Differential activation of adenylyl cyclase by protein kinase C isoenzymes. *J Biol Chem* **269**:16554-16558.

Khan SM, Sleno R, Gora S, Zylbergold P, Laverdure JP, Labbe JC, Miller GJ and Hebert TE (2013) The expanding roles of Gbetagamma subunits in G protein-coupled receptor signaling and drug action. *Pharmacol Rev* **65**:545-577.

Kim KS, Kim H, Baek IS, Lee KW and Han PL (2011) Mice lacking adenylyl cyclase type 5 (AC5) show increased ethanol consumption and reduced ethanol sensitivity. *Psychopharmacology (Berl)* **215**:391-398.

Kim KS, Kim J, Back SK, Im JY, Na HS and Han PL (2007) Markedly attenuated acute and chronic pain responses in mice lacking adenylyl cyclase-5. *Genes Brain Behav* **6**:120-127.

Kim KS, Lee KW, Lee KW, Im JY, Yoo JY, Kim SW, Lee JK, Nestler EJ and Han PL (2006) Adenylyl cyclase type 5 (AC5) is an essential mediator of morphine action. *Proc Natl Acad Sci U S A* **103**:3908-3913.

Kinast L, von der Ohe J, Burhenne H and Seifert R (2012) Impairment of adenylyl cyclase 2 function and expression in hypoxanthine phosphoribosyltransferase-deficient rat B103 neuroblastoma cells as model for Lesch-Nyhan disease: BODIPY-forskolin as pharmacological tool. *Naunyn Schmiedebergs Arch Pharmacol* **385**:671-683.

Kleinboelting S, Diaz A, Moniot S, van den Heuvel J, Weyand M, Levin LR, Buck J and Steegborn C (2014) Crystal structures of human soluble adenylyl cyclase reveal mechanisms of catalysis and of its activation through bicarbonate. *Proc Natl Acad Sci U S A* **111**:3727-3732.

Koch WJ, Hawes BE, Inglese J, Luttrell LM and Lefkowitz RJ (1994) Cellular expression of the carboxyl terminus of a G protein-coupled receptor kinase attenuates G beta gamma-mediated signaling. *J Biol Chem* **269**:6193-6197.

Krupinski J, Coussen F, Bakalyar HA, Tang WJ, Feinstein PG, Orth K, Slaughter C, Reed RR and Gilman AG (1989) Adenylyl cyclase amino acid sequence: possible channel- or transporter-like structure. *Science* **244**:1558-1564.

Lai HL, Yang TH, Messing RO, Ching YH, Lin SC and Chern Y (1997) Protein kinase C inhibits adenylyl cyclase type VI activity during desensitization of the A2a-adenosine receptor-mediated cAMP response. *J Biol Chem* **272**:4970-4977.

Lee E, Linder ME and Gilman AG (1994) Expression of G-protein alpha subunits in Escherichia coli. *Methods Enzymol* **237**:146-164.

Levin LR and Reed RR (1995) Identification of functional domains of adenylyl cyclase using in vivo chimeras. *J Biol Chem* **270**:7573-7579.

Li S, Lee ML, Bruchas MR, Chan GC, Storm DR and Chavkin C (2006) Calmodulin-stimulated adenylyl cyclase gene deletion affects morphine responses. *Mol Pharmacol* **70**:1742-1749.

Li Y, Baldwin TA, Wang Y, Subramaniam J, Carbajal AG, Brand CS, Cunha SR and Dessauer CW (2017) Loss of type 9 adenylyl cyclase triggers reduced phosphorylation of Hsp20 and diastolic dysfunction. *Sci Rep* **7**:5522.

Li Y, Chen L, Kass RS and Dessauer CW (2012) The A-kinase anchoring protein Yotiao facilitates complex formation between adenylyl cyclase type 9 and the IKs potassium channel in heart. *J Biol Chem* **287**:29815-29824.

Litvin TN, Kamenetsky M, Zarifyan A, Buck J and Levin LR (2003) Kinetic properties of "soluble" adenylyl cyclase. Synergism between calcium and bicarbonate. *J Biol Chem* **278**:15922-15926.

Logue JS and Scott JD (2010) Organizing signal transduction through A-kinase anchoring proteins (AKAPs). *FEBS J* **277**:4370-4375.

Lohse MJ, Benovic JL, Codina J, Caron MG and Lefkowitz RJ (1990) beta-Arrestin: a protein that regulates beta-adrenergic receptor function. *Science* **248**:1547-1550.

Ludwig MG and Seuwen K (2002) Characterization of the human adenylyl cyclase gene family: cDNA, gene structure, and tissue distribution of the nine isoforms. *J Recept Signal Transduct Res* **22**:79-110.

Macdougall DA, Wachten S, Ciruela A, Sinz A and Cooper DM (2009) Separate elements within a single IQ-like motif in adenylyl cyclase type 8 impart ca2+/calmodulin binding and autoinhibition. *J Biol Chem* **284**:15573-15588.

Mahoney JP and Sunahara RK (2016) Mechanistic insights into GPCR-G protein interactions. *Curr Opin Struct Biol* **41**:247-254.

Maier T, Guell M and Serrano L (2009) Correlation of mRNA and protein in complex biological samples. *FEBS Lett* **583**:3966-3973.

Mamluk R, Defer N, Hanoune J and Meidan R (1999) Molecular identification of adenylyl cyclase 3 in bovine corpus luteum and its regulation by prostaglandin F2alpha-induced signaling pathways. *Endocrinology* **140**:4601-4608.

Mann L, Heldman E, Bersudsky Y, Vatner SF, Ishikawa Y, Almog O, Belmaker RH and Agam G (2009) Inhibition of specific adenylyl cyclase isoforms by lithium and carbamazepine, but not valproate, may be related to their antidepressant effect. *Bipolar Disord* **11**:885-896.

Masada N, Ciruela A, Macdougall DA and Cooper DM (2009) Distinct mechanisms of regulation by Ca2+/calmodulin of type 1 and 8 adenylyl cyclases support their different physiological roles. *J Biol Chem* **284**:4451-4463.

Masada N, Schaks S, Jackson SE, Sinz A and Cooper DM (2012) Distinct mechanisms of calmodulin binding and regulation of adenylyl cyclases 1 and 8. *Biochemistry* **51**:7917-7929.

Maurice DH, Ke H, Ahmad F, Wang Y, Chung J and Manganiello VC (2014) Advances in targeting cyclic nucleotide phosphodiesterases. *Nat Rev Drug Discov* **13**:290-314.

McCudden CR, Hains MD, Kimple RJ, Siderovski DP and Willard FS (2005) G-protein signaling: back to the future. *Cell Mol Life Sci* **62**:551-577.

McVey M, Hill J, Howlett A and Klein C (1999) Adenylyl cyclase, a coincidence detector for nitric oxide. *J Biol Chem* **274**:18887-18892.

Mochona B, Qi X, Euynni S, Sikazwi D, Mateeva N and Soliman KF (2016) Design and evaluation of novel oxadiazole derivatives as potential prostate cancer agents. *Bioorg Med Chem Lett* **26**:2847-2851.

Moore CA, Milano SK and Benovic JL (2007) Regulation of receptor trafficking by GRKs and arrestins. *Annu Rev Physiol* **69**:451-482.

Mou TC, Masada N, Cooper DM and Sprang SR (2009) Structural basis for inhibition of mammalian adenylyl cyclase by calcium. *Biochemistry* **48**:3387-3397.

Naga Prasad SV, Barak LS, Rapacciuolo A, Caron MG and Rockman HA (2001) Agonist-dependent recruitment of phosphoinositide 3-kinase to the membrane by beta-adrenergic receptor kinase 1. A role in receptor sequestration. *J Biol Chem* **276**:18953-18959.

Nelson EJ, Hellevuo K, Yoshimura M and Tabakoff B (2003) Ethanol-induced phosphorylation and potentiation of the activity of type 7 adenylyl cyclase. Involvement of protein kinase C delta. *J Biol Chem* **278**:4552-4560.

Nevo I, Avidor-Reiss T, Levy R, Bayewitch M, Heldman E and Vogel Z (1998) Regulation of adenylyl cyclase isozymes on acute and chronic activation of inhibitory receptors. *Mol Pharmacol* **54**:419-426.

Ngo T, Kufareva I, Coleman J, Graham RM, Abagyan R and Smith NJ (2016) Identifying ligands at orphan GPCRs: current status using structure-based approaches. *Br J Pharmacol* **173**:2934-2951.

Nguyen CH and Watts VJ (2006) Dexamethasone-induced Ras protein 1 negatively regulates protein kinase C delta: implications for adenylyl cyclase 2 signaling. *Mol Pharmacol* **69**:1763-1771.

Nielsen MD, Chan GC, Poser SW and Storm DR (1996) Differential regulation of type I and type VIII Ca2+-stimulated adenylyl cyclases by Gi-coupled receptors in vivo. *J Biol Chem* **271**:33308-33316.

Okumura S, Kawabe J, Yatani A, Takagi G, Lee MC, Hong C, Liu J, Takagi I, Sadoshima J, Vatner DE, Vatner SF and Ishikawa Y (2003) Type 5 adenylyl cyclase disruption alters not only sympathetic but also parasympathetic and calcium-mediated cardiac regulation. *Circ Res* **93**:364-371.

Oldham WM and Hamm HE (2008) Heterotrimeric G protein activation by G-protein-coupled receptors. *Nat Rev Mol Cell Biol* **9**:60-71.

Ostrom RS, Gregorian C, Drenan RM, Xiang Y, Regan JW and Insel PA (2001) Receptor number and caveolar co-localization determine receptor coupling efficiency to adenylyl cyclase. *J Biol Chem* **276**:42063-42069.

Ostrom RS and Insel PA (2004) The evolving role of lipid rafts and caveolae in G protein-coupled receptor signaling: implications for molecular pharmacology. *Br J Pharmacol* **143**:235-245.

Ostrom RS, Liu X, Head BP, Gregorian C, Seasholtz TM and Insel PA (2002) Localization of adenylyl cyclase isoforms and G protein-coupled receptors in vascular smooth muscle cells: expression in caveolin-rich and noncaveolin domains. *Mol Pharmacol* **62**:983-992.

Ostrom RS, Violin JD, Coleman S and Insel PA (2000) Selective enhancement of beta-adrenergic receptor signaling by overexpression of adenylyl cyclase type 6: colocalization of receptor and adenylyl cyclase in caveolae of cardiac myocytes. *Mol Pharmacol* **57**:1075-1079.

Pagano M, Clynes MA, Masada N, Ciruela A, Ayling LJ, Wachten S and Cooper DM (2009) Insights into the residence in lipid rafts of adenylyl cyclase AC8 and its regulation by capacitative calcium entry. *Am J Physiol Cell Physiol* **296**:C607-619.

Paramonov VM, Mamaeva V, Sahlgren C and Rivero-Muller A (2015) Genetically-encoded tools for cAMP probing and modulation in living systems. *Front Pharmacol* **6**:196.

Paterson JM, Smith SM, Harmar AJ and Antoni FA (1995) Control of a novel adenylyl cyclase by calcineurin. *Biochem Biophys Res Commun* **214**:1000-1008.

Pierre S, Eschenhagen T, Geisslinger G and Scholich K (2009) Capturing adenylyl cyclases as potential drug targets. *Nat Rev Drug Discov* **8**:321-335.

Pinto C, Papa D, Hubner M, Mou TC, Lushington GH and Seifert R (2008) Activation and inhibition of adenylyl cyclase isoforms by forskolin analogs. *J Pharmacol Exp Ther* **325**:27-36.

Pitman JL, Wheeler MC, Lloyd DJ, Walker JR, Glynne RJ and Gekakis N (2014) A gain-of-function mutation in adenylate cyclase 3 protects mice from diet-induced obesity. *PLoS One* **9**:e110226.

Qualls-Creekmore E, Gupta R and Yoshimura M (2017) The effect of alcohol on recombinant proteins derived from mammalian adenylyl cyclase. *Biochem Biophys Rep* **10**:157-164.

Ran FA, Hsu PD, Wright J, Agarwala V, Scott DA and Zhang F (2013) Genome engineering using the CRISPR-Cas9 system. *Nat Protoc* **8**:2281-2308.

Rasmussen SG, DeVree BT, Zou Y, Kruse AC, Chung KY, Kobilka TS, Thian FS, Chae PS, Pardon E, Calinski D, Mathiesen JM, Shah ST, Lyons JA, Caffrey M, Gellman SH, Steyaert J, Skiniotis G, Weis WI, Sunahara RK and Kobilka BK (2011) Crystal structure of the beta2 adrenergic receptor-Gs protein complex. *Nature* **477**:549-555.

Rees S, Kittikulsuth W, Roos K, Strait KA, Van Hoek A and Kohan DE (2014) Adenylyl cyclase 6 deficiency ameliorates polycystic kidney disease. *J Am Soc Nephrol* **25**:232-237.

Risoe PK, Ryg U, Wang YY, Rutkovskiy A, Smedsrod B, Valen G and Dahle MK (2011) Cecal ligation and puncture sepsis is associated with attenuated expression of adenylyl cyclase 9 and increased miR142-3p. *Shock* **36**:390-395.

Ross EM, Howlett AC, Ferguson KM and Gilman AG (1978) Reconstitution of hormone-sensitive adenylate cyclase activity with resolved components of the enzyme. *J Biol Chem* **253**:6401-6412.

Roth DM, Gao MH, Lai NC, Drumm J, Dalton N, Zhou JY, Zhu J, Entrikin D and Hammond HK (1999) Cardiac-directed adenylyl cyclase expression improves heart function in murine cardiomyopathy. *Circulation* **99**:3099-3102.

Sadana R and Dessauer CW (2009) Physiological roles for G protein-regulated adenylyl cyclase isoforms: insights from knockout and overexpression studies. *Neurosignals* **17**:5-22.

Saeed S, Bonnefond A, Tamanini F, Mirza MU, Manzoor J, Janjua QM, Din SM, Gaitan J, Milochau A, Durand E, Vaillant E, Haseeb A, De Graeve F, Rabearivelo I, Sand O, Queniat G, Boutry R, Schott DA, Ayesha H, Ali M, Khan WI, Butt TA, Rinne T, Stumpel C, Abderrahmani A, Lang J, Arslan M and Froguel P (2018) Loss-of-function mutations in ADCY3 cause monogenic severe obesity. *Nat Genet* **50**:175-179.

Sanabra C and Mengod G (2011) Neuroanatomical distribution and neurochemical characterization of cells expressing adenylyl cyclase isoforms in mouse and rat brain. *J Chem Neuroanat* **41**:43-54.

Sassone-Corsi P (2012) The cyclic AMP pathway. *Cold Spring Harb Perspect Biol* **4**.

Schaefer ML, Wong ST, Wozniak DF, Muglia LM, Liauw JA, Zhuo M, Nardi A, Hartman RE, Vogt SK, Luedke CE, Storm DR and Muglia LJ (2000) Altered stress-induced anxiety in adenylyl cyclase type VIII-deficient mice. *J Neurosci* **20**:4809-4820.

Schneider EH and Seifert R (2010) Sf9 cells: a versatile model system to investigate the pharmacological properties of G protein-coupled receptors. *Pharmacol Ther* **128**:387-418.

Scott JK, Huang SF, Gangadhar BP, Samoriski GM, Clapp P, Gross RA, Taussig R and Smrcka AV (2001) Evidence that a protein-protein interaction 'hot spot' on heterotrimeric G protein betagamma subunits is used for recognition of a subclass of effectors. *EMBO J* **20**:767-776.

Seifert R, Lushington GH, Mou TC, Gille A and Sprang SR (2012) Inhibitors of membranous adenylyl cyclases. *Trends Pharmacol Sci* **33**:64-78.

Seneviratne AMPB, Burroughs M, Giralt E and Smrcka AV (2011) Direct-reversible binding of small molecules to G protein βγ subunits. *Biochimica et Biophysica Acta (BBA) - Proteins and Proteomics* **1814**:1210-1218.

Sethna F, Feng W, Ding Q, Robison AJ, Feng Y and Wang H (2017) Enhanced expression of ADCY1 underlies aberrant neuronal signalling and behaviour in a syndromic autism model. *Nat Commun* **8**:14359.

Shen JX, Wachten S, Halls ML, Everett KL and Cooper DM (2012) Muscarinic receptors stimulate AC2 by novel phosphorylation sites, whereas Gbetagamma subunits exert opposing effects depending on the G-protein source. *Biochem J* **447**:393-405.

Simonds WF (1999) G protein regulation of adenylate cyclase. *Trends Pharmacol Sci* **20**:66-73.

Skalhegg BS and Tasken K (2000) Specificity in the cAMP/PKA signaling pathway. Differential expression,regulation, and subcellular localization of subunits of PKA. *Front Biosci* **5**:D678-693.

Skyba DA, Radhakrishnan R, Bement MKH and Sluka KA (2004) The cAMP pathway and pain: potential targets for drug development. *Drug Discovery Today: Disease Models* **1**:115-119.

Smith JS and Rajagopal S (2016) The beta-Arrestins: Multifunctional Regulators of G Protein-coupled Receptors. *J Biol Chem* **291**:8969-8977.

Smith KE, Gu C, Fagan KA, Hu B and Cooper DM (2002) Residence of adenylyl cyclase type 8 in caveolae is necessary but not sufficient for regulation by capacitative Ca(2+) entry. *J Biol Chem* **277**:6025-6031.

Smrcka AV (2008) G protein betagamma subunits: central mediators of G protein-coupled receptor signaling. *Cell Mol Life Sci* **65**:2191-2214.

Smrcka AV, Lehmann DM and Dessal AL (2008) G protein betagamma subunits as targets for small molecule therapeutic development. *Comb Chem High Throughput Screen* **11**:382-395.

Sprang SR (1997) G protein mechanisms: insights from structural analysis. *Annu Rev Biochem* **66**:639-678.

Sriram K and Insel PA (2018) G Protein-Coupled Receptors as Targets for Approved Drugs: How Many Targets and How Many Drugs? *Mol Pharmacol* **93**:251-258.

Steegborn C (2014) Structure, mechanism, and regulation of soluble adenylyl cyclases - similarities and differences to transmembrane adenylyl cyclases. *Biochim Biophys Acta* **1842**:2535-2547.

Steiner D, Avidor-Reiss T, Schallmach E, Butovsky E, Lev N and Vogel Z (2005) Regulation of adenylate cyclase type VIII splice variants by acute and chronic Gi/o-coupled receptor activation. *Biochem J* **386**:341-348.

Storm DR, Hansel C, Hacker B, Parent A and Linden DJ (1998) Impaired cerebellar long-term potentiation in type I adenylyl cyclase mutant mice. *Neuron* **20**:1199-1210.

Sunahara RK, Dessauer CW and Gilman AG (1996) Complexity and diversity of mammalian adenylyl cyclases. *Annu Rev Pharmacol Toxicol* **36**:461-480.

Sunahara RK, Dessauer CW, Whisnant RE, Kleuss C and Gilman AG (1997) Interaction of Gsalpha with the cytosolic domains of mammalian adenylyl cyclase. *J Biol Chem* **272**:22265-22271.

Sunahara RK and Insel PA (2016) The Molecular Pharmacology of G Protein Signaling Then and Now: A Tribute to Alfred G. Gilman. *Mol Pharmacol* **89**:585-592.

Surve CR, Lehmann D and Smrcka AV (2014) A chemical biology approach demonstrates G protein betagamma subunits are sufficient to mediate directional neutrophil chemotaxis. *The Journal of biological chemistry* **289**:17791-17801.

Sutherland EW and Rall TW (1958) Fractionation and characterization of a cyclic adenine ribonucleotide formed by tissue particles. *J Biol Chem* **232**:1077-1091.

Sutherland EW, Rall TW and Menon T (1962) Adenyl cylase. I. Distribution, preparation, and properties. *J Biol Chem* **237**:1220-1227.

Tang T, Gao MH, Lai NC, Firth AL, Takahashi T, Guo T, Yuan JX, Roth DM and Hammond HK (2008) Adenylyl cyclase type 6 deletion decreases left ventricular function via impaired calcium handling. *Circulation* **117**:61-69.

Tang T, Hammond HK, Firth A, Yang Y, Gao MH, Yuan JX and Lai NC (2011) Adenylyl cyclase 6 improves calcium uptake and left ventricular function in aged hearts. *J Am Coll Cardiol* **57**:1846-1855.

Tang T, Lai NC, Roth DM, Drumm J, Guo T, Lee KW, Han PL, Dalton N and Gao MH (2006) Adenylyl cyclase type V deletion increases basal left ventricular function and reduces left ventricular contractile responsiveness to beta-adrenergic stimulation. *Basic Res Cardiol* **101**:117-126.

Tang T, Lai NC, Wright AT, Gao MH, Lee P, Guo T, Tang R, McCulloch AD and Hammond HK (2013) Adenylyl cyclase 6 deletion increases mortality during sustained beta-adrenergic receptor stimulation. *J Mol Cell Cardiol* **60**:60-67.

Tang WJ and Hurley JH (1998) Catalytic mechanism and regulation of mammalian adenylyl cyclases. *Mol Pharmacol* **54**:231-240.

Tang WJ, Krupinski J and Gilman AG (1991) Expression and characterization of calmodulin-activated (type I) adenylylcyclase. *J Biol Chem* **266**:8595-8603.

Taussig R, Iniguez-Lluhi JA and Gilman AG (1993a) Inhibition of adenylyl cyclase by Gi alpha. *Science* **261**:218-221.

Taussig R, Quarmby LM and Gilman AG (1993b) Regulation of purified type I and type II adenylylcyclases by G protein beta gamma subunits. *J Biol Chem* **268**:9-12.

Taussig R, Tang WJ, Hepler JR and Gilman AG (1994) Distinct patterns of bidirectional regulation of mammalian adenylyl cyclases. *J Biol Chem* **269**:6093-6100.

Taussig R and Zimmermann G (1998) Type-specific regulation of mammalian adenylyl cyclases by G protein pathways. *Adv Second Messenger Phosphoprotein Res* **32**:81-98.

Tesmer JJ, Sunahara RK, Gilman AG and Sprang SR (1997) Crystal structure of the catalytic domains of adenylyl cyclase in a complex with Gsalpha.GTPgammaS. *Science* **278**:1907-1916.

Tidow H and Nissen P (2013) Structural diversity of calmodulin binding to its target sites. *FEBS J* **280**:5551-5565.

Ubersax JA and Ferrell JE, Jr. (2007) Mechanisms of specificity in protein phosphorylation. *Nat Rev Mol Cell Biol* **8**:530-541.

Vadakkan KI, Wang H, Ko SW, Zastepa E, Petrovic MJ, Sluka KA and Zhuo M (2006) Genetic reduction of chronic muscle pain in mice lacking calcium/calmodulin-stimulated adenylyl cyclases. *Mol Pain* **2**:7.

Vasudevan NT, Mohan ML, Gupta MK, Martelli EE, Hussain AK, Qin Y, Chandrasekharan UM, Young D, Feldman AM, Sen S, Dorn GW, 2nd, Dicorleto PE and Naga Prasad SV (2013) Gbetagamma-independent recruitment of G-protein coupled receptor kinase 2 drives tumor necrosis factor alpha-induced cardiac beta-adrenergic receptor dysfunction. *Circulation* **128**:377-387.

Vatner SF, Pachon RE and Vatner DE (2015) Inhibition of adenylyl cyclase type 5 increases longevity and healthful aging through oxidative stress protection. *Oxid Med Cell Longev* **2015**:250310.

Vatner SF, Park M, Yan L, Lee GJ, Lai L, Iwatsubo K, Ishikawa Y, Pessin J and Vatner DE (2013) Adenylyl cyclase type 5 in cardiac disease, metabolism, and aging. *Am J Physiol Heart Circ Physiol* **305**:H1-8.

Vatner SF, Yan L, Ishikawa Y, Vatner DE and Sadoshima J (2009) Adenylyl cyclase type 5 disruption prolongs longevity and protects the heart against stress. *Circ J* **73**:195-200.

Vercellino I, Rezabkova L, Olieric V, Polyhach Y, Weinert T, Kammerer RA, Jeschke G and Korkhov VM (2017) Role of the nucleotidyl cyclase helical domain in catalytically active dimer formation. *Proc Natl Acad Sci U S A* **114**:E9821-E9828.

Villacres EC, Wong ST, Chavkin C and Storm DR (1998) Type I adenylyl cyclase mutant mice have impaired mossy fiber long-term potentiation. *J Neurosci* **18**:3186-3194.

Vorherr T, Knopfel L, Hofmann F, Mollner S, Pfeuffer T and Carafoli E (1993) The calmodulin binding domain of nitric oxide synthase and adenylyl cyclase. *Biochemistry* **32**:6081-6088.

Wall MA, Coleman DE, Lee E, Iniguez-Lluhi JA, Posner BA, Gilman AG and Sprang SR (1995) The structure of the G protein heterotrimer Gi alpha 1 beta 1 gamma 2. *Cell* **83**:1047-1058.

Wang H, Ferguson GD, Pineda VV, Cundiff PE and Storm DR (2004) Overexpression of type-1 adenylyl cyclase in mouse forebrain enhances recognition memory and LTP. *Nat Neurosci* **7**:635-642.

Wang H, Gong B, Vadakkan KI, Toyoda H, Kaang BK and Zhuo M (2007) Genetic evidence for adenylyl cyclase 1 as a target for preventing neuronal excitotoxicity mediated by N-methyl-D-aspartate receptors. *J Biol Chem* **282**:1507-1517.

Wang H, Pineda VV, Chan GC, Wong ST, Muglia LJ and Storm DR (2003) Type 8 adenylyl cyclase is targeted to excitatory synapses and required for mossy fiber long-term potentiation. *J Neurosci* **23**:9710-9718.

Wang H, Xu H, Wu LJ, Kim SS, Chen T, Koga K, Descalzi G, Gong B, Vadakkan KI, Zhang X, Kaang BK and Zhuo M (2011a) Identification of an adenylyl cyclase inhibitor for treating neuropathic and inflammatory pain. *Sci Transl Med* **3**:65ra63.

Wang T, Wei JJ, Sabatini DM and Lander ES (2014) Genetic screens in human cells using the CRISPR-Cas9 system. *Science* **343**:80-84.

Wang Z, Balet Sindreu C, Li V, Nudelman A, Chan GC and Storm DR (2006) Pheromone detection in male mice depends on signaling through the type 3 adenylyl cyclase in the main olfactory epithelium. *J Neurosci* **26**:7375-7379.

Wang Z, Li V, Chan GC, Phan T, Nudelman AS, Xia Z and Storm DR (2009) Adult type 3 adenylyl cyclase-deficient mice are obese. *PLoS One* **4**:e6979.

Wang Z, Phan T and Storm DR (2011b) The type 3 adenylyl cyclase is required for novel object learning and extinction of contextual memory: role of cAMP signaling in primary cilia. *J Neurosci* **31**:5557-5561.

Wang Z and Storm DR (2011) Maternal behavior is impaired in female mice lacking type 3 adenylyl cyclase. *Neuropsychopharmacology* **36**:772-781.

Watson PA, Krupinski J, Kempinski AM and Frankenfield CD (1994) Molecular cloning and characterization of the type VII isoform of mammalian adenylyl cyclase expressed widely in mouse tissues and in S49 mouse lymphoma cells. *J Biol Chem* **269**:28893-28898.

Watts VJ (2007) Adenylyl cyclase isoforms as novel therapeutic targets: an exciting example of excitotoxicity neuroprotection. *Mol Interv* **7**:70-73.

Watts VJ (2018) Selective Adenylyl Cyclase Type 1 Inhibitors as Potential Opioid Alternatives For Chronic Pain. *Neuropsychopharmacology* **43**:215-216.

Watts VJ and Neve KA (1997) Activation of type II adenylate cyclase by D2 and D4 but not D3 dopamine receptors. *Mol Pharmacol* **52**:181-186.

Watts VJ and Neve KA (2005) Sensitization of adenylate cyclase by Galpha i/o-coupled receptors. *Pharmacol Ther* **106**:405-421.

Wei F, Qiu CS, Kim SJ, Muglia L, Maas JW, Pineda VV, Xu HM, Chen ZF, Storm DR, Muglia LJ and Zhuo M (2002) Genetic elimination of behavioral sensitization in mice lacking calmodulin-stimulated adenylyl cyclases. *Neuron* **36**:713-726.

Wei J, Wayman G and Storm DR (1996) Phosphorylation and inhibition of type III adenylyl cyclase by calmodulin-dependent protein kinase II in vivo. *J Biol Chem* **271**:24231-24235.

Wei J, Zhao AZ, Chan GC, Baker LP, Impey S, Beavo JA and Storm DR (1998) Phosphorylation and inhibition of olfactory adenylyl cyclase by CaM kinase II in Neurons: a mechanism for attenuation of olfactory signals. *Neuron* **21**:495-504.

Weitmann S, Schultz G and Kleuss C (2001) Adenylyl cyclase type II domains involved in Gbetagamma stimulation. *Biochemistry* **40**:10853-10858.

Willoughby D, Halls ML, Everett KL, Ciruela A, Skroblin P, Klussmann E and Cooper DM (2012) A key phosphorylation site in AC8 mediates regulation of Ca(2+)-dependent cAMP dynamics by an AC8-AKAP79-PKA signalling complex. *J Cell Sci* **125**:5850-5859.

Willoughby D, Masada N, Wachten S, Pagano M, Halls ML, Everett KL, Ciruela A and Cooper DM (2010) AKAP79/150 interacts with AC8 and regulates Ca2+-dependent cAMP synthesis in pancreatic and neuronal systems. *J Biol Chem* **285**:20328-20342.

Wittpoth C, Scholich K, Yigzaw Y, Stringfield TM and Patel TB (1999) Regions on adenylyl cyclase that are necessary for inhibition of activity by beta gamma and G(ialpha) subunits of heterotrimeric G proteins. *Proc Natl Acad Sci U S A* **96**:9551-9556.

Wong ST, Athos J, Figueroa XA, Pineda VV, Schaefer ML, Chavkin CC, Muglia LJ and Storm DR (1999) Calcium-stimulated adenylyl cyclase activity is critical for hippocampus-dependent long-term memory and late phase LTP. *Neuron* **23**:787-798.

Wong ST, Trinh K, Hacker B, Chan GC, Lowe G, Gaggar A, Xia Z, Gold GH and Storm DR (2000) Disruption of the type III adenylyl cyclase gene leads to peripheral and behavioral anosmia in transgenic mice. *Neuron* **27**:487-497.

Wu YS, Chen CC, Chien CL, Lai HL, Jiang ST, Chen YC, Lai LP, Hsiao WF, Chen WP and Chern Y (2017) The type VI adenylyl cyclase protects cardiomyocytes from beta-adrenergic stress by a PKA/STAT3-dependent pathway. *J Biomed Sci* **24**:68.

Xia ZG, Refsdal CD, Merchant KM, Dorsa DM and Storm DR (1991) Distribution of mRNA for the calmodulin-sensitive adenylate cyclase in rat brain: expression in areas associated with learning and memory. *Neuron* **6**:431-443.

Yan K, Gao LN, Cui YL, Zhang Y and Zhou X (2016) The cyclic AMP signaling pathway: Exploring targets for successful drug discovery (Review). *Mol Med Rep* **13**:3715-3723.

Yan L, Vatner DE, O'Connor JP, Ivessa A, Ge H, Chen W, Hirotani S, Ishikawa Y, Sadoshima J and Vatner SF (2007) Type 5 adenylyl cyclase disruption increases longevity and protects against stress. *Cell* **130**:247-258.

Yan SZ, Beeler JA, Chen Y, Shelton RK and Tang WJ (2001) The regulation of type 7 adenylyl cyclase by its C1b region and Escherichia coli peptidylprolyl isomerase, SlyD. *J Biol Chem* **276**:8500-8506.

Yan SZ, Huang ZH, Andrews RK and Tang WJ (1998) Conversion of forskolin-insensitive to forskolin-sensitive (mouse-type IX) adenylyl cyclase. *Mol Pharmacol* **53**:182-187.

Yoshimura M and Cooper DM (1992) Cloning and expression of a Ca(2+)-inhibitable adenylyl cyclase from NCB-20 cells. *Proc Natl Acad Sci U S A* **89**:6716-6720.

Yoshimura M and Cooper DM (1993) Type-specific stimulation of adenylylcyclase by protein kinase C. *J Biol Chem* **268**:4604-4607.

Yoshimura M, Pearson S, Kadota Y and Gonzalez CE (2006) Identification of ethanol responsive domains of adenylyl cyclase. *Alcohol Clin Exp Res* **30**:1824-1832.

Yoshimura M and Tabakoff B (1995) Selective effects of ethanol on the generation of cAMP by particular members of the adenylyl cyclase family. *Alcohol Clin Exp Res* **19**:1435-1440.

Yu P, Sun M, Villar VA, Zhang Y, Weinman EJ, Felder RA and Jose PA (2014) Differential dopamine receptor subtype regulation of adenylyl cyclases in lipid rafts in human embryonic kidney and renal proximal tubule cells. *Cell Signal* **26**:2521-2529.

Zachariou V, Liu R, LaPlant Q, Xiao G, Renthal W, Chan GC, Storm DR, Aghajanian G and Nestler EJ (2008) Distinct roles of adenylyl cyclases 1 and 8 in opiate dependence: behavioral, electrophysiological, and molecular studies. *Biol Psychiatry* **63**:1013-1021.

Zhang P, Covic L and Kuliopulos A (2015) Pepducins and Other Lipidated Peptides as Mechanistic Probes and Therapeutics. *Methods Mol Biol* **1324**:191-203.

Zhuang LK, Xu GP, Pan XR, Lou YJ, Zou QP, Xia D, Yan WW, Zhang YT, Jia PM and Tong JH (2014) MicroRNA-181a-mediated downregulation of AC9 protein decreases intracellular cAMP level and inhibits ATRA-induced APL cell differentiation. *Cell Death Dis* **5**:e1161.

Zhuo M (2012) Targeting neuronal adenylyl cyclase for the treatment of chronic pain. *Drug Discov Today* **17**:573-582.

Ziegler M, Bassler J, Beltz S, Schultz A, Lupas AN and Schultz JE (2017) Characterization of a novel signal transducer element intrinsic to class IIIa/b adenylate cyclases and guanylate cyclases. *FEBS J* **284**:1204-1217.

Zippin JH, Levin LR and Buck J (2001) CO(2)/HCO(3)(-)-responsive soluble adenylyl cyclase as a putative metabolic sensor. *Trends Endocrinol Metab* **12**:366-370.

VITA

Monica Soto Velasquez, Ph.D.

Educational Background

Ph.D. in Molecular Pharmacology, *GPA: 3.89.* *May 2018*
Purdue University, West Lafayette, IN

Bachelor of Science in Biochemistry, *GPA: 3.74.* *May 2012*
College of Saint Scholastica, Duluth, MN

Positions Held

GRADUATE RESEARCH ASSISTANT *January 2012 – May 2018*
Department of Medicinal Chemistry and Molecular Pharmacology,
Purdue University, West Lafayette, IN

Graduate student working with Val J. Watts, Ph.D., Professor of Medicinal Chemistry and Molecular Pharmacology.

- Graduate student working with Val J. Watts, Ph.D., Professor of Medicinal Chemistry and Molecular Pharmacology.
- Identified the most potent inhibitor to date of adenylyl cyclase type 1 (AC1) activity using high-throughput screening, hit compound validation and counter-screens.
- Collaborated with medicinal chemists in structure-activity relationship studies for lead optimization of the newly identified AC1 inhibitor scaffolds.
- Constructed CRISPR/Cas9-based cell lines to selectively evaluate adenylyl cyclase isoforms activities.
- Designed and completed a high-throughput screen of 17,000 compounds for selective inhibitors of adenylyl cyclase type 8 (AC8).
- Characterized the inhibitory properties of a peptide derived from adenylyl cyclase type 2 as a selective inhibitor of Gβγ-mediated AC2 activity.

INSTRUMENT TEACHING ASSISTANT *May 2014– May 2015*
Department of Medicinal Chemistry and Molecular Pharmacology,
Purdue University, West Lafayette, IN

- Trained graduate students, undergraduate students, postdocs, and visitor scholars on the departmental shared instrumentation (plate readers, centrifuges, gel scanners) in the Department of Medicinal Chemistry and Molecular Pharmacology.

- Helped users troubleshoot problems that were experienced with instrumentation.

TEACHING ASSISTANT *August 2012 – May 2013*
Department of Medicinal Chemistry and Molecular Pharmacology,
Purdue University, West Lafayette, IN

- Teaching assistant for MCMP 204L/205L

RESEARCH VOLUNTEER *September 2011– May 2012*
Department of Chemistry and Biochemistry
University of Minnesota, Duluth, MN

- Undergraduate research assistant working with Ahmed Heikal, Ph.D., Adjunct Professor Pharmacy Practice and Pharmaceutical Sciences.

- Studied the effects of macromolecular crowding on the fraction of free and LDH-bound NADH, employing Time resolving Anisotropy.

SUMMER UNDERGRADUATE RESEARCH ASSISTANT *June – August 2011*
Department of Chemistry and Biochemistry
University of Minnesota, Duluth, MN

- Examined the interaction of cholesterol and lipid molecules in a Triton X-100 micellar system by using the techniques Fluorescence correlation Spectroscopy (FCS) and Dual-Color Fluorescence Cross-Correlation Spectroscopy (DCFCS).

TEACHER ASSISTANT *August 2010 – May 2012*
College of Saint Scholastica, Duluth, MN

- Teaching assistant for CHML 1110/1120

Technical Skills

- Cell-Based Assay Development for Small Molecule Drug Discovery (assay development, experience with automated liquid handling systems and plate readers, lead optimization and SAR development)
- Cell culture of mammalian cell lines and iPSCs-derived neurons (transfection and transduction of mammalian cells. stable cell line generation, production and handling of adenoviral expression systems)

- Experience with cell-based assay technologies (reporter-based, FRET-based, luminescence-based, FACS, live-cell imaging, HTRF, sensors)
- Gene Editing for target validation (CRISPR/Cas9 and RNA interference (siRNA))
- Microscopy (confocal microscopy, fluorescence microscopy)
- Molecular Biology (RNA and DNA isolation and analysis, PCR, gibson assembly, qPCR, DNA cloning, vector construction, and gel electrophoresis)
- Biochemistry (protein quantification, ELISA, SDS/PAGE, Western Blotting, and protein expression)
- Tissue processing and preparation for enzyme activity assays, RNA/DNA extraction or protein quantification.
- Additional skills (Microsoft Office, Adobe Photoshop, GraphPad Prism, Snapgene, Vector NTI)

Awards and Honors

- Graduate Student Travel Award—ASPET annual meeting at Experimental Biology (2018)
- College of Pharmacy Graduate Student Travel Award— Purdue University (2018)
- Neuroscience Collaborative Research Award—PIIN, Purdue University (2017)
- Graduate Student Travel Award—ASPET annual meeting at Experimental Biology (2017)
- Graduate Student Travel Award—ASPET annual meeting at Experimental Biology (2016)
- Graduate Student Travel Award—ASPET annual meeting at Experimental Biology (2014)

Professional Society Memberships

American Society for Pharmacology and Experimental Therapeutics—ASPET (2013-Present)

Publications

- ***Soto-Velasquez, M.**, Hayes, M.P., Alpsoy, A., Dykhuizen, E.C., and Watts, V.J.,* A Novel CRISPR/Cas9-Based Cellular Model to Explore Adenylyl Cyclase and Cyclic AMP Signaling. *Mol. Pharmacol*, (Accepted).

- *Frydrych, J., Skácel, J., Šmídková, M., Mertlíková-Kaiserová, H., Dračínský M., Gnanasekaran, R., Lepšík, M.,* ***Soto-Velasquez, M.**, Watts, V. J., Janeba, Z.*. Synthesis of α-branched acyclic nucleoside phosphonates as potential inhibitors of bacterial adenylate cyclases. *ChemMedChem*, (2018).

- *Hayes, M.P.,* ***Soto Velasquez, M.**, Fowler, C.A., Watts, V.J., Roman, D.L.*. Identification of FDA-Approved Small Molecules Capable of Disrupting the Calmodulin-Adenylyl Cyclase 8 Interaction through Direct Binding to Calmodulin. *ACS Chem. Neurosci.*, (2017).

- *Brust, T. F., Alongkronrusmee, D.,* ***Soto Velasquez, M.P.****, Ye, Z., Dai, M., van Rijn, R.M., Watts, V. J.*.
- Identification of a selective small-molecule inhibitor of type 1 adenylyl cyclase activity with analgesic properties. *Sci. Signal.*, (2017).
- *Rana, N, Conley, J.M., Leon, F., Cutler, S. J,* ***Soto Velasquez, M.P.****, Watts, V. J., Lill, M.A.*. Molecular Modeling Evaluation of the Enantiomers of a Novel Adenylyl Cyclase 2 Inhibitor. *J. Chem. Inf. Model.*, 57, 322–334 (2017).
- *Břehová, P., Šmídková, M., Skácel, J., Dračínský, M., Mertlíková-Kaiserová, H.,* ***Velasquez, M. P. S.****, Watts, V. J., Janeba, Z.*. Design and Synthesis of Fluorescent Acyclic Nucleoside Phosphonates as Potent Inhibitors of Bacterial Adenylate Cyclases. *ChemMedChem*, *11*(22), 2534–2546 (2016).
- *Alfveby, J., Timerman, R.,* ***Soto Velasquez, M. P****., Wickramasinghe, D. W. P. M., Bartusek, J., Heikal, A. A.* Time- and polarization-resolved cellular autofluorescence towards quantitative biochemistry on living cells. *Proc. of SPIE*, 91980U–91980U–15 (2014).